

Discovery of N1-(4-((7-cyclopentyl-6-(dimethylcarbamoyl)-7H-pyrrolo[2,3-d] pyrimidin-2-yl) amino) phenyl)-N8-hydroxyoctanediamide as a Novel Inhibitor Targeting Cyclin Dependent Kinase 4/9 (CDK4/9) and Histone Deacetylase1 (HDAC1) against Malignant Cancer

Yongtao Li, Xiaohe Luo, Qingxiang Guo, Yongwei Nie, Tianqi Wang, Chao Zhang, Zhi Huang, Xin Wang, Yanhua Liu, Yanan Chen, Jian-Yu Zheng, Shengyong Yang, Yan Fan, and Rong Xiang

J. Med. Chem., **Just Accepted Manuscript** • DOI: 10.1021/acs.jmedchem.8b00209 • Publication Date (Web): 08 Mar 2018

Downloaded from <http://pubs.acs.org> on March 9, 2018

Just Accepted

"Just Accepted" manuscripts have been peer-reviewed and accepted for publication. They are posted online prior to technical editing, formatting for publication and author proofing. The American Chemical Society provides "Just Accepted" as a service to the research community to expedite the dissemination of scientific material as soon as possible after acceptance. "Just Accepted" manuscripts appear in full in PDF format accompanied by an HTML abstract. "Just Accepted" manuscripts have been fully peer reviewed, but should not be considered the official version of record. They are citable by the Digital Object Identifier (DOI®). "Just Accepted" is an optional service offered to authors. Therefore, the "Just Accepted" Web site may not include all articles that will be published in the journal. After a manuscript is technically edited and formatted, it will be removed from the "Just Accepted" Web site and published as an ASAP article. Note that technical editing may introduce minor changes to the manuscript text and/or graphics which could affect content, and all legal disclaimers and ethical guidelines that apply to the journal pertain. ACS cannot be held responsible for errors or consequences arising from the use of information contained in these "Just Accepted" manuscripts.



Discovery**of**

N1-(4-((7-cyclopentyl-6-(dimethylcarbamoyl)-7H-pyrrolo[2,3-d]pyrimidin-2-yl) amino) phenyl)-N8-hydroxyoctanediamide as a Novel Inhibitor Targeting Cyclin Dependent Kinase 4/9 (CDK4/9) and Histone Deacetylase1 (HDAC1) against Malignant Cancer

Yongtao Li,¹ Xiaohe Luo,¹ Qingxiang Guo,¹ Yongwei Nie,¹ Tianqi Wang,¹ Chao Zhang,¹ Zhi Huang,¹ Xin Wang,¹ Yanhua Liu,¹ Yanan Chen,¹ Jianyu Zheng,⁴ Shengyong Yang,⁵ Yan Fan*^{1,2,3} and Rong Xiang*^{1,2,3}

¹ Department of Medicinal Chemistry, School of Medicine, Nankai University, 94 Weijin Road, Tianjin 300071, China

² State Key Laboratory of Medicinal Chemical Biology, 94 Weijin Road, Tianjin 300071, China

³ 2011 Project Collaborative Innovation Center for Biotherapy of Ministry of Education, 94 Weijin Road, Tianjin 300071, China

⁴ State Key Laboratory and Institute of Elemento-Organic Chemistry, Collaborative Innovation Center of Chemical Science and Engineering, Nankai University, Tianjin 300071, China.

⁵ Medical Oncology, Cancer Center, State Key Laboratory of Biotherapy, West China Hospital, Sichuan University, Chengdu 610041, China

Abstract

A series of novel, highly potent, selective inhibitors targeting both CDK4/9 and HDAC1 have been designed and synthesized. N1-(4-((7-cyclopentyl-6-(dimethylcarbamoyl)-7H-pyrrolo[2,3-d]pyrimidin-2-yl) amino) phenyl)-N8-hydroxyoctanediamide (**6e**) was discovered. The lead compound **6e** with excellent CDK4/9 and HDAC1 inhibitory activity of $IC_{50} = 8.8$ nM, 12 nM and 2.2 nM respectively, can effectively induce apoptosis of cancer cell lines. The kinase profiling of compound **6e** showed excellent selectivity and specificity. **6e** induces G2/M arrest in high concentration and G0/G1 arrest in low concentration to prevent the proliferation and differentiation of cancer cells. Mice bared-breast cancer treated with **6e** showed significant antitumor efficacy. The insight into mechanisms of **6e** indicated that it could induce cancer cell death via cell apoptosis based on CDK4/9 and HDAC1 repression and phosphorylation of p53. Our data demonstrated the novel compound **6e** could be a promising drug candidate for cancer therapy.

Keywords: CDK4, HDAC1, CDK9, Inhibitor, Cancer

1. INTRODUCTION

Cancer is believed to result from dysregulation of normal cell cycle that leads to abnormal proliferation and inability of cells to undergo differentiation and/or apoptosis. The cell cycle consists of four phases, G1, S, G2 and M phase, which play a critical and central role in control of cell growth and proliferation.¹⁻⁴ Cyclins and their catalytic binding partners, cyclin-dependent kinases (CDKs) maintain the regulation of the cell cycle. CDK4 formed a complex with cyclinD1 is important component of cell cycle activation and control the key progression step, G1 phase, where cells grow and synthesize proteins in preparation for DNA synthesis. Deregulation of the CDK4-cyclinD-Rb pathway and CDK4 overexpression has been observed in cancer. Inhibition of CDK4 associated with cell cycle regulation by inhibitors can lead to a G1 arrest and cell cycle progression halt, which provides an effective approach to the control of tumor growth.⁵⁻¹¹

Many researchers have focused their efforts on the development of small molecule inhibitors of CDK4. The first generation of CDK4 inhibitors was nonselective and caused severe toxic side effects in clinical trials. Toxicity due to poor specificity has limited their therapeutic efficacy.^{12, 13} In an attempt to overcome the toxicity, potent and selective CDK4 inhibitors have received significant attentions. palbociclib and ribociclib that entered clinical trials are highly specific for CDK4.¹⁴⁻¹⁸ They all need to combine with letrozole for the treatment of ER+/HER2– metastatic breast cancer. These studies suggest that monotherapy targeting on CDK4 to induce tumor cell death may be insufficient.^{19, 20} Additionally, many studies have shown synergistic outcomes in reduction of tumor burden by simultaneous inhibition of more than one activated protein.²¹⁻²³ Therefore, we reasoned that development of single drugs with multiple biological targets based on CDK4 might improve efficacy in cancer treatment.

Histone deacetylases (HDACs) catalyze the deacetylation from lysine residues in histones tails, leading to chromatin condensation, thus controlling the transcriptional regulation, cell cycle progression and apoptosis.²⁴⁻²⁷ Inhibition of HDACs significantly suppress cancer cell proliferation, angiogenesis, and metastasis and induce apoptosis. Interestingly, HDAC1 inhibitors that possess synergistic or

additive antitumor effects in rational combinations with anticancer drugs have been investigated.²⁸⁻³¹ Following the success of synergy between HDAC inhibitor and CDK inhibitor in treating neuroblastomas and melanoma,³² we conceived that multitarget inhibition using of HDAC1 inhibitor in combination with CDK4 target agent to increase the efficiencies the CDK inhibitor. There is few report in the literature concerning bifunctional targeting of CDK and HDAC1 by single chemical inhibitors. With this approach, a novel single molecule targeting CDK4 and HDAC1, was designed to avoid side effect of more separate agents, such as drug-drug interaction or different physicochemical properties.

In our study, a series of novel dual-action compounds targeting CDK4 and HDAC1 were designed and synthesized. In vitro antiproliferative activity and kinase profiling revealed that the most active compound, **6e** was a multikinase inhibitor with excellent CDK4 inhibitory activity ($IC_{50} = 8.8$ nM), HDAC1 inhibitory activity ($IC_{50} = 2.2$ nM) and CDK9 inhibitory activity ($IC_{50} = 9$ nM). The lead compound can induce apoptosis of a wide variety of tumor cell lines and significantly induce G2/M arrest in high concentration and induces G₀/G₁ arrest in low concentration. In vivo it is effective in a 4T1 xenograft model in BALB/c mice. On the basis of these findings, it appears that compound **6e** offers potential for the treatment of a variety of tumor diseases. Herein, we report the synthesis, structure-activity relationship (SAR), kinase inhibitory profile, in vitro cytotoxicity, and tumor regression studies of this lead compound. The selection of key drug-like parameters comprising Log P and Log D were measured. This work provides a novel approach in the development of new chemotherapy for further exploration of dual CDK-HDAC1 pathway inhibition achieved with single molecule.

2. RESULTS AND DISCUSSION

2.1. Dual CDK4-HDAC1 Inhibitors Design Strategy. Rather than linking two inhibitors together with a long chain, a merged pharmacophore is more desirable order to avoid high molecular weight. Since there is no 3D structure of CDK4-ligand complex reported at present, the structure of CDK6 in complex with an inhibitor (PDB entry: 4EZ5) was used as a template for homology modeling.³³ Analyzing the X-ray cocrystal structure and the third generation of CDK-directed drugs, we found all of

1 them interact with the hinge region using the 2-aminopyrimidine group. Analysis of the structural
2 information in Figure S1 and Figure 1 suggested that His100 in CDK6 (His92 in CDK4), an amino acid
3 that is rarely conserved in other kinases. Previously reported structural studies with CDK inhibitors
4 bound to CDK6 propose 2-amino and N-3 position of the pyrrolo[2,3-d] pyrimidine ring forming two
5 hydrogen bonds with His100 (His92 in CDK4) as an important determinant for CDK enzyme inhibition.
6 The 2-aminopyrimidine group, which interacts with the hinge region as its core CDK6-binding scaffold
7 provides a suitable moiety to explore our hypothesis. Thus, it was postulated that inserting the HDAC1
8 binding group here would retain CDK activity. An intrinsic property that affects kinase selectivity for
9 many drugs is lipophilicity³⁴, quantified by cLogP. As the cLogP of ribociclib (2.3) is significantly
10 lower than abemaciclib (5.5) or palbociclib (2.7), we selected pyrrolo[2,3-d] pyrimidines-2-amine as the
11 backbone because this class of compound showed to possess higher CDK kinase inhibitory activity and
12 kinase selectivity. Most HDACis, such as vorinostat, are characterized by a widely accepted
13 pharmacophore model including three moieties, the capping group, linker region and zinc binding
14 group. The capping group that interacts with residues at the entry point of the active site tunnel. The
15 linker chain plus a connecting unit interacting mainly with hydrophobic residues of the tunnel. The zinc
16 binding functional group, such as hydroxamic acid, binds strongly to the zinc cation or a monodentate
17 group at the active site. According to the structural information, the zinc binding group plays a critical
18 role in chelation of zinc ion for HDAC1 inhibition.³⁵ The hydroxamic acids moiety consistently inserts
19 into the catalytic outer tunnel of HDAC and chelates a zinc ion, which is important for the catalytic
20 process of HDAC. We further designed a merged molecule (Figure 1), in which the two essential
21 pharmacophoric elements, pyrrolo[2,3-d] pyrimidines-2-amine and hydroxamic acid moiety. Thus, we
22 design single compound that selectively inhibits both CDK and HDAC1 enzymes to improve efficacy in
23 cancer treatment compared to a single inhibitor alone.

24
25
26
27
28
29
30
31
32
33
34
35
36
37
38
39
40
41
42
43
44
45
46
47
48
49
50
51
52
53 **2.2. Chemistry.** All target compounds were prepared by routes outlined in Schemes 1–3. First, we
54 synthesized the key intermediates and the general synthetic routes are illustrated in Scheme 1. Briefly,
55 commercially available **1a-1d** reacted with phenylenediamine (**2a-2c**) to provide aniline intermediate

3a-3f (40–87% yield).³⁶⁻³⁸ Commercial compound **4** with intermediate anilines **3a-3f** through palladium catalyzed cross-coupling reaction provided compounds **5a-5f**. Similarly, commercially available **7a-7d** reacted with 4-aminobenzoic acid (**8**) which were purchased from market to provide aniline intermediate **9a-9d**. After that, **10a-10d** were obtained by **9a-9d** with one step. Those methyl carbonate analogues (**5a-5f**, **10a-10d**) were directly converted into the hydroxamic acids analogues (**6a-6f**, **11a-11d**) by NH_2OH in CH_3OH .³⁵ Aniline intermediate **13a-13f** were acquired by **12a-12d** with *p*-phenylenediamine (**2c**). Then, intermediate **13a-13d** with compound **4** to provide compounds **14a-14d**.³⁹⁻⁴¹ A primary amine **7b** was reacted with triphosgene and trimethylamine to provide isocyanate derivative **15**, which was then reacted with *p*-phenylenediamine to produce aniline intermediate **16**.⁴² **16** underwent $\text{S}_{\text{N}}\text{Ar}$ with compound **4** to produce **17**, which was then directly converted into **18** by NH_2OH in CH_3OH .

In Scheme 2, Compound **4** was coupled to the diphenylmethanimine to obtain **8**, which was not necessary to further purify and treated with concentrated HCl to obtain **20**.⁴³ Compound **4** was heated with $\text{N}_2\text{H}_4 \cdot \text{H}_2\text{O}$ in EtOH to give **21**.⁴⁴ Compound **1c** was condensed with **20**, **21**, ribociclib, 4-(Aminomethyl)anilinedihydrochloride and tert-butyl (5-aminopyridin-2-yl)carbamate to provide **22**, **23**, **24**, **26** and **29**, respectively. Similarly, **26** underwent $\text{S}_{\text{N}}\text{Ar}$ with **4** to produce **27**, which was then directly converted into **28** by NH_2OH in CH_3OH . Removal the protecting group of **29** provided aniline **30**, which underwent $\text{S}_{\text{N}}\text{Ar}$ with **4** to produce **31**. **31** was heated with NH_2OH in MeOH to give **32**. **33** was obtained by the procedure from **1c** reacting with 5-nitropyridin-2-amine, and the nitro was reduced to produce **34**. The syntheses procedure of **35** is similar with **31**.

In Scheme 3, to viewing the contribution of the *N,N*-dimethylamide substituent, the unsubstituted intermediates 2-chloro-9-cyclopentyl-9*H*-purine (**40**) and 5-chloro-3-cyclopentyl-3*H*-[1,2,3]triazolo[4,5-*d*]pyrimidine (**43**) were required. Commercially available 2,4-dichloro-5-nitropyrimidine (**36**) as the starting material reacted with cyclopentylamine (**37**) to give compound **38**,⁴⁵ which was treated with $\text{SnCl}_2 \cdot 2\text{H}_2\text{O}$ for reduction of nitro to obtain compound **39**.⁴⁶ The compound **40** was prepared from **39** by treatment with trimethyl orthoformate in 47% yield.

Compound **39** was treated with NaNO₂ under concentrated HCl conditions to produce compound **43**. A palladium catalyzed cross-coupling reaction of compounds **40** and **43** with intermediate anilines **3e** provided compounds **41** and **44** followed by converted into the hydroxamic acids compounds **42** and **45** by NH₂OH in CH₃OH. The compound **46** was prepared by reduction of compound **5e** with lithium aluminum hydride in THF.⁴⁷ Hydrolysis of **5e** gave the acetic acid derivative **47**, followed by condensation with dimethylamine in the presence of EDCI and HOBt and DIEA to afford the amide derivative **48**.⁴⁸

2.3. Enzyme Inhibitory Activity and SAR. It is evident from Table 1 that the nature of substituents Y-6 position in the general structure specifies the enzyme activity of the molecules on CDK4/cyclinD.⁴⁹ Placing dimethylcarbamoyl in Y-6 position and keeping other positions constant, the molecule showed better activity targeting CDK4. As the dimethylcarbamoyl was displaced, inhibitory properties of compounds as shown **41**, **42**, **44** and **45**, were decreased by several fold compared to other molecules. These data clearly show that a dimethylcarbamoyl group at Y-6 position is the most optimal substituent, suggesting that the dimethylcarbamoyl group at the Y-6 position of the pyrrolo[2,3-d] pyrimidine ring is critical for its activity.

Once we identified suitable substituents for the Y-6 position, we then investigate whether the aromatic ring moiety, between the pyrrolo[2,3-d] pyrimidine and zinc binding group, was important for potent inhibition of CDK4/cyclinD. The results of enzyme inhibitory activity studies showed that all of the molecules with phenyl substituent between the pyrrolo[2,3-d] pyrimidine and zinc binding group were similar active with CDK inhibitor ribociclib. These compounds fared better with half-maximal inhibitory concentrations (IC₅₀) values ranging from 4.8 nM to 30 nM, such as compounds **5b-f**, **6b-6f**, **10a-d**, **11a-d**, **14a-b**, **18**, **27**, **28**, and **46** to **48**. Other derivatives focusing on the position connecting to the C-2 position of the pyrrolo [2,3-d] pyrimidine-6-one was varied in an attempt to further improve the potency for CDK4/cyclinD. When the position changed to pyridine moiety, the molecules (**31** and **32**) were several-fold less active than aboved compounds. Compound **5a** and **6a**, which possess an ortho-aniline group instead of a para-aniline, showed lower binding affinity (IC₅₀ > 5000 nM), most

likely because of unfavorable steric interactions with the pocket of CDK4/cyclinD. Analogues **22** and **23** with progressive decrease of IC_{50} values were also observed. 5-(Piperazin-1-yl) pyridin-2-yl group in **24** and **25** conferred high CDK4/cyclinD potency.

Several substituents, such as hydroxamic acids, methyl ester, dimethylcarbamoyl group, alkyl and hydroxy, were designed as a zinc binding group. We have selected some representative compounds to detect the HDAC1 inhibition activities. Among these compounds, the ester group, dimethylcarbamoyl group, alkyl and hydroxy were completely inactive against HDAC1 at the highest concentration tested (5 μ M) in Table 1, due to the weak chelating effect to the zinc cation in the HDAC1 active site. Therefore, hydroxamic acid is essential for good zinc binding and activity, thus the hydroxamic derivatives showed significant inhibition of HDAC1 activity in Table 1. These compounds were 10-100-fold more potent than positive control, HDAC1 Inhibitor (vorinostat). Compounds afforded strong HDAC1 inhibition, such as **6b**, **6e**, **6f**, **11c**, **11d** and **44**, especially compound **6b** (IC_{50} = 0.84 nM) and **11b** (IC_{50} = 0.53 nM). The SAR appears to mirror that observed for a series of homologues in which the linking section between the hydroxamic acid and amide must be at least five carbon atoms in length, with length of five being optimal.⁵⁰ Compound **6c** (IC_{50} = 27 nM) did not demonstrated outstanding HDAC1 inhibition activity, probably due to the short distance between the acid and the pyrrolo[2,3-d]pyrimidine. Compound **6a** was not particularly active, probably because the dimethylcarbamoyl is ortho to 2-aminopyrimidine group resulting in steric hindrance. With HDAC1 inhibitory of IC_{50} = 53 nM, the compound **28** with a methylene spacer was found to be less active than the parent molecule, probably because of the benzyl amine group increasing the flexibility of the zinc binding moiety. In comparison with vorinostat, compound **11a-d** was made as reversed amide. The observed low HDAC1 inhibitoion of **25**, **32** and **45** is probably due to the differences in the cap binding region of the CDK.

2.4. Cellular Assays. We focused our efforts on the evaluation of our bifunctional inhibitors. Whether or not the kinase inhibitory activity of the dual-action molecules transfer to tumor cell lines was next explored with cancer cell proliferation assays. We screened dual-acting compounds exhibiting better kinase inhibitory than ribiciclib and vorinostat to do the preliminary cell inhibition assays (Table

S1). Then, IC₅₀ values were further detected on compounds that exhibit better cell inhibition in a panel of cancer cell lines growth using standard CCK8 assay. Despite being highly potent against both CDK4 and HDAC1, analogues **6d**, **6f** and **11b**, with five or seven carbon atoms in length of the linking section between the hydroxamic acid and amide, were only weakly antitumor activities in these cells (Table S2). The best tumor cell potency of these analogues was obtained for six carbon linked molecule **6e**, which was also outstanding inhibitor of CDK4 and HDAC1 with IC₅₀ values of 8.8 and 2.2 nM. It was probably due to compound **6e** with a comfortable and optimal merged pharmacophore for cell uptake. As attributes of a truly merged bispecific pharmacophore and the results of antitumor activity in cell lines showed that **6e** is the best in this class, we performed all subsequent in vitro and in vivo biological studies using this compound. The compound was next evaluated in a dose response study against breast cancer cell lines (4T1, T47D and MDA-MB-231), lung cancer cell lines (A549 and H460), and liver cancer cell lines (HepG2 and Hep3B) to test cytotoxic activity (Table 2 and Table S3).⁵¹ Compounds ribociclib and vorinostat were used as references. Compound **6e** showed potent profile in vitro, with around 1 μM IC₅₀ values in the 4T1, MDA-MB-231, A549, H1299 and Hep3B cell lines and about 2-3 μM in other cell lines. The CDK4 selective inhibitor ribociclib was not potent in these cells, which indicated CDK4 monotherapy lack sensitivity. This result demonstrated that combination CDK and HDAC1 inhibition in a single molecule, led to synergy at the cellular level more efficiently.

2.5. Kinase Selectivity Profiling. To investigate the kinase selectivity, kinase inhibition profiling assays with a fixed concentration of 1 μM of compound **6e** were first carried out against a series of 375 kinases through the Eurofins kinase profiling. The results are provided in Figure 2 and Table S4. Further IC₅₀ values of the kinases that showed a high inhibitory rate at 1 μM, were examined and the results are shown in Table 3. Interestingly, ribociclib with highly selective for CDK4/6 relative to other human protein,⁵² was detected with the IC₅₀ of CDK4/cyclinD, 13 nM and IC₅₀ of CDK9/cyclinT, 197 nM. Our compound **6e** showed higher inhibitory activity against CDK4/cyclinD (IC₅₀ = 8.8 nM) and CDK9/cyclinT (IC₅₀ = 9 nM) over other CDKs. Resulting from high homology, identical substrate specificities and enzymatic activities CDK4 and CDK6 have overlapping functions in development. In

light of this fact, many of the third generation CDK4 inhibitors such as abemaciclib, dinaciclib, ribociclib, palbociclib and AG-024322 also inhibited CDK6.⁵² Therefore, the development of ATP-competitive CDK4 inhibitors that are selective over CDK6 may offer an improved therapeutic potential as well as dual CDK4/CDK6 inhibitors. CDK4 along with cyclins D is involved in the regulation of cell cycle, while CDK9 along with cyclins T is key player in transcription regulation/RNA processing. Compound **6e** that target cell cycle-related CDK4 and transcription-related CDK9, might contribute to the antitumor activity. Compound **6e** has additional kinase activities (6 human protein kinases have $IC_{50} < 50$ nmol/L), all of which are intimately associated with the growth, survival, and metastasis in tumor cells.

2.6. Molecular Modeling of Compound 6e. Molecular docking studies were carried out to investigate the binding modes of compound **6e** in CDK4, CDK9, and HDAC1, respectively. Since there is no 3D structure of CDK4-ligand complex reported at present, the structure of CDK6 in complex with an inhibitor (PDB entry: 4EZ5) was used as a template for homology modeling. MODELLER⁵³ in the Discovery Studio (DS, Accelrys Inc., USA) was employed for the homology modeling. Then the compound **6e** was docked to CDK4, CDK9 (PDB code: 4BCF) and HDAC1 (PDB code: 4BKX) by GOLD (version 5.0). Hydrogen atoms were added to the proteins by using DS 3.1. GoldScore was selected as the scoring function, and other parameters were set as default. The image was created using PyMOL.⁵⁴

Figures 3 illustrate the predicted binding modes and the detailed protein-inhibitor interactions of compound **6e** with CDK4, HDAC1 and CDK9, respectively. For comparison, the binding mode of **6e** was superimposed on that of ribociclib or vorinostat. Compound **6e** is a potent inhibitor of CDK4 with an IC_{50} of 8.8 nM and ribociclib shows a similar level of CDK4 inhibition, with an IC_{50} of 13 nM. As shown in Figure 3A, **6e** could tightly bind to the ATP-binding site of CDK4 in a binding mode similar to that of ribociclib. Hydrogen bonds appear to be formed between the aminopyrimidine and the backbone residue of VAL96 and HIS95. Given that these hydrogen bonds are critical for binding to CDK4, it is satisfying to find that NH of aminopyrimidine may also be serving a similar role in its interactions with

HDAC1. From this point of view, **6e** displays attributes of a truly merged bispecific pharmacophore. In an attempt to find the reasons for the HDAC1 inhibitory of the compound **6e**, we docked compound **6e** into the HDAC1 protein. As shown in Figure 3B, the hydroxamic acid could insert into the catalytic outer tunnel of HDAC1 and the group also chelates a zinc ion, which is important for the catalytic process of HDAC1. In addition, the 2-aminopyrimidine group contribute to the hydrogen-bonding interaction with the residue in the catalytic tunnel. In contrast to vorinostat that contain simple heterocycle to exert cap action, our results of molecular modeling reveal that placing 2-aminopyrimidine substituents at proper locations forms a hydrogen bonding interaction with GLU-98. This deeper and closer binding of compound **6e** to HDAC1 may explain the better binding affinity of compound **6e** for HDAC1, about 10 fold than vorinostat. The CDK9 inhibitory IC_{50} of compound **6e** is 9 nM, while ribociclib is 197 nM. From Figure 3C, we can see that, compared with ribociclib, compound **6e** gains another new hydrogen bonding interaction between hydroxamic acid group and THR-29, which could be used to interpret the phenomena that **6e** showed a stronger activity against the CDK9 kinase than ribociclib.

In order to illustrate the SARs more rational, molecular modeling studies are employed to select **5c** and **11b** as the best candidate for CDK4 and HDAC1 enzyme inhibition, respectively. As shown in Figure S2. Compared with **6e**, compound **5c** gains another new hydrogen bonding interaction with ARG101, which could explain **5c** showed a stronger CDK4 inhibition than **6e** and ribociclib. As shown in Figure S3, the length of the linking section with four carbon atoms between the hydroxamic acid and amide made the structure of compound **11b** expanded, which lead to it is more suitable in the active pocket of HDAC1. That may be the reason for the inhibition difference between compound **6e** and **11b**. The SARs findings according to the docking poses are coordinating with our SAR results discussed above.

2.7. Effect of Compound 6e on Cell Cycle Progression. We therefore wondered whether this cell apoptotic and kinase inhibition effect could partly result from growth arrest induction and cell cycle inhibition. We next investigated the effect of compound **6e** treatment on breast cancer cell lines (T47D

and MDA-MB-231), lung cancer cell lines (A549 and H460), and liver cancer cell lines (HepG2 and Hep3B) cell cycle kinetics (Figure 4). Cells were treated with compound **6e** with varying concentrations according to IC_{50} values, ribociclib and vehicle (DMSO) for 24 h, which were stained with propidium iodide, and subjected to flow cytometric analysis to determine the distribution of cells in various phases of the cell cycle. Similar effects were observed in three type cells. Compared to the vehicle-treated cells, cancer cells treated with compound **6e** demonstrate a loss of S-phase cells and an increase in the percentage of cells in G2 and G0/G1. Ribociclib treatment led to a massive accumulation of cells in G0/G1. It was evident that compound **6e** blocked the cells in G2 at high dose of 2.5 and 10 μ M, while at low dose of 625 nM, induced an increase in cells in G0/G1 phase, which resulted in decreased S-phase populations. It is well known that CDK4 plays a critical role in the G1/S transition of the cell cycle. Inhibition of cellular CDK4 activity is expected inhibition of cell cycle arrest in the G1 phase. Analyses of our result demonstrated the ability of compound **6e** to affect the activities of CDK4 in cells and led to support the hypothesis of a blockage during the G1 phase of compound **6e** with lower concentration. The effects on G0/G1-phase inhibition are consistent with the inhibition of CDK4. Compound **6e** blocked both G0/G1 and G2-M transitions. The G2 phase inhibition is indicative of cells undergoing apoptosis.⁵⁵ Additionally, there may be a role for inhibition of CDK9 and HDAC1, which are inhibited by compound **6e** with similar potency as CDK4. This result indicated that compound **6e** has cellular HDAC1 or CDK9 inhibitory activity at a higher concentration and a cellular CDK4 inhibitory activity with a lower concentration. The results confirmed that compound **6e** had antiproliferative properties, suggesting the existence of multi-intracellular targets.

2.8. Effect of Compound 6e on Cell Apoptosis. The Hoechst 33342 staining was used to verify if the compound **6e** was able to affect cell growth through apoptosis. As shown by representative pictures of T47D (Figure 5A), the apoptotic bodies of cells have been investigated that revealed a dose-dependent increase of apoptosis in cell cultures after 48h of incubation with compound **6e**, consistent with the effect on cell proliferation. Compound **6e** generated an increase of the presence of apoptotic cells compared to untreated cells.

1 It was subjected to an apoptotic assay for further evaluation of the antiproliferative activities of our
2 compound against breast, lung and liver cancer cell lines. Cells were treated with compound **6e**,
3 vorinostat as reference drugs and vehicle (DMSO) for 48h, which were analyzed by annexin V/PI
4 staining (Figure 5B). Compound **6e** induced cell apoptosis in a dose-dependent manner. The percentage
5 of apoptotic cells was defined as the sum of early and late apoptosis (annexin V-positive and PI-positive
6 cells). Compared with the vehicle condition, compound **6e** was significantly more active in apoptosis
7 induction as the concentration increased. **6e**-treated T47D, H460 and HepG2 cells exhibited
8 significantly better inhibition. Taken together, compound **6e** could induce cell death via apoptosis.

18 **2.9. Molecular Mechanisms of Activity for Compound 6e.** As compound **6e** exhibited clear cell
19 cycle suppression and significant induction of apoptosis, we decided to characterize the cellular effects
20 of compound **6e** in more detail. To further confirm the CDK inhibitory, we first performed western blot
21 analysis to evaluate the protein levels of CDK4 inhibition (Figure 6A). Similar results were obtained for
22 six types cell. Compound **6e** exhibited stronger inhibition of CDK4 enzymes. Treated cells exhibited
23 dose-dependent reductions in the level of the protein CDK4 and Cyclin D1, which is consistent with the
24 known mechanisms of action for CDK4 inhibitors. Compound suppressed CDK4 at 1 μ M in cells,
25 which is in accord with the IC₅₀ value in cell viability assays. To evaluate if the antiproliferative activity
26 of compound **6e** is caused by inhibition of cellular CDK4 and CDK9, we selected inhibition of Rb
27 phosphorylation at the CDK-specific sites Ser807/811. The results of this study (Figure 6A) show that
28 compound **6e** effectively suppressed phosphorylation of Rb Ser807/811 at 1 μ M, confirming that CDK
29 is one target of this compound. The intracellular histone acetylation status is a direct marker of class I
30 HDAC1 inhibition. To further investigate whether the dual enzyme inhibition profile of compound **6e**
31 translates into intracellular inhibition against HDAC1 pathway, we performed western blot analysis to
32 study the effect of compound **6e** in the six type cell lines. As shown in Figure 6B, compound **6e** affected
33 acetyl-histone H3 expression level, resulting in upregulation of acetyl-histone H3, especially in breast
34 cancer cell lines and lung cancer cell lines. In liver cancer cell line, the assay showed that compound **6e**
35 showed a similar level of acetyl-histone H3 with vorinostat.

As illustrated in Figure 6B, to confirm further the apoptosis induction of compound **6e**, we examined the expression of apoptotic proteins Bcl-2 and the cleavage states of caspase 3. Cells were treated with or without compound **6e** and control for 48h and then lysed and analyzed by Western blot. It was revealed that treatment with compound **6e** dramatically increased the relative levels of antiapoptotic Bcl-2 expression in a dose-dependent manner. Furthermore, compound **6e** resulted in more significant cleaved caspase 3 to different extents than the control group. Additionally, the inhibition of both HDAC1 and transcriptional CDK9 might also induce cell death through the down-regulation of these short-lived anti-apoptotic proteins Bcl-2. This implies that compound **6e** may induce cell death by both transcriptional and HDAC1 repression. It is well known that phosphorylation of p53 results of DNA damage induced by treatment with HDAC1 inhibitors. Next, we wanted to detected whether compound **6e** induced apoptosis depends on the expression of p53. Protein level of P-p53 detected by western blot, was enhanced in compound **6e**-treated cells in respect to control groups. This finding led to the conclusion that compound **6e**-induced apoptosis is associated with p53 phosphorylation.

The above results re-emphasized that compound **6e** inhibits CDK4/9 and HDAC1 activity and is efficient in cultured breast cancer cells, lung cancer cells and liver cancer cells. The correlation between the suppression of CDK4, Rb-phosphorylation and onset of apoptosis suggests that the mechanism of action of compound **6e**, in these six cancer cell lines proceed through inhibition of CDK and HDAC1 critical.

Immunofluorescence (Figure 7) were carried out to demonstrate the inhibitory activity of compound **6e** on CDK4 and deacetylation of histone H3. A549 cell line has been selected as a representative model because it resulted as being nearly the most sensitive to the compound **6e** antiproliferative effect. It was demonstrated above that compound **6e** induced an increase in cells in G0/G1 phase at low concentration, which is consistent with the inhibition of CDK4. The 100 nM concentration and 1 μ M concentrations of compound **6e** were chosen and used in the immunofluorescence assay to detect the effect on CDK4 and acetyl-histone H3, respectively. After 24 h of treatment with compound **6e** and vehicle condition, a

significant inhibition of CDK4 and increase of acetylation, observable staining of CDK4 and acetyl-histone H3, were detected by immunofluorescence analysis (Figure 7).

2.10. Lipophilicity. Log P and Log D describe a compound's lipophilicity, and values often correlate with a number of key biopharmaceutical parameters in drug discovery. We detected the experimental Log P, Log D_{7.4} values and calculated Log P (cLogP) value for compound **6e**. The values were measured using the traditional shake flask method. The LogP value for **6e** is 2.62 and LogD_{7.4} value is 2.02. Using ChemDraw Ultra 12 software, the cLogP for the virtual compound **6e**, is 2.08. Our results indicated that compound **6e** has a reasonable lipophilicity. We also detected the solubility of **6e**. The solubility of **6e** in PBS at pH 7.4 is 0.35 µg/mL and in the methanesulfonic acid formulation is 526 µg/ mL. Methanesulfonic acid formulation is compound **6e** combined with one equiv methanesulfonic acid. As the solubility of compound **6e** in other acid formulation was not good, data were not shown. Despite its limited solubility, **6e** exhibited good lipophilicity.

2.11. Pharmacokinetic Properties of 6e in Rats. Considering the excellent anti-tumor activities of compounds **6e** both in vitro and in vivo, pharmacokinetic (PK) properties of these compound was further evaluated. Key PK parameters are summarized in Table 4. After per iv administration of 20 mg/kg compound **6e**, the area under the concentration–time curve (AUC_{0–∞}) was about 6158 µg/L*h and the half-life (t_{1/2}) was about 10.76 h. After per ip administration of 20 mg/kg compound **6e**, the area under the concentration–time curve (AUC_{0–∞}) was about 2133.7 µg/L*h and the half-life (t_{1/2}) was about 9.65 h. In addition, after per ip compound **6e** achieved a maximum plasma concentration (C_{max}) of 359.6 µg/L and showed a clearance rate (CL) of 12.61 L/h/kg and apparent distribution volume (V_{ss}) of 119.94 L/kg. When administered 20 mg/kg compound **6e** orally, the area under the concentration–time curve (AUC_{0–∞}) was about 1130.6 µg/L*h and the half-life (t_{1/2}) was about 14.91 h. After per op compound **6e** achieved a maximum plasma concentration (C_{max}) of 136.8 µg/L and showed a clearance rate (CL) of 20.62 L/h/kg and apparent distribution volume (V_{ss}) of 431.52 L/kg. All of these indicated that compound **6e** has moderate PK properties.

2.12. In Vivo Anticancer Activity of Compound 6e. We next carried out studies to determine the maximum tolerated dose of compound **6e** in mice. BALB/c female mice ($n = 4$) received different doses (45 mg/kg, 90 mg/kg and 130 mg/kg) of compound **6e** intraperitoneally for 16 consecutive days and were monitored over signs of toxicity (Figure 8A). No signs of toxicity or weight loss were observed. 4T1 cells were labeled with a reporter system encoding of firefly luciferase (Fluc) by lentiviral transduction. To determine the efficacy of compound **6e** in vivo using tumor xenograft models, Fluc-4T1 cells were orthotopically implanted into the mammary fat pads of 6–8 weeks old female BALB/c mice. Once the tumors reached an average volume of 100 mm³, compound **6e** was administered daily via IP injection based on the toxicity results and literature^{14, 56-58}. The bioluminescence imagings were performed on the representative animals at 8 days and 25 days for Fluc reporter gene expression to reflect the number of viable tumor cells (Figure 8B). The tumor treated with compound **6e** therapy demonstrated a great decrease in the strength of Fluc signal which suggested a considerable extent of tumor inhibition. Quantitative analysis of bioluminescence imaging signals at day 25 demonstrated that compound **6e** showed significantly better inhibition (Figure 8C). The results of this study (Figure 8D) showed that compound **6e** administered on this schedule led to a dose-dependent inhibition of tumor growth. Tumor growth inhibitions of 78.4% and 84.8% were observed at doses of 90 and 130 mg/kg, respectively. In contrast, vorinostat and ribociclib as the positive controls were less potent (76.8%) and (68.5%) than **6e** at the same dose, respectively. As positive controls, 130 mg/kg vorinostat and ribociclib showed weaker antitumor activities compared with that of the compound **6e**. A decrease in tumor weight was also observed at the end-point of the study (Figure 8E). No overt signs of toxicity were observed in the **6e** treated groups (body weights was not shown), indicating that the compound **6e** is well-tolerated in vivo. Administration of compound **6e** by oral gavage was also effective. IHC staining showed that the expression level of p-Rb and Bcl-2 was suppressed in **6e** treatment groups (Figure 9). Tumor growth inhibitions of 70.3%, 79.3% were observed in the 4T1 model at doses of 90 and 130 mg/kg, respectively. In contrast, vorinostat and ribociclib as the positive controls were less potent (75.6%) and (38.9%) than **6e** at the same dose, respectively. **6e** exhibited

potent activity in vivo after both intraperitoneal and oral administration. Intraperitoneal administration showed a high antitumor efficacy compared with oral administration at the same doses, which are coordinating with our bioavailability results as shown in Table 4.

3. CONCLUSIONS

Through designing and structural optimization targeting on CDK4 and HDAC1, we finally discovered a new compound **6e**. Compound **6e** is a multikinase inhibitor, which potently inhibited CDK4, CDK9 and HDAC1 with IC_{50} values of 8.8 nM, 9 nM and 2.2 nM, respectively. **6e** also inhibited several kinases, such as the Aurora-A/B/C, Flt4, LIMK1 and TrkA, with $IC_{50} < 50$ nmol/L. Even so, it is not a promiscuous agent and showed good selectivity in a kinase profiling assay against 375 kinases. In vitro cellular assays, **6e** showed potent activities against breast cancer cell lines, T47D and MDA-MB-231 (triple negative breast cancer cell line), lung cancer cell lines, A549 and H460, liver cancer cell lines, HepG2 and Hep3B. In cell cycle assays, compound **6e** could block the six tumor cells mentioned above in G2 at high dose of 2.5 and 10 μ M, while at low dose of 625 nM, induce an increase in cells in G0/G1 phase, which resulted in decreased S-phase populations. The effect on the cell cycle progression confirmed that compound **6e** has cellular HDAC1 or CDK9 inhibitory activity at a higher concentration and a cellular CDK4 inhibitory activity with a lower concentration. In vivo antitumor activity assays showed that intraperitoneal and oral administration of compound **6e** led to potent tumor regression in the 4T1 xenograft models. Studies of mechanisms of action indicated that **6e** down-regulated the activity of CDK4 and cyclinD1 kinase and the phosphorylation of protein Rb. In addition, **6e** significantly upregulation of acetyl-histone H3 and the relative levels of antiapoptotic Bcl-2 expression and cleaved-caspase-3. **6e** also enhanced the protein level of P-p53, which led to the conclusion that compound **6e**-induced apoptosis is associated with DNA damage. All of the studies presented here support **6e** as a novel drug candidate targeting on CDK4/9 and HDAC1 and deserve further research and development.

4. EXPERIMENTAL SECTION

4.1 Chemistry Methods. All reagents and solvents were obtained from commercial suppliers and used without further purification unless otherwise indicated. Melting points (mp) were taken in open capillaries on a Mettler MP 50 melting-point system. All reactions were monitored by thin-layer chromatography (TLC), and silica gel plates with fluorescence F-254 were used and visualized with UV light. ^1H NMR (400 MHz) and ^{13}C NMR (101 MHz) spectra were taken on a Bruker AV-400 MHz spectrometer and chemical shifts were reported in ppm downfield from internal Me_4Si . High-resolution mass spectra (HRMS) were recorded on a VG ZAB-HS mass spectrometer under electron spray ionization (ESI). All of the solvents were purified and distilled according to the standard procedure. The commercially obtained materials were used directly without further purification unless otherwise noted. All of the final compounds were purified to > 95% purity, as determined by high-performance liquid chromatography (HPLC). The purity by HPLC analysis on a Shimadzu Prominence-i LC-2030C 3D system (column, InertSustain C18, 4.6 mm \times 250 mm, 5 μM ; mobile phase, gradient elution of methanol/ H_2O ; low rate, 1.0 mL/min; UV wavelength, 190–800 nm; temperature, 40 $^\circ\text{C}$; injection volume, 10 μL). ^1H and ^{13}C spectra of test compounds are provided in Supporting Information Appendix.

General Procedure for the Synthesis of 3a-f. A mixture of acid **1a-1d** (30 mmol, 1 equiv), amine **2b-2c** (60 mmol, 2 equiv), EDCI (8.27 g, 45 mmol, 1.5 equiv), HOBT (4.87 g, 36 mmol, 1.2 equiv), and DIEA (7.76 g, 60 mmol, 2 equiv) was stirred in DMF (60 mL) at room temperature for 12 hours. After completion of the reaction, the mixture was quenched by water and extracted by ethyl acetate. The combined organic layer was washed with brine solution and dried by MgSO_4 . The solvent was evaporated, and the residue was purified by silica gel column chromatography (dichloromethane – methanol, gradient 100:0 \rightarrow 98:2) to yield the desired aniline reagents **3a-3f**.

4.1.1. methyl 8-((2-aminophenyl)amino)-8-oxooctanoate (3a). Light-brown solid; 69% yield; mp 81.7 $^\circ\text{C}$; ^1H NMR (400 MHz, Chloroform-*d*) δ 7.40 (d, J = 12.0 Hz, 1H), 7.19 – 7.12 (m, 1H), 7.04 (td, J = 7.7, 1.4 Hz, 1H), 6.81 – 6.73 (m, 2H), 3.66 (s, 3H), 2.39 – 2.27 (m, 4H), 1.77 – 1.57 (m, 4H), 1.43 – 1.29 (m, 4H). ^{13}C NMR (101 MHz, CDCl_3) δ 174.26, 171.85, 140.74, 127.14, 125.27, 124.40, 119.54,

118.23, 51.53, 36.78, 33.95, 28.81, 28.74, 25.56, 24.70. ESI-HRMS m/z calcd for $C_{15}H_{23}N_2O_3^+$ 279.1703, found 279.1703 $[M + H]^+$. HPLC purity 97%.

4.1.2. methyl 8-((3-aminophenyl)amino)-8-oxooctanoate (3b). Yellow oil; 78% yield; 1H NMR (400 MHz, Chloroform- d) δ 7.52 – 7.41 (m, 1H), 7.17 (t, J = 2.2 Hz, 1H), 7.04 (t, J = 8.0 Hz, 1H), 6.67 (dd, J = 7.9, 2.1 Hz, 1H), 6.40 (dd, J = 8.2, 2.1 Hz, 1H), 3.65 (s, 3H), 2.32 – 2.26 (m, 4H), 1.65 (dt, J = 30.0, 7.1 Hz, 4H), 1.40 – 1.28 (m, 4H). ^{13}C NMR (101 MHz, $CDCl_3$) δ 174.31, 171.42, 147.22, 139.08, 129.63, 110.90, 109.63, 106.56, 51.53, 37.63, 33.96, 28.78, 28.76, 25.38, 24.71. ESI-HRMS m/z calcd for $C_{15}H_{23}N_2O_3^+$ 279.1703, found 279.1705 $[M + H]^+$. HPLC purity 96%.

4.1.3. methyl 6-((4-aminophenyl)amino)-6-oxohexanoate (3c). Grey solid; 39% yield; mp 70.7 °C; 1H NMR (400 MHz, Chloroform- d) δ 7.26 – 7.20 (m, 2H), 6.59 (dt, J = 8.8, 2.0 Hz, 2H), 3.65 (s, 3H), 2.35 – 2.23 (m, 4H), 1.74 – 1.61 (m, 4H). ^{13}C NMR (101 MHz, $CDCl_3$) δ 174.14, 170.90, 143.28, 129.35, 122.14, 115.34, 51.63, 36.86, 33.71, 25.08, 24.39. ESI-HRMS m/z calcd for $C_{13}H_{19}N_2O_3^+$ 251.1390, found 251.1390 $[M + H]^+$. HPLC purity 97%.

4.1.4. methyl 7-((4-aminophenyl)amino)-7-oxoheptanoate (3d). Grey solid; 77% yield; mp 80.3 °C; 1H NMR (400 MHz, Chloroform- d) δ 7.26 – 7.19 (m, 2H), 6.62 – 6.54 (m, 2H), 3.63 (s, 3H), 3.57 (br, 2H), 2.33 – 2.21 (m, 4H), 1.74 – 1.55 (m, 4H), 1.39 – 1.29 (m, 2H). ^{13}C NMR (101 MHz, $CDCl_3$) δ 174.28, 171.23, 143.18, 129.42, 122.08, 115.37, 51.56, 37.05, 33.84, 28.65, 25.32, 24.55. ESI-HRMS m/z calcd for $C_{14}H_{21}N_2O_3^+$ 265.1547, found 265.1546 $[M + H]^+$. HPLC purity 95%.

4.1.5. methyl 8-((4-aminophenyl)amino)-8-oxooctanoate(3e). Off-white solid; 63% yield; mp 77.6 °C; 1H NMR (400 MHz, DMSO- d_6) δ 9.42 (s, 1H), 7.19 (d, J = 8.5 Hz, 2H), 6.47 (d, J = 8.5 Hz, 2H), 4.82 (s, 2H), 3.57 (s, 3H), 2.29 (t, J = 7.4 Hz, 2H), 2.19 (t, J = 7.4 Hz, 2H), 1.53 (h, J = 7.4 Hz, 4H), 1.35 – 1.19 (m, 4H). ^{13}C NMR (101 MHz, DMSO- d_6) δ 173.82, 170.64, 144.98, 129.04, 121.31, 114.22, 51.62, 36.60, 33.69, 28.83, 28.72, 25.61, 24.80. ESI-HRMS m/z calcd for $C_{15}H_{23}N_2O_3^+$ 279.1703, found 279.1704 $[M + H]^+$. HPLC purity 99%.

4.1.6. methyl 9-((4-aminophenyl)amino)-9-oxononanoate(3f). Reddish solid; 80% yield; mp 93.7 °C; 1H NMR (400 MHz, Chloroform- d) δ 7.23 (d, J = 8.2 Hz, 2H), 6.57 (d, J = 7.4 Hz, 2H), 3.63 (s,

3H), 2.31 – 2.19 (m, 4H), 1.68 – 1.50 (m, 4H), 1.34 – 1.24 (m, 6H). ^{13}C NMR (101 MHz, CDCl_3) δ 174.41, 171.45, 143.20, 129.46, 122.02, 115.31, 51.52, 37.37, 34.03, 29.03, 28.97, 28.92, 25.67, 24.85. ESI-HRMS m/z calcd for $\text{C}_{16}\text{H}_{25}\text{N}_2\text{O}_3^+$ 293.1860, found 293.1861 $[\text{M} + \text{H}]^+$. HPLC purity 98%.

General Procedure for the Synthesis of 5a-f. To a suspension of 2-chloro-7-cyclopentyl-N,N-dimethyl-7H-pyrrolo[2,3-d]pyrimidine-6-carboxamide (**4**) (586 mg, 2 mmol, 1 equiv) in 20 mL 1,4-dioxane was added compound **3a-f** (2 mmol, 1 equiv), $\text{Pd}(\text{OAc})_2$ (11 mg, 0.05 mmol, 0.25 equiv), BINAP (62 mg, 0.1 mmol, 0.05 equiv) and Cs_2CO_3 (1.37 g, 4.2 mmol, 2.1 equiv) and the flask was purged with N_2 . Then the flask was sealed and the mixture was heated for 12 h at 100 °C. The reaction was cooled to room temperature, and the solvent was removed under reduced pressure. The residue was purified by silica gel column chromatography (dichloromethane – methanol, gradient 100:0 \rightarrow 96:4) to obtain the desired product **5a-f**.

4.1.7. methyl 8-((2-((7-cyclopentyl-6-(dimethylcarbamoyl)-7H-pyrrolo[2,3-d]pyrimidin-2-yl)amino) phenyl)amino)-8-oxooctanoate (5a). White solid; 83% yield; mp 52.1 °C; ^1H NMR (400 MHz, Chloroform-*d*) δ 8.59 (s, 1H), 8.10 (s, 1H), 7.85 – 7.79 (m, 1H), 7.65 – 7.57 (m, 1H), 7.38 (s, 1H), 7.15 (dq, J = 6.8, 4.1, 2.6 Hz, 2H), 6.38 (s, 1H), 4.78 – 4.61 (m, 1H), 3.63 (s, 3H), 3.12 (s, 6H), 2.36 – 2.19 (m, 6H), 2.02 – 1.91 (m, 2H), 1.88 – 1.76 (m, 2H), 1.70 – 1.46 (m, 6H), 1.36 – 1.20 (m, 4H). ^{13}C NMR (101 MHz, CDCl_3) δ 174.19, 171.76, 164.71, 163.98, 156.81, 152.36, 151.77, 132.08, 131.84, 131.74, 125.19, 124.63, 124.08, 112.52, 100.86, 57.62, 51.45, 37.35, 33.95, 30.61, 28.79, 28.74, 25.39, 24.86, 24.69. ESI-HRMS m/z calcd for $\text{C}_{29}\text{H}_{39}\text{N}_6\text{O}_4^+$ 535.3027, found 535.3030 $[\text{M} + \text{H}]^+$. HPLC purity 99%.

4.1.8. methyl 8-((3-((7-cyclopentyl-6-(dimethylcarbamoyl)-7H-pyrrolo[2,3-d]pyrimidin-2-yl)amino) phenyl)amino)-8-oxooctanoate (5b). White solid; 84% yield; mp 128.5 °C; ^1H NMR (400 MHz, Chloroform-*d*) δ 8.63 (s, 1H), 7.83 (s, 1H), 7.56 – 7.45 (m, 3H), 7.23 (t, J = 8.1 Hz, 1H), 7.16 (d, J = 8.1 Hz, 1H), 6.40 (s, 1H), 4.91 – 4.70 (m, 1H), 3.64 (s, 3H), 3.13 (s, 6H), 2.60 – 2.45 (m, 2H), 2.36 – 2.24 (m, 4H), 2.11 – 1.92 (m, 4H), 1.76 – 1.55 (m, 6H), 1.42 – 1.28 (m, 4H). ^{13}C NMR (101 MHz, CDCl_3) δ

174.24, 171.26, 164.16, 155.40, 152.09, 151.57, 140.75, 138.57, 131.88, 129.18, 114.52, 113.27, 112.39, 110.05, 101.00, 57.73, 51.50, 37.58, 33.97, 30.26, 28.82, 28.79, 25.34, 24.71, 24.69. ESI-HRMS m/z calcd for $C_{29}H_{39}N_6O_4^+$ 535.3027, found 535.3030 $[M + H]^+$. HPLC purity 97%.

4.1.9.**Methyl**

6-((4-((7-cyclopentyl-6-(dimethylcarbamoyl)-7H-pyrrolo[2,3-d]pyrimidin-2-yl)amino)phenyl)amino)-6-oxohexanoate (5c). White solid; 89% yield; mp 164.9 °C; 1H NMR (400 MHz, Chloroform- d) δ 8.51 (s, 1H), 8.20 (s, 1H), 7.96 (s, 1H), 7.51 (d, J = 8.4 Hz, 2H), 7.25 (d, J = 8.0 Hz, 2H), 6.29 (s, 1H), 4.64 (q, J = 8.8 Hz, 1H), 3.63 (s, 3H), 3.11 (s, 6H), 2.57 – 2.46 (m, 2H), 2.33 (t, J = 6.7 Hz, 4H), 2.04 – 1.91 (m, 4H), 1.78 – 1.57 (m, 6H). ^{13}C NMR (101 MHz, $CDCl_3$) δ 174.04, 170.89, 164.46, 155.43, 151.97, 151.48, 136.69, 131.95, 131.42, 120.99, 118.87, 112.02, 100.88, 57.99, 51.58, 36.87, 33.74, 30.07, 25.10, 24.60, 24.44. ESI-HRMS m/z calcd for $C_{27}H_{35}N_6O_4^+$ 507.2714, found 507.2714 $[M + H]^+$. HPLC purity 99%.

4.1.10.**methyl**

7-((4-((7-cyclopentyl-6-(dimethylcarbamoyl)-7H-pyrrolo[2,3-d]pyrimidin-2-yl)amino)phenyl)amino)-7-oxoheptanoate (5d). White solid; 73% yield; mp 151.7 °C; 1H NMR (400 MHz, Chloroform- d) δ 8.54 (s, 1H), 8.07 (s, 1H), 7.82 (s, 1H), 7.54 (d, J = 8.4 Hz, 2H), 7.30 (d, J = 8.4 Hz, 2H), 6.32 (s, 1H), 4.66 (p, J = 8.9 Hz, 1H), 3.64 (s, 3H), 3.13 (s, 6H), 2.59 – 2.44 (m, 2H), 2.35 – 2.27 (m, 4H), 2.03 – 1.96 (m, 4H), 1.76 – 1.63 (m, 6H), 1.47 – 1.32 (m, 2H). ^{13}C NMR (101 MHz, $CDCl_3$) δ 174.19, 171.19, 164.40, 155.47, 151.99, 151.56, 136.65, 132.03, 131.46, 120.87, 118.90, 112.06, 100.91, 57.97, 51.52, 37.10, 33.84, 30.08, 28.70, 25.29, 24.61, 24.57. ESI-HRMS m/z calcd for $C_{28}H_{37}N_6O_4^+$ 521.2871, found 521.2872 $[M + H]^+$. HPLC purity 99%.

4.1.11.**methyl**

8-((4-((7-cyclopentyl-6-(dimethylcarbamoyl)-7H-pyrrolo[2,3-d]pyrimidin-2-yl)amino)phenyl)amino)-8-oxooctanoate (5e). White solid; 82% yield; mp 171.0 °C; 1H NMR (400 MHz, Chloroform- d) δ 8.57 (s, 1H), 7.77 (s, 1H), 7.65 – 7.53 (m, 3H), 7.37 (d, J = 8.4 Hz, 2H), 6.36 (s, 1H), 4.70 (p, J = 8.9 Hz, 1H), 3.65 (s, 3H), 3.14 (s, 6H), 2.55 (t, J = 10.7 Hz, 2H), 2.31 (dt, J = 11.1, 7.5 Hz,

5H), 2.08 – 1.93 (m, 5H), 1.77 – 1.57 (m, 4H), 1.36 (dq, $J = 8.6, 4.5$ Hz, 4H). ^{13}C NMR (101 MHz, DMSO- d_6) δ 173.76, 171.13, 163.38, 156.04, 152.52, 151.74, 136.78, 133.41, 131.79, 119.80, 118.91, 111.73, 101.18, 57.41, 51.58, 36.71, 35.03, 33.68, 30.03, 28.84, 28.72, 25.49, 24.79, 24.65. ESI-HRMS m/z calcd for $\text{C}_{29}\text{H}_{39}\text{N}_6\text{O}_4^+$ 535.3027, found 535.3031 $[\text{M} + \text{H}]^+$. HPLC purity 99%.

4.1.12.

methyl

9-((4-((7-cyclopentyl-6-(dimethylcarbamoyl)-7H-pyrrolo[2,3-d]pyrimidin-2-yl)amino)phenyl)amino)-9-oxononanoate (5f). White solid; 73% yield; mp 139.8 °C; ^1H NMR (400 MHz, Chloroform- d) δ 8.58 (s, 1H), 7.68 (s, 1H), 7.59 (d, $J = 8.5$ Hz, 2H), 7.54 (s, 1H), 7.40 (d, $J = 8.4$ Hz, 2H), 6.37 (s, 1H), 4.71 (t, $J = 8.9$ Hz, 1H), 3.65 (s, 3H), 3.14 (s, 6H), 2.69 – 2.41 (m, 2H), 2.40 – 2.24 (m, 4H), 2.11 – 1.95 (m, 4H), 1.80 – 1.51 (m, 6H), 1.42 – 1.24 (m, 6H). ^{13}C NMR (101 MHz, CDCl_3) δ 174.34, 171.30, 164.30, 155.44, 152.09, 151.49, 136.57, 132.22, 131.70, 120.75, 119.05, 112.18, 100.99, 57.99, 51.51, 37.54, 34.07, 30.16, 29.09, 29.00, 28.96, 25.61, 24.89, 24.67. ESI-HRMS m/z calcd for $\text{C}_{30}\text{H}_{41}\text{N}_6\text{O}_4^+$ 549.3184, found 549.3179 $[\text{M} + \text{H}]^+$. HPLC purity 99%.

General Procedure for the Synthesis of 6a-f. To a stirred solution of the compound **5a-f** (1 mmol,) in methanol (20 mL) was added a solution of hydroxylamine (50% in water, 5.5 mL). The resulting solution was stirred for 18 h under reflux. Then the solvent was removed under vacuum and the crude residue purified by chromatography on a silica gel column (dichloromethane – methanol, gradient 100:0 → 90:10) to obtain the desired hydroxamic acids **6a-f**.

4.1.13.

N1-(2-((7-cyclopentyl-6-(dimethylcarbamoyl)-7H-pyrrolo[2,3-d]pyrimidin-2-yl)amino)phenyl) -N8-hydroxyoctanediamide (6a). White solid; 62% yield; mp 166.9 °C (decompose); ^1H NMR (400 MHz, DMSO- d_6) δ 9.72 (s, 1H), 8.71 (s, 1H), 8.37 (s, 1H), 7.99 (d, $J = 8.1$ Hz, 1H), 7.39 (d, $J = 7.9$ Hz, 1H), 7.23 – 7.12 (m, 1H), 7.04 (t, $J = 7.6$ Hz, 1H), 6.56 (s, 1H), 4.67 (p, $J = 8.7$ Hz, 1H), 3.04 (s, 6H), 2.50 (t, $J = 2.0$ Hz, 1H), 2.41 – 2.22 (m, 4H), 1.92 (t, $J = 7.3$ Hz, 4H), 1.86 – 1.78 (m, 2H), 1.64 – 1.40 (m, 6H), 1.34 – 1.20 (m, 4H). ^{13}C NMR (101 MHz, DMSO- d_6) δ 172.44, 169.48, 163.33, 156.20, 152.67, 151.74, 133.77, 132.12, 129.65, 125.37, 123.31, 123.17, 112.33, 100.97, 57.11, 36.30, 35.05, 32.72, 30.53, 28.89, 28.79, 25.70, 25.51, 24.95. ESI-HRMS m/z calcd for

$C_{28}H_{38}N_7O_4^+$ 536.2980, found 536.2985 $[M + H]^+$. HPLC purity 98%.

4.1.14.

N1-((7-cyclopentyl-6-(dimethylcarbamoyl)-7H-pyrrolo

[2,3-d]pyrimidin-2-yl)amino)phenyl) -N8-hydroxyoctanediamide (6b). White solid; 49% yield; mp 176.2 °C (decompose); 1H NMR (400 MHz, DMSO- d_6) δ 10.36 (s, 1H), 9.78 (s, 1H), 9.48 (s, 1H), 8.73 (s, 1H), 8.69 (s, 1H), 8.08 (s, 1H), 7.54 – 7.43 (m, 1H), 7.17 (t, J = 8.0 Hz, 1H), 7.07 (d, J = 8.0 Hz, 1H), 6.57 (s, 1H), 4.86 (p, J = 8.9 Hz, 1H), 3.14 – 2.96 (m, 6H), 2.41 – 2.24 (m, 4H), 2.01 – 1.81 (m, 6H), 1.67 – 1.53 (m, 4H), 1.48 (q, J = 7.1 Hz, 2H), 1.35 – 1.19 (m, 4H). ^{13}C NMR (101 MHz, DMSO- d_6) δ 171.41, 169.54, 163.53, 156.14, 152.38, 151.85, 141.60, 139.81, 131.86, 128.70, 114.17, 113.01, 111.81, 110.66, 101.13, 56.88, 36.79, 32.72, 30.38, 28.95, 28.93, 25.53, 24.67. ESI-HRMS m/z calcd for $C_{28}H_{38}N_7O_4^+$ 536.2980, found 536.2988 $[M + H]^+$. HPLC purity 97%.

4.1.15.

N1-4-((7-cyclopentyl-6-(dimethylcarbamoyl)-7H-pyrrolo

[2,3-d]pyrimidin-2-yl)amino)phenyl) -N6-hydroxyadipamide (6c). White solid; 48% yield; mp 211.9 °C (decompose); 1H NMR (400 MHz, DMSO- d_6) δ 10.38 (s, 1H), 9.77 (s, 1H), 9.45 (s, 1H), 8.78 – 8.63 (m, 2H), 7.74 (d, J = 8.5 Hz, 2H), 7.51 (d, J = 8.5 Hz, 2H), 6.57 (s, 1H), 4.72 (t, J = 8.8 Hz, 1H), 3.05 (s, 6H), 2.49 – 2.40 (m, 2H), 2.33 – 2.22 (m, 2H), 2.04 – 1.89 (m, 6H), 1.72 – 1.61 (m, 2H), 1.60 – 1.46 (m, 4H). ^{13}C NMR (101 MHz, DMSO- d_6) δ 170.66, 169.11, 163.06, 155.71, 152.24, 151.41, 136.47, 133.05, 131.51, 119.49, 118.61, 111.42, 100.85, 57.07, 36.25, 34.75, 32.34, 29.71, 25.07, 24.33. ESI-HRMS m/z calcd for $C_{26}H_{34}N_7O_4^+$ 508.2667, found 508.2671 $[M + H]^+$. HPLC purity 96%.

4.1.16.

N1-4-((7-cyclopentyl-6-(dimethylcarbamoyl)-7H-pyrrolo

[2,3-d]pyrimidin-2-yl)amino)phenyl) -N7-hydroxyheptanediamide (6d). White solid; 57% yield; mp 180.7 °C (decompose); 1H NMR (400 MHz, DMSO- d_6) δ 10.36 (s, 1H), 9.76 (s, 1H), 9.46 (s, 1H), 8.72 (s, 1H), 8.71 – 8.67 (m, 1H), 7.74 (d, J = 8.8 Hz, 2H), 7.51 (d, J = 8.7 Hz, 2H), 6.56 (s, 1H), 4.72 (p, J = 8.9 Hz, 1H), 3.16 – 2.95 (m, 6H), 2.49 – 2.39 (m, 2H), 2.27 (t, J = 7.3 Hz, 2H), 2.03 – 1.88 (m, 6H), 1.72 – 1.46 (m, 6H), 1.34 – 1.21 (m, 2H). ^{13}C NMR (101 MHz, DMSO- d_6) δ 171.08, 169.51, 163.37, 156.02, 152.56, 151.72, 136.76, 133.39, 131.81, 119.78, 118.91, 111.73, 101.19, 57.39, 36.63, 32.63, 30.03, 28.76, 25.43, 25.39, 24.65. ESI-HRMS m/z calcd for $C_{27}H_{36}N_7O_4^+$ 522.2823, found 522.2825 $[M$

+ H]⁺. HPLC purity 98%.

4.1.17.

N₁-(4-((7-cyclopentyl-6-(dimethylcarbamoyl)-7H-pyrrolo

[2,3-d]pyrimidin-2-yl)amino)phenyl) -N8-hydroxyoctanediamide (6e). White solid; 76% yield; mp 182.7 °C (decompose); ¹H NMR (400 MHz, DMSO-d₆) δ 10.33 (s, 1H), 9.73 (s, 1H), 9.42 (s, 1H), 8.71 (s, 1H), 8.66 (s, 1H), 7.79 – 7.65 (m, 2H), 7.58 – 7.46 (m, 2H), 6.56 (s, 1H), 4.80 – 4.62 (m, 1H), 3.05 (s, 6H), 2.50 – 2.39 (m, 2H), 2.27 (t, *J* = 7.4 Hz, 2H), 2.03 – 1.89 (m, 6H), 1.70 – 1.45 (m, 6H), 1.35 – 1.22 (m, 4H). ¹³C NMR (101 MHz, DMSO-d₆) δ 171.15, 169.57, 163.42, 156.05, 152.53, 151.76, 136.77, 133.41, 131.86, 119.83, 118.96, 111.75, 101.15, 57.40, 36.75, 32.73, 30.05, 28.94, 28.89, 25.57, 25.52, 24.65. ESI-HRMS *m/z* calcd for C₂₈H₃₈N₇O₄⁺ 536.2980, found 536.2985 [M + H]⁺. HPLC purity 98%.

4.1.18.

N₁-(4-((7-cyclopentyl-6-(dimethylcarbamoyl)-7H-pyrrolo

[2,3-d]pyrimidin-2-yl)amino)phenyl) -N9-hydroxynonanediamide (6f). White solid; 49% yield; mp 185.5 °C (decompose); ¹H NMR (400 MHz, DMSO-d₆) δ 10.36 (s, 1H), 9.75 (s, 1H), 9.46 (s, 1H), 8.71 (s, 1H), 8.69 (s, 1H), 7.74 (d, *J* = 8.5 Hz, 2H), 7.51 (d, *J* = 8.5 Hz, 2H), 6.56 (s, 1H), 4.72 (p, *J* = 8.9 Hz, 1H), 3.05 (t, *J* = 6.8 Hz, 6H), 2.49 – 2.40 (m, 2H), 2.27 (t, *J* = 7.4 Hz, 2H), 2.05 – 1.87 (m, 6H), 1.69 – 1.42 (m, 6H), 1.33 – 1.18 (m, 6H). ¹³C NMR (101 MHz, DMSO-d₆) δ 171.18, 169.58, 163.38, 156.02, 152.55, 151.72, 136.76, 133.40, 131.81, 119.80, 118.93, 111.73, 101.19, 65.38, 57.39, 36.78, 32.72, 30.03, 29.10, 29.02, 28.95, 25.64, 25.58, 24.65. ESI-HRMS *m/z* calcd for C₂₉H₄₀N₇O₄⁺ 550.3136, found 550.3141 [M + H]⁺. HPLC purity 97%.

General Procedure for the Synthesis of 9a-9d.

The title compound was prepared from **7a-7d** (14.6 mmol, 1 equiv), 4-aminobenzoic acid (**8**) (2 g, 14.6 mmol, 1 equiv), EDCI (4.2 g, 21.9 mmol, 1.5 equiv), HOBt (2.37 g, 17.52 mmol, 1.2 equiv), DIEA (5.06 g, 43.8 mmol, 3 equiv) and DMF (30 mL) using the procedure described for compound **3a-3f** to obtain the desired product **9a-9d**.

4.1.19. methyl 5-(4-aminobenzamido)pentanoate (9a). Light-brown oil; 63% yield; ¹H NMR (400 MHz, Chloroform-*d*) δ 7.66 – 7.56 (m, 2H), 6.69 – 6.61 (m, 2H), 6.21 (s, 1H), 3.66 (s, 3H), 3.41 (q, *J* =

6.6 Hz, 2H), 2.36 (t, $J = 7.1$ Hz, 2H), 1.76 – 1.52 (m, 4H). ^{13}C NMR (101 MHz, CDCl_3) δ 174.10, 167.28, 149.44, 128.60, 124.22, 114.17, 51.63, 39.34, 33.53, 29.15, 22.12. ESI-HRMS m/z calcd for $\text{C}_{13}\text{H}_{19}\text{N}_2\text{O}_3^+$ 251.1390, found 251.1395 $[\text{M} + \text{H}]^+$. HPLC purity 99%.

4.1.20. methyl 6-(4-aminobenzamido)hexanoate (9b). Light-brown solid; 66% yield; mp 118.3°C; ^1H NMR (400 MHz, DMSO-d_6) δ 7.97 (t, $J = 5.5$ Hz, 1H), 7.67 – 7.48 (m, 2H), 6.62 – 6.47 (m, 2H), 5.57 (s, 2H), 3.57 (s, 3H), 3.18 (q, $J = 6.6$ Hz, 2H), 2.29 (t, $J = 7.2$ Hz, 2H), 1.50 (dp, $J = 23.1$, 7.5 Hz, 4H), 1.28 (td, $J = 8.6$, 4.1 Hz, 2H). ^{13}C NMR (101 MHz, DMSO-d_6) δ 173.30, 166.08, 151.39, 128.57, 121.40, 112.46, 51.11, 38.71, 33.20, 29.03, 25.94, 24.20. ESI-HRMS m/z calcd for $\text{C}_{14}\text{H}_{21}\text{N}_2\text{O}_3^+$ 265.1547, found 265.1550 $[\text{M} + \text{H}]^+$. HPLC purity 99%.

4.1.21. methyl 7-(4-aminobenzamido)heptanoate (9c). Light-brown solid; 87% yield; mp 95.8 °C; ^1H NMR (400 MHz, Chloroform-d) δ 7.57 (dd, $J = 8.5$, 2.4 Hz, 2H), 6.72 – 6.49 (m, 2H), 6.40 – 6.05 (m, 1H), 4.03 (s, 2H), 3.63 (s, 3H), 3.40 – 3.27 (m, 2H), 2.35 – 2.22 (m, 2H), 1.56 (dp, $J = 15.5$, 7.4 Hz, 4H), 1.41 – 1.24 (m, 4H). ^{13}C NMR (101 MHz, CDCl_3) δ 174.27, 167.38, 149.62, 128.59, 124.09, 114.09, 51.50, 39.79, 33.96, 29.58, 28.78, 26.61, 24.79. ESI-HRMS m/z calcd for $\text{C}_{15}\text{H}_{23}\text{N}_2\text{O}_3^+$ 279.1703, found 279.1704 $[\text{M} + \text{H}]^+$. HPLC purity 99%.

4.1.22. methyl 8-(4-aminobenzamido)octanoate (9d). Light-brown solid; 73% yield; mp 59.6 °C; ^1H NMR (400 MHz, Chloroform-d) δ 7.62 – 7.55 (m, 2H), 6.63 (dd, $J = 8.7$, 2.4 Hz, 2H), 3.64 (s, 3H), 3.37 (td, $J = 7.2$, 5.8 Hz, 2H), 2.28 (t, $J = 7.5$ Hz, 2H), 1.58 (dt, $J = 14.2$, 7.2 Hz, 4H), 1.37 – 1.27 (m, 6H). ^{13}C NMR (101 MHz, CDCl_3) δ 174.31, 167.26, 149.36, 128.56, 124.36, 114.18, 51.49, 39.87, 34.03, 29.73, 29.01, 28.95, 26.80, 24.83. ESI-HRMS m/z calcd for $\text{C}_{16}\text{H}_{25}\text{N}_2\text{O}_3^+$ 293.1860, found 293.1856 $[\text{M} + \text{H}]^+$. HPLC purity 95%.

General Procedure for the Synthesis of 10a-10d.

The title compound was prepared from **9a-9d** (2 mmol, 1 equiv), compound **4** (586 mg, 2 mmol, 1 equiv), $\text{Pd}(\text{OAc})_2$ (11 mg, 0.05 mmol, 0.025 equiv), BINAP (62 mg, 0.1 mmol, 0.05 equiv) and Cs_2CO_3 (1.37 g, 4.2 mmol, 2.1 equiv) and 1,4-dioxane (20 mL) using the procedure described for compound **5a-5f** to obtain the desired product **10a-10d**.

4.1.23. methyl 5-(4-((7-cyclopentyl-6-(dimethylcarbamoyl)-7H-pyrrolo[2,3-d]pyrimidin-2-yl)amino) benzamido)pentanoate (10a). White solid; 77% yield; mp 195.0 °C; ¹H NMR (400 MHz, DMSO-*d*₆) δ 9.81 (s, 1H), 8.79 (s, 1H), 8.29 (t, *J* = 5.7 Hz, 1H), 7.97 – 7.88 (m, 2H), 7.84 – 7.73 (m, 2H), 6.61 (s, 1H), 4.86 – 4.66 (m, 1H), 3.58 (s, 3H), 3.25 (q, *J* = 6.2 Hz, 2H), 3.06 (s, 6H), 2.50 – 2.42 (m, 2H), 2.35 (t, *J* = 6.9 Hz, 2H), 2.07 – 1.95 (m, 4H), 1.74 – 1.63 (m, 2H), 1.62 – 1.48 (m, 4H). ¹³C NMR (101 MHz, DMSO-*d*₆) δ 173.75, 166.17, 163.32, 155.52, 152.53, 151.49, 144.04, 132.53, 128.23, 126.89, 117.36, 112.41, 101.05, 57.51, 51.63, 40.01, 39.10, 33.45, 30.39, 30.11, 29.22, 24.66, 22.48. ESI-HRMS *m/z* calcd for C₂₇H₃₅N₆O₄⁺ 507.2714, found 507.2720 [M + H]⁺. HPLC purity 99%.

4.1.24. methyl 6-(4-((7-cyclopentyl-6-(dimethylcarbamoyl)-7H-pyrrolo[2,3-d]pyrimidin-2-yl)amino) benzamido)hexanoate (10b). White solid; 84% yield; mp 190.1 °C; ¹H NMR (400 MHz, Chloroform-*d*) δ 8.66 (s, 1H), 7.79 – 7.73 (m, 4H), 7.71 (s, br, 1H), 6.44 (s, 1H), 6.30 – 6.22 (m, 1H), 4.85 – 4.67 (m, 1H), 3.65 (s, 3H), 3.46 (q, *J* = 6.7 Hz, 2H), 3.15 (s, 6H), 2.68 – 2.49 (m, 2H), 2.33 (t, *J* = 7.4 Hz, 2H), 2.15 – 1.98 (m, 4H), 1.80 – 1.58 (m, 6H), 1.50 – 1.35 (m, 2H). ¹³C NMR (101 MHz, CDCl₃) δ 174.14, 167.07, 163.94, 154.73, 151.78, 151.49, 143.09, 132.40, 127.87, 127.27, 117.45, 112.79, 100.89, 58.05, 51.56, 39.71, 33.88, 30.14, 29.42, 26.45, 24.66, 24.49. ESI-HRMS *m/z* calcd for C₂₈H₃₇N₆O₄⁺ 521.2871, found 521.2873 [M + H]⁺. HPLC purity 99%.

4.1.25. methyl 7-(4-((7-cyclopentyl-6-(dimethylcarbamoyl)-7H-pyrrolo[2,3-d]pyrimidin-2-yl)amino) benzamido)heptanoate (10c). White solid; 76% yield; mp 87.2 °C; ¹H NMR (400 MHz, Chloroform-*d*) δ 8.65 (s, 1H), 7.90 (d, *J* = 9.5 Hz, 1H), 7.74 (s, 4H), 6.42 (s, 1H), 6.29 (q, *J* = 5.4 Hz, 1H), 4.83 – 4.68 (m, 1H), 3.64 (s, 3H), 3.42 (q, *J* = 6.8 Hz, 2H), 3.14 (s, 6H), 2.64 – 2.51 (m, 2H), 2.29 (t, *J* = 7.5 Hz, 2H), 2.10 – 1.99 (m, 4H), 1.73 – 1.57 (m, 6H), 1.43 – 1.29 (m, 4H). ¹³C NMR (101 MHz, CDCl₃) δ 174.23, 167.11, 163.96, 154.80, 151.76, 151.52, 143.12, 132.33, 127.84, 127.29, 117.46, 112.75, 100.89, 58.04, 51.52, 39.90, 33.96, 30.13, 29.59, 28.79, 26.63, 24.80, 24.65. ESI-HRMS *m/z* calcd for C₂₉H₃₉N₆O₄⁺ 535.3027, found 535.3029 [M + H]⁺. HPLC purity 99%.

4.1.26. methyl 8-(4-((7-cyclopentyl-6-(dimethylcarbamoyl)-7H-pyrrolo

[2,3-d]pyrimidin-2-yl)amino) benzamido)octanoate (10d). White solid; 78% yield; mp 166.2 °C; ¹H NMR (400 MHz, Chloroform-*d*) δ 8.65 (d, *J* = 3.2 Hz, 1H), 7.82 – 7.65 (m, 4H), 6.43 (d, *J* = 4.8 Hz, 1H), 4.91 – 4.53 (m, 1H), 3.65 (s, 3H), 3.52 – 3.32 (m, 2H), 3.15 (s, 6H), 2.67 – 2.50 (m, 2H), 2.36 – 2.24 (m, 2H), 2.15 – 1.98 (m, 4H), 1.70 (t, *J* = 6.1 Hz, 2H), 1.67 – 1.54 (m, 4H), 1.41 – 1.25 (m, 6H). ¹³C NMR (101 MHz, CDCl₃) δ 174.30, 167.09, 163.96, 154.74, 151.78, 151.52, 143.05, 132.40, 127.85, 127.36, 117.46, 112.79, 100.89, 58.04, 51.51, 40.00, 34.03, 30.14, 29.73, 29.03, 28.96, 26.82, 24.83, 24.66. ESI-HRMS *m/z* calcd for C₃₀H₄₁N₆O₄⁺ 549.3184, found 549.3189 [M + H]⁺. HPLC purity 99%.

General Procedure for the Synthesis of 11a-11d.

The title compound was prepared from **10a-10d** (2 mmol, 1 equiv), solution of hydroxylamine (50% in water, 10 mL). and CH₃OH (20 mL) using the procedure described for compound **6a-6f** to obtain the desired product **11a-11d**.

4.1.27.

7-cyclopentyl-2-((4-((5-(hydroxyamino)-5-oxopentyl)

carbamoyl)phenyl)amino)-N,N-dimethyl -7H-pyrrolo[2,3-d]pyrimidine-6-carboxamide (11a).

White solid; 62% yield; mp 189.0 °C (decompose); ¹H NMR (400 MHz, DMSO-*d*₆) δ 10.38 (s, 1H), 9.83 (s, 1H), 8.79 (s, 1H), 8.70 (s, 1H), 8.31 (t, *J* = 5.7 Hz, 1H), 7.92 (d, *J* = 8.4 Hz, 2H), 7.82 (d, *J* = 8.5 Hz, 2H), 6.60 (s, 1H), 5.75 (s, 1H), 4.83 – 4.63 (m, 1H), 3.25 (q, *J* = 6.2 Hz, 2H), 3.12 – 2.95 (m, 6H), 2.51 – 2.43 (m, 2H), 2.10 – 1.92 (m, 6H), 1.76 – 1.60 (m, 2H), 1.62 – 1.43 (m, 4H). ¹³C NMR (101 MHz, DMSO-*d*₆) δ 169.51, 166.16, 163.31, 155.51, 152.54, 151.48, 144.03, 132.51, 128.25, 126.89, 117.35, 112.40, 101.07, 57.51, 55.37, 35.09, 32.54, 30.10, 29.46, 24.66, 23.28. ESI-HRMS *m/z* calcd for C₂₆H₃₄N₇O₄⁺ 508.2667, found 508.2671 [M + H]⁺. HPLC purity 98%.

4.1.28.

7-cyclopentyl-2-((4-((6-(hydroxyamino)-6-oxohexyl)

carbamoyl)phenyl)amino)-N,N-dimethyl -7H-pyrrolo[2,3-d]pyrimidine-6-carboxamide (11b).

White solid; 62% yield; mp 94.5 °C (decompose); ¹H NMR (400 MHz, DMSO-*d*₆) δ 10.36 (s, 1H), 9.84 (s, 1H), 8.79 (s, 1H), 8.69 (s, 1H), 8.30 (t, *J* = 5.8 Hz, 1H), 7.99 – 7.76 (m, 4H), 6.61 (s, 1H), 4.75 (p, *J* = 8.9 Hz, 1H), 3.23 (q, *J* = 6.7 Hz, 2H), 3.06 (s, 6H), 2.50 – 2.40 (m, 2H), 2.09 – 1.88 (m, 6H), 1.77 – 1.63 (m, 2H), 1.56 – 1.42 (m, 4H), 1.37 – 1.23 (m, 2H). ¹³C NMR (101 MHz, DMSO-*d*₆) δ 169.52,

166.10, 163.29, 155.50, 152.56, 151.46, 144.01, 132.49, 128.24, 126.89, 117.32, 112.38, 101.09, 57.50, 35.11, 32.72, 30.09, 29.58, 27.85, 26.64, 25.43, 24.66. ESI-HRMS m/z calcd for $C_{27}H_{36}N_7O_4^+$ 522.2823, found 522.2831 $[M + H]^+$. HPLC purity 98%.

4.1.29.

7-cyclopentyl-2-((4-((7-(hydroxyamino)-7-oxoheptyl)

carbamoyl)phenyl)amino)-N,N-dimethyl -7H-pyrrolo[2,3-d]pyrimidine-6-carboxamide (11c).

White solid; 58% yield; mp 112.2°C (decompose); 1H NMR (400 MHz, DMSO- d_6) δ 10.36 (s, 1H), 9.85 (s, 1H), 8.79 (s, 1H), 8.29 (t, $J = 5.7$ Hz, 1H), 7.91 (d, $J = 8.6$ Hz, 2H), 7.81 (d, $J = 8.5$ Hz, 2H), 6.61 (s, 1H), 4.75 (p, 1H), 3.24 (q, $J = 6.7$ Hz, 2H), 3.05 (s, 6H), 2.49 – 2.40 (m, 2H), 2.07 – 1.97 (m, 4H), 1.94 (t, $J = 7.3$ Hz, 2H), 1.76 – 1.60 (m, 2H), 1.57 – 1.43 (m, 4H), 1.38 – 1.22 (m, 4H). ^{13}C NMR (101 MHz, DMSO- d_6) δ 169.55, 166.12, 163.29, 155.50, 152.56, 151.45, 144.00, 132.48, 128.24, 126.91, 117.33, 112.38, 101.09, 57.50, 35.06, 32.71, 30.08, 29.71, 28.85, 26.75, 25.59, 24.98, 24.66. ESI-HRMS m/z calcd for $C_{28}H_{38}N_7O_4^+$ 536.2980, found 536.2985 $[M + H]^+$. HPLC purity 98%.

4.1.30.

7-cyclopentyl-2-((4-((8-(hydroxyamino)-8-oxooctyl)carbamoyl)phenyl)amino)-N,N-dimethyl

-7H-pyrrolo[2,3-d]pyrimidine-6-carboxamide (11d). White solid; 71% yield; mp 105.9 °C (decompose); 1H NMR (400 MHz, DMSO- d_6) δ 10.35 (s, 1H), 9.85 (s, 1H), 8.79 (s, 1H), 8.30 (t, $J = 5.7$ Hz, 1H), 7.91 (d, $J = 8.5$ Hz, 2H), 7.81 (d, $J = 8.5$ Hz, 2H), 6.61 (s, 1H), 4.75 (p, 1H), 3.24 (q, $J = 6.7$ Hz, 2H), 3.05 (s, 6H), 2.52 – 2.39 (m, 2H), 2.07 – 1.96 (m, 4H), 1.93 (t, $J = 7.4$ Hz, 2H), 1.74 – 1.63 (m, 2H), 1.55 – 1.42 (m, 4H), 1.33 – 1.18 (m, 6H). ^{13}C NMR (101 MHz, DMSO- d_6) δ 169.56, 166.12, 163.29, 155.50, 152.56, 151.45, 144.00, 132.48, 128.24, 126.91, 117.33, 112.38, 101.08, 57.50, 35.06, 32.72, 30.09, 29.78, 29.04, 29.00, 26.93, 25.57, 24.66. ESI-HRMS m/z calcd for $C_{29}H_{40}N_7O_4^+$ 550.3136, found 550.3141 $[M + H]^+$. HPLC purity 99%.

General Procedure for the Synthesis of 13a-13d.

The title compound was prepared from **12a-12d** (60 mmol, 1 equiv), *p*-Phenylenediamine (**2c**) (6.49 g, 60 mmol, 2 equiv), EDCI (8.27 g, 45 mmol, 1.5 equiv), HOBT (4.87 g, 36 mmol, 1.2 equiv), DIEA (7.76 g, 60 mmol, 2 equiv) and DMF (60 mL) using the procedure described for compound **3a-3f** to obtain the

desired product **13a-13d**.

4.1.31. N-(4-aminophenyl)hexanamide (13a). White solid; 60% yield; mp 87.8 °C; ^1H NMR (400 MHz, Chloroform-*d*) δ 7.78 (s, 1H), 7.26 – 7.21 (m, 2H), 6.58 – 6.53 (m, 2H), 3.57 (s, 2H), 2.31 – 2.19 (m, 2H), 1.75 – 1.59 (m, 2H), 1.36 – 1.26 (m, 4H), 0.90 – 0.84 (m, 3H). ^{13}C NMR (101 MHz, CDCl_3) δ 171.74, 143.17, 129.50, 122.16, 115.33, 37.41, 31.48, 25.53, 22.47, 14.00. ESI-HRMS m/z calcd for $\text{C}_{12}\text{H}_{19}\text{N}_2\text{O}^+$ 207.1492, found 207.1494 $[\text{M} + \text{H}]^+$. HPLC purity 99%.

4.1.32. N-(4-aminophenyl)heptanamide (13b). White solid; 40% yield; mp 89.2 °C; ^1H NMR (400 MHz, Chloroform-*d*) δ 7.31 – 7.23 (m, 2H), 7.15 (s, 1H), 6.62 (d, J = 8.6 Hz, 2H), 3.67 – 3.37 (m, 2H), 2.29 (t, J = 7.6 Hz, 2H), 1.69 (p, J = 7.5 Hz, 2H), 1.42 – 1.22 (m, 6H), 0.91 – 0.86 (m, 3H). ^{13}C NMR (101 MHz, CDCl_3) δ 171.25, 143.19, 129.39, 122.01, 115.39, 37.63, 31.59, 28.99, 25.75, 22.53, 14.06. ESI-HRMS m/z calcd for $\text{C}_{13}\text{H}_{21}\text{N}_2\text{O}^+$ 221.1648, found 221.1650 $[\text{M} + \text{H}]^+$. HPLC purity 99%.

4.1.33. N-(4-aminophenyl)octanamide (13c). White solid; 82% yield; mp 98.8 °C; ^1H NMR (400 MHz, Chloroform-*d*) δ 7.63 (s, 1H), 7.26 – 7.21 (m, 2H), 6.60 – 6.54 (m, 2H), 3.57 (br, 2H), 2.26 (t, J = 7.6 Hz, 2H), 1.66 (t, J = 7.3 Hz, 2H), 1.37 – 1.18 (m, 8H), 0.86 (t, J = 6.6 Hz, 3H). ^{13}C NMR (101 MHz, CDCl_3) δ 171.63, 143.17, 129.47, 122.13, 115.34, 37.51, 31.73, 29.30, 29.11, 25.85, 22.64, 14.12. ESI-HRMS m/z calcd for $\text{C}_{14}\text{H}_{23}\text{N}_2\text{O}^+$ 235.1805, found 235.1807 $[\text{M} + \text{H}]^+$. HPLC purity 99%.

4.1.34. N-(4-aminophenyl)nonanamide (13d). White solid; 66% yield; mp 99.2 °C; ^1H NMR (400 MHz, Chloroform-*d*) δ 7.28 (d, J = 3.6 Hz, 2H), 7.10 (s, 1H), 6.64 (d, J = 8.4 Hz, 2H), 3.59 (s, 2H), 2.31 (t, J = 7.6 Hz, 2H), 1.71 (p, J = 7.4 Hz, 2H), 1.41 – 1.21 (m, 10H), 0.89 (t, J = 6.5 Hz, 3H). ^{13}C NMR (101 MHz, CDCl_3) δ 171.22, 143.19, 129.38, 122.00, 115.39, 37.65, 31.84, 29.37, 29.32, 29.17, 25.78, 22.66, 14.11. ESI-HRMS m/z calcd for $\text{C}_{15}\text{H}_{25}\text{N}_2\text{O}^+$ 249.1961, found 249.1963 $[\text{M} + \text{H}]^+$. HPLC purity 99%.

General Procedure for the Synthesis of 14a-14d.

The title compound was prepared from **13a-13d** (2 mmol, 1 equiv), compound **4** (586 mg, 2 mmol, 1 equiv), $\text{Pd}(\text{OAc})_2$ (11 mg, 0.05 mmol, 0.025 equiv), BINAP (62 mg, 0.1 mmol, 0.05 equiv) and Cs_2CO_3 (1.37 g, 4.2 mmol, 2.1 equiv) and 1,4-dioxane (20 mL) using the procedure described for compound

5a-5f to obtain the desired product **14a-14d**.

4.1.35.

7-cyclopentyl-2-((4-hexanamidophenyl)

amino)-N,N-dimethyl-7H-pyrrolo[2,3-d]pyrimidine -6-carboxamide (14a). White solid; 84% yield; mp 171.8 °C; ¹H NMR (400 MHz, DMSO-d₆) δ 9.72 (s, 1H), 9.42 (s, 1H), 8.72 (s, 1H), 7.78 – 7.60 (m, 2H), 7.57 – 7.43 (m, 2H), 6.56 (s, 1H), 4.80 – 4.62 (m, 1H), 3.05 (s, 6H), 2.49 – 2.39 (m, 2H), 2.27 (t, *J* = 7.4 Hz, 2H), 2.05 – 1.86 (m, 4H), 1.73 – 1.52 (m, 4H), 1.39 – 1.22 (m, 4H), 0.87 (t, *J* = 6.8 Hz, 3H). ¹³C NMR (101 MHz, DMSO-d₆) δ 171.17, 163.41, 156.06, 152.53, 151.76, 136.76, 133.43, 131.85, 119.81, 118.96, 111.75, 101.15, 57.40, 36.76, 31.41, 30.05, 27.62, 25.35, 24.64, 22.38, 14.34. ESI-HRMS *m/z* calcd for C₂₆H₃₅N₆O₂⁺ 463.2816, found 463.2822 [M + H]⁺. HPLC purity 99%.

4.1.36.

7-cyclopentyl-2-((4-heptanamidophenyl)

amino)-N,N-dimethyl-7H-pyrrolo[2,3-d]pyrimidine -6-carboxamide (14b). White solid; 82% yield; mp 114.0 °C; ¹H NMR (400 MHz, DMSO-d₆) δ 9.72 (s, 1H), 9.42 (s, 1H), 8.72 (s, 1H), 7.78 – 7.66 (m, 2H), 7.55 – 7.45 (m, 2H), 6.56 (s, 1H), 4.79 – 4.65 (m, 1H), 3.05 (s, 6H), 2.50 – 2.38 (m, 2H), 2.27 (t, *J* = 7.4 Hz, 2H), 1.97 – 1.92 (m, 2H), 1.71 – 1.50 (m, 4H), 1.34 – 1.20 (m, 6H), 0.86 (t, *J* = 6.8 Hz, 3H). ¹³C NMR (101 MHz, DMSO-d₆) δ 171.17, 163.41, 156.06, 152.53, 151.76, 136.76, 133.43, 131.85, 119.81, 118.96, 111.75, 101.14, 57.40, 36.80, 31.52, 30.05, 28.85, 25.63, 24.64, 22.47, 14.39. ESI-HRMS *m/z* calcd for C₂₇H₃₇N₆O₂⁺ 477.2973, found 477.2977 [M + H]⁺. HPLC purity 99%.

4.1.37.

7-cyclopentyl-N,N-dimethyl-2-((4-octanamidophenyl)amino)-7H-pyrrolo[2,3-d]pyrimidine

-6-carboxamide (14c). White solid; 81% yield; mp 176.4 °C; ¹H NMR (400 MHz, DMSO-d₆) δ 9.72 (s, 1H), 9.42 (s, 1H), 8.71 (s, 1H), 7.81 – 7.61 (m, 2H), 7.55 – 7.45 (m, 2H), 6.56 (s, 1H), 4.80 – 4.60 (m, 1H), 3.05 (s, 6H), 2.50 – 2.41 (m, 2H), 2.27 (t, *J* = 7.4 Hz, 2H), 2.04 – 1.89 (m, 4H), 1.74 – 1.52 (m, 4H), 1.35 – 1.19 (m, 8H), 0.84 (t, *J* = 6.8 Hz, 3H). ¹³C NMR (101 MHz, DMSO-d₆) δ 171.17, 163.41, 156.06, 152.52, 151.76, 136.77, 133.43, 131.84, 119.82, 118.95, 111.74, 101.15, 57.40, 36.80, 31.65, 30.05, 29.15, 28.95, 25.67, 24.64, 22.54, 14.39. ESI-HRMS *m/z* calcd for C₂₈H₃₉N₆O₂⁺ 491.3129, found 491.3132 [M + H]⁺. HPLC purity 99%.

4.1.38.**7-cyclopentyl-N,N-dimethyl-2-((4-nonanamidophenyl)amino)-7H-pyrrolo[2,3-d]pyrimidine-**

6-carboxamide (14d). White solid; 80% yield; mp 168.2 °C; ¹H NMR (400 MHz, DMSO-d₆) δ 9.72 (s, 1H), 9.42 (s, 1H), 8.71 (s, 1H), 7.79 – 7.58 (m, 2H), 7.58 – 7.44 (m, 2H), 6.56 (s, 1H), 4.72 (p, *J* = 8.9 Hz, 1H), 3.05 (s, 6H), 2.49 – 2.41 (m, 2H), 2.26 (t, *J* = 7.4 Hz, 2H), 1.97 (dtd, *J* = 15.7, 8.7, 7.9, 3.9 Hz, 4H), 1.69 – 1.51 (m, 4H), 1.34 – 1.19 (m, 10H), 0.84 (t, *J* = 6.8 Hz, 3H). ¹³C NMR (101 MHz, DMSO-d₆) δ 171.16, 163.41, 156.05, 152.52, 151.75, 136.76, 133.42, 131.84, 119.81, 118.94, 111.74, 101.15, 57.40, 36.80, 31.73, 30.05, 29.25, 29.18, 29.07, 25.66, 24.64, 22.55, 14.41. ESI-HRMS *m/z* calcd for C₂₉H₄₁N₆O₂⁺ 505.3286, found 505.3290 [M + H]⁺. HPLC purity 99%.

4.1.39. methyl 6-(3-(4-aminophenyl)ureido)hexanoate (16). To a methyl 6-aminohexanoate hydrochloride (**7b**) (3.63 g, 20 mmol) in 50 mL dichloromethane was added triphosgene (7.05 g, 24 mmol) at 0 °C. Then triethylamine (5.06 g, 50 mmol) was added dropwise. After the completion of the dropwise addition, the cooling bath was removed and the reaction mixture was stirred at room temperature for about 3 hours. Then the mixture dropwise into *p*-Phenylenediamine (**2c**) (4.33 g, 40 mmol) and triethylamine (2.02 g, 20 mmol) in 50 mL DMF, and the reaction mixture was stirred at room temperature for about 12 hours. The solvent was removed under reduced pressure, and the residue was added sodium bicarbonate solution 200 mL and extracted by ethyl acetate. The combine organic was washed by water and brine. The organic phase was dried over MgSO₄, filtered and evaporated. The residue was purified by silica gel column chromatography (dichloromethane – methanol, gradient 100:0 → 95:5) to obtain 4.4 g (78%) of **16** as a white solid, mp 100.4 °C. ¹H NMR (400 MHz, DMSO-d₆) δ 7.83 (s, 1H), 7.01 – 6.96 (m, 2H), 6.50 – 6.42 (m, 2H), 5.87 (t, *J* = 5.6 Hz, 1H), 4.67 (s, 2H), 3.58 (s, 3H), 3.02 (q, *J* = 6.6 Hz, 2H), 2.30 (t, *J* = 7.4 Hz, 2H), 1.60 – 1.47 (m, 2H), 1.46 – 1.33 (m, 2H), 1.32 – 1.21 (m, 2H). ¹³C NMR (101 MHz, DMSO-d₆) δ 173.80, 156.16, 143.75, 130.11, 120.65, 114.59, 51.65, 39.36, 33.71, 30.09, 26.34, 24.69. ESI-HRMS *m/z* calcd for C₁₄H₂₂N₃O₃⁺ 280.1656, found 280.1660 [M + H]⁺. HPLC purity 99%.

4.1.40. methyl 6-(3-(4-((7-cyclopentyl-6-(dimethylcarbamoyl)-7H-pyrrolo[2,3-d]pyrimidin-2-yl)

amino)phenyl)ureido)hexanoate (17). The title compound was prepared from compound **4** (586 mg, 2 mmol), compound **16** (558 mg, 2 mmol), Pd(OAc)₂ (11 mg, 0.05 mmol), BINAP (62 mg, 0.1 mmol), Cs₂CO₃ (1.37 g, 4.2 mmol) and 1,4-dioxane (20 mL) using the procedure described for **5a-f** in 45% yield as a white solid, mp 161.5 °C. ¹H NMR (400 MHz, DMSO-d₆) δ 9.35 (s, 1H), 8.70 (s, 1H), 8.26 (s, 1H), 7.66 (d, *J* = 8.6 Hz, 2H), 7.29 (d, *J* = 8.6 Hz, 2H), 6.56 (s, 1H), 6.02 (t, *J* = 5.7 Hz, 1H), 4.71 (p, *J* = 9.0 Hz, 1H), 3.58 (s, 3H), 3.13 – 2.94 (m, 8H), 2.45 (t, *J* = 10.5 Hz, 2H), 2.31 (t, *J* = 7.4 Hz, 2H), 1.96 (q, *J* = 9.0, 8.4 Hz, 4H), 1.71 – 1.59 (m, 2H), 1.54 (p, *J* = 7.5 Hz, 2H), 1.41 (p, *J* = 7.1 Hz, 2H), 1.34 – 1.24 (m, 2H). ¹³C NMR (101 MHz, DMSO-d₆) δ 173.79, 163.40, 156.18, 155.82, 152.55, 151.81, 135.18, 134.72, 131.62, 119.35, 118.47, 111.54, 101.21, 57.36, 51.65, 33.71, 30.03, 26.34, 24.68, 24.64. ESI-HRMS *m/z* calcd for C₂₈H₃₈N₇O₄⁺ 537.3013, found 537.2932 [M + H]⁺. HPLC purity 99%.

4.1.41.

7-cyclopentyl-2-((4-(3-(6-(hydroxyamino)-6-oxohexyl)ureido)phenyl)amino)-N,N-dimethyl-7H-pyrrolo[2,3-d]pyrimidine-6-carboxamide (18). The title compound was prepared from compound **17** (900 mg, 1.71 mmol), solution of hydroxylamine (50% in water, 9 mL) and CH₃OH (36 mL) using the procedure described for **6a-f** in 68% yield as a white solid, mp 210.8 °C (decompose). ¹H NMR (400 MHz, DMSO-d₆) δ 10.35 (s, 1H), 9.30 (s, 1H), 8.69 (s, 1H), 8.30 (s, 1H), 7.66 (d, *J* = 8.4 Hz, 2H), 7.30 (d, *J* = 8.3 Hz, 2H), 6.55 (s, 1H), 6.07 (s, 1H), 4.71 (p, *J* = 8.8 Hz, 1H), 3.18 – 2.98 (m, 8H), 2.49 – 2.40 (m, 2H), 2.03 – 1.87 (m, 6H), 1.71 – 1.58 (m, 2H), 1.51 (p, *J* = 7.4 Hz, 2H), 1.45 – 1.37 (m, 2H), 1.27 (q, *J* = 7.7 Hz, 2H). ¹³C NMR (101 MHz, DMSO-d₆) δ 169.47, 163.44, 156.21, 155.87, 152.51, 151.85, 135.17, 134.79, 131.67, 119.40, 118.50, 111.56, 101.17, 57.36, 39.47, 32.70, 30.08, 30.07, 26.54, 26.50, 25.40, 24.65. ESI-HRMS *m/z* calcd for C₂₇H₃₇N₈O₄⁺ 537.2932, found 537.2932 [M + H]⁺. HPLC purity 99%.

4.1.42. 2-amino-7-cyclopentyl-N,N-dimethyl-7H-pyrrolo[2,3-d] pyrimidine-6-carboxamide (20).

To a suspension of 2-chloro-7-cyclopentyl-N,N-dimethyl-7H-pyrrolo[2,3-d]pyrimidine-6-carboxamide (**a**) (2.93 g, 10 mmol) in 50 mL 1,4-dioxane were added diphenylmethanimine (1.95 g, 10.5 mmol), Pd(OAc)₂ (110 mg, 0.5 mmol), BINAP (0.31 mg, 0.5 mmol) and Cs₂CO₃ (4.89 g, 15 mmol) and the

flask was purged with N₂. Then the flask was sealed and the mixture was heated for 12 h at 100 °C. The reaction was cooled to room temperature, then the suspension was added with ethyl acetate and water. The solvent was extracted with ethyl acetate, and the organic phase was dried over Na₂SO₄, filtered and evaporated. The residue was without purified to obtain 4.16 g of 7-cyclopentyl-2-((diphenylmethylene)amino)-N,N-dimethyl-7H-pyrrolo[2,3-d]pyrimidine-6-carboxamide (**19**) as a yellow solid. The residue was added THF 30 mL and concentrated HCl 5 mL, and the mixture was stirred for 3 hours. This solvent was basified to pH 10 with aqueous 25percent NaOH solution and extracted with ethyl acetate. The organic phase was dried over Na₂SO₄, filtered and evaporated. The residue was purified by silica gel column chromatography (dichloromethane – methanol, gradient 100:0 → 94:6) to obtain 2.28 g (84%, two steps) of **20** as a white solid, mp 132.1 °C. ¹H NMR (400 MHz, Chloroform-*d*) δ 8.52 (s, 1H), 6.35 (s, 1H), 4.95 (s, 2H), 4.74 (p, *J* = 8.7 Hz, 1H), 3.11 (s, 6H), 2.38 (ddd, *J* = 14.5, 6.4, 3.4 Hz, 2H), 2.10 – 1.85 (m, 4H), 1.68 – 1.52 (m, 2H). ¹³C NMR (101 MHz, DMSO-*d*₆) δ 163.75, 160.37, 153.29, 152.44, 130.51, 110.45, 101.30, 56.42, 34.97, 30.44, 24.65. ESI-HRMS *m/z* calcd for C₁₄H₂₀N₅O⁺ 274.1662, found 274.1660 [M + H]⁺. HPLC purity 99%.

4.1.43. 7-cyclopentyl-2-hydrazinyl-N,N-dimethyl-7H-pyrrolo[2,3-d]pyrimidine-6-carboxamide (21). To a suspension of 2-chloro-7-cyclopentyl-N,N-dimethyl-7H-pyrrolo[2,3-d]pyrimidine-6-carboxamide (**4**) (2.93 g, 10 mmol) in 10 mL ethanol were added N₂H₄·H₂O (80% in water, 2.5 mL). The mixture was heated for 6 h at 80 °C. The reaction was cooled to room temperature, the solvent was removed under reduced pressure, and the residue was purified by silica gel column chromatography (dichloromethane – methanol, gradient 100:0 → 93:7) to obtain 2.28 g (79%) of **21** as a light-yellow solid, mp 121.5 °C. ¹H NMR (400 MHz, DMSO-*d*₆) δ 8.57 (s, 1H), 7.93 (s, 1H), 6.49 (s, 1H), 4.87 – 4.63 (m, 1H), 4.15 (s, 2H), 3.11 – 2.94 (m, 7H), 2.41 – 2.26 (m, 2H), 2.01 – 1.85 (m, 4H), 1.58 (q, *J* = 6.2 Hz, 2H). ¹³C NMR (101 MHz, DMSO-*d*₆) δ 163.13, 161.33, 152.24, 151.86, 130.26, 110.31, 100.76, 56.18, 34.48, 30.09, 24.65. ESI-HRMS *m/z* calcd for C₁₄H₂₁N₆O⁺ 289.1771, found 289.1767 [M + H]⁺. HPLC purity 99%.

4.1.44. methyl 8-((7-cyclopentyl-6-(dimethylcarbamoyl)-7H-pyrrolo[2,3-d]pyrimidin-2-yl)amino)-8-oxooctanoate (22). To a two-necked flask, compound **20** (547 mg, 2 mmol), suberic acid monomethyl ester (**1c**) (412 mg, 2.2 mmol), DCC (454 mg, 2.2 mmol), DMAP (280 mg, 2.2 mmol) and dichloromethane (20 mL) were charged. The mixture was stirred at reflux for 36 hours, then quenched by saturated aqueous NaHCO₃ solution. The mixture was extracted by dichloromethane, and the combined organic layers were dried by anhydrous magnesium sulphate. The solvent was evaporated, and the residue was purified by silica gel column chromatography (dichloromethane – methanol, gradient 100:0 → 95:5) to obtain 638 mg (72%) of **22** as a white solid, mp 149.9 °C. ¹H NMR (400 MHz, DMSO-d₆) δ 10.32 (s, 1H), 8.85 (s, 1H), 6.64 (s, 1H), 4.82 – 4.61 (m, 1H), 3.56 (s, 3H), 3.03 (s, 6H), 2.53 (t, *J* = 8.3 Hz, 2H), 2.41 – 2.31 (m, 2H), 2.28 (t, *J* = 7.4 Hz, 2H), 1.96 (dq, *J* = 16.5, 8.8, 7.1 Hz, 4H), 1.65 – 1.44 (m, 6H), 1.37 – 1.23 (m, 4H). ¹³C NMR (101 MHz, DMSO-d₆) δ 173.77, 171.90, 163.18, 152.59, 151.89, 151.25, 134.33, 114.59, 100.25, 57.29, 51.60, 36.70, 34.98, 33.68, 30.68, 28.80, 28.74, 25.00, 24.80, 24.75. ESI-HRMS *m/z* calcd for C₂₃H₃₄N₅O₄⁺ 444.2605, found 444.2604 [M + H]⁺. HPLC purity 98%.

4.1.45. methyl 8-(2-(7-cyclopentyl-6-(dimethylcarbamoyl)-7H-pyrrolo[2,3-d]pyrimidin-2-yl)hydrazinyl)-8-oxooctanoate (23). To a two-necked flask, suberic acid monomethyl ester (**1c**) (482 mg, 2.4 mmol), compound **21** (577 mg, 2 mmol), EDCI (575 mg, 3 mmol), HOBt (325 mg, 2.4 mmol), DIEA (517 mg, 4 mmol) and DMF (10 mL) were charged. The mixture was stirred at 60 °C for 12 hours, then quenched by water. The mixture was extracted by ethyl acetate, and the combined organic layer was washed with brine solution and dried by anhydrous magnesium sulphate. The solvent was evaporated, and the residue was purified by silica gel column chromatography (dichloromethane – methanol, gradient 100:0 → 95:5) to obtain 293 mg (32%) of **23** as an off-white solid, mp 131.5 °C. ¹H NMR (400 MHz, DMSO-d₆) δ 9.63 (d, *J* = 2.1 Hz, 1H), 8.62 (s, 1H), 8.56 (d, *J* = 2.0 Hz, 1H), 6.52 (s, 1H), 4.68 (p, *J* = 8.5 Hz, 1H), 3.58 (s, 3H), 3.03 (s, 6H), 2.35 – 2.26 (m, 4H), 2.16 (t, *J* = 7.5 Hz, 2H), 1.97 – 1.81 (m, 4H), 1.60 – 1.48 (m, 6H), 1.33 – 1.18 (m, 4H). ¹³C NMR (101 MHz, DMSO-d₆) δ

173.78, 172.26, 163.48, 159.93, 152.49, 152.19, 131.74, 112.19, 100.80, 56.90, 51.62, 35.02, 33.70, 30.54, 28.85, 28.69, 25.25, 24.99, 24.78. ESI-HRMS m/z calcd for $C_{23}H_{35}N_6O_4^+$ 459.2714, found 459.2707 $[M + H]^+$. HPLC purity 99%.

4.1.46. methyl 8-(4-(6-((7-cyclopentyl-6-(dimethylcarbamoyl)-7H-pyrrolo[2,3-d]pyrimidin-2-yl)amino)pyridin-3-yl)piperazin-1-yl)-8-oxooctanoate (24). To a two-necked flask, suberic acid monomethyl ester (**1c**) (0.55 mmol, 104 mg), Lee011 (0.46 mmol, 200 mg), EDCI (0.69 mmol, 132 mg), DIEA (0.69 mmol, 89 mg) and DMF (3 mL) were charged. The mixture was stirred at room temperature for 12 hours, then quenched by water. The mixture was extracted by ethyl acetate, and the combined organic layer was washed with brine solution and dried by anhydrous magnesium sulphate. The solvent was evaporated, and the residue was purified by silica gel column chromatography (dichloromethane – methanol, gradient 100:0 → 95:5) to obtain 135 mg (49%) of **24** as a light-brown solid, mp 159.6 °C. 1H NMR (400 MHz, DMSO- d_6) δ 9.64 (s, 1H), 8.82 (s, 1H), 8.21 (d, J = 9.0 Hz, 1H), 8.08 (d, J = 3.0 Hz, 1H), 7.47 (dd, J = 9.2, 3.1 Hz, 1H), 6.60 (s, 1H), 4.74 (p, J = 8.9 Hz, 1H), 3.72 – 3.52 (m, 7H), 3.16 – 2.96 (m, 10H), 2.48 – 2.38 (m, 2H), 2.38 – 2.23 (m, 4H), 1.98 (p, J = 10.3, 8.9 Hz, 4H), 1.70 – 1.59 (m, 2H), 1.58 – 1.46 (m, 4H), 1.38 – 1.22 (m, 4H). ^{13}C NMR (101 MHz, DMSO- d_6) δ 173.78, 171.06, 163.34, 155.16, 152.58, 151.66, 147.04, 142.51, 136.71, 132.37, 126.46, 112.95, 112.29, 101.08, 57.43, 51.61, 49.95, 49.54, 45.21, 41.26, 33.69, 32.58, 30.19, 28.87, 28.76, 25.07, 24.80, 24.67. ESI-HRMS m/z calcd for $C_{32}H_{45}N_8O_4^+$ 605.3558, found 605.3563 $[M + H]^+$. HPLC purity 99%.

4.1.47. 7-cyclopentyl-2-((5-(4-(8-(hydroxyamino)-8-oxooctanoyl)piperazin-1-yl)pyridin-2-yl)amino)-N,N-dimethyl-7H-pyrrolo[2,3-d] pyrimidine-6-carboxamide (25). The title compound was prepared from compound **24** (750 mg, 1.24 mmol), solution of hydroxylamine (50% in water, 7.5 mL) and CH_3OH (30 mL) using the procedure described for **6a-f** in 67% yield as a white solid, mp 135.5 °C (decompose). 1H NMR (400 MHz, DMSO- d_6) δ 10.34 (s, 1H), 9.67 (s, 1H), 8.82 (s, 1H), 8.67 (s, 1H), 8.21 (d, J = 8.9 Hz, 1H), 8.09 (s, 1H), 7.48 (d, J = 9.2 Hz, 1H), 6.61 (s, 1H), 4.74 (p, J = 8.8 Hz, 1H), 3.68 – 3.49 (m, 4H), 3.18 – 2.96 (m, 10H), 2.47 – 2.38 (m, 2H), 2.07 – 1.87 (m, 8H), 1.74 – 1.56 (m, 2H), 1.54 – 1.42 (m, 4H), 1.35 – 1.19 (m, 4H). ^{13}C NMR (101 MHz, DMSO- d_6) δ 171.09, 169.57,

163.35, 155.15, 152.58, 151.66, 147.04, 142.51, 136.68, 132.39, 126.51, 112.96, 112.30, 101.10, 57.44, 49.95, 49.54, 45.22, 41.26, 32.73, 32.66, 30.20, 28.98, 28.93, 25.52, 25.16, 24.68. ESI-HRMS m/z calcd for $C_{31}H_{44}N_9O_4^+$ 606.3511, found 606.3521 $[M + H]^+$. HPLC purity 98%.

4.1.48. methyl 8-((4-aminobenzyl)amino)-8-oxooctanoate (26). To a two-necked flask, Suberic acid monomethyl ester (**1c**) (4.82 g, 25.6 mmol), 4-(Aminomethyl)anilinedihydrochloride (5 g, 25.63 mmol), EDCI (7.34 g, 38.45 mmol), HOBt (4.16 g, 30.76 mmol), DIEA (13.25 g, 102.54 mmol) and DMF (50 mL) were charged. The mixture was stirred at room temperature for 12 hours, then quenched by water. The mixture was extracted by ethyl acetate, and the combined organic layer was washed with brine solution and dried by anhydrous magnesium sulphate. The solvent was evaporated, and the residue was purified by silica gel column chromatography (dichloromethane – methanol, gradient 100:0 → 96:4) to obtain 5.032 g (67%) of **26** as a light-brown solid, mp 87.3 °C. 1H NMR (400 MHz, Chloroform-*d*) δ 7.04 (dt, J = 8.8, 2.5 Hz, 2H), 6.62 (dt, J = 7.2, 2.6 Hz, 2H), 4.28 (dt, J = 6.2, 3.0 Hz, 2H), 3.64 (d, J = 2.6 Hz, 3H), 2.27 (dd, J = 9.2, 6.2 Hz, 2H), 2.15 (dd, J = 9.4, 6.3 Hz, 2H), 1.69 – 1.52 (m, 4H), 1.30 (p, J = 3.7 Hz, 4H). ^{13}C NMR (101 MHz, $CDCl_3$) δ 174.23, 172.69, 145.88, 129.17, 128.15, 115.19, 51.50, 43.24, 36.66, 33.97, 28.87, 28.79, 25.54, 24.75. ESI-HRMS m/z calcd for $C_{16}H_{25}N_2O_3^+$ 293.1860, found 293.1859 $[M + H]^+$. HPLC purity 98%.

4.1.49. methyl 8-((4-((7-cyclopentyl-6-(dimethylcarbamoyl)-7H-pyrrolo[2,3-d]pyrimidin-2-yl)amino)benzyl) amino)-8-oxooctanoate (27). The title compound was prepared from compound **4** (586 mg, 2 mmol), compound **26** (558 mg, 2 mmol), $Pd(OAc)_2$ (11 mg, 0.05 mmol), BINAP (62 mg, 0.1 mmol), Cs_2CO_3 (1.37 g, 4.2 mmol) and 1,4-dioxane (20 mL) using the procedure described for **5a-f** in 79% yield as a light-yellow solid, mp 54.8 °C. 1H NMR (400 MHz, Chloroform-*d*) δ 8.59 (s, 1H), 7.84 (s, 1H), 7.67 – 7.57 (m, 2H), 7.16 (d, J = 8.1 Hz, 2H), 6.37 (s, 1H), 6.10 (s, 1H), 4.73 (p, J = 9.1 Hz, 1H), 4.35 (d, J = 5.5 Hz, 2H), 3.62 (s, 3H), 3.11 (s, 6H), 2.61 – 2.46 (m, 2H), 2.31 – 2.22 (m, 2H), 2.21 – 2.12 (m, 2H), 2.07 – 1.92 (m, 4H), 1.72 – 1.51 (m, 6H), 1.35 – 1.24 (m, 4H). ^{13}C NMR (101 MHz, $CDCl_3$) δ 174.23, 172.88, 164.17, 155.45, 152.04, 151.64, 139.65, 131.87, 131.57, 128.37, 118.70, 112.32, 100.99, 57.97, 51.52, 43.19, 36.65, 34.02, 30.16, 28.96, 28.87, 25.63, 24.80,

24.69. ESI-HRMS m/z calcd for $C_{30}H_{41}N_6O_4^+$ 549.3184, found 549.3186 $[M + H]^+$. HPLC purity 99%.

4.1.50. N1-(4-((7-cyclopentyl-6-(dimethylcarbamoyl)-7H-pyrrolo[2,3-d]pyrimidin-2-yl)amino)benzyl)-N8-hydroxyoctanediamide (28). The title compound was prepared from compound **27** (710 mg, 1.29 mmol), solution of hydroxylamine (50% in water, 7 mL) and CH_3OH (28 mL) using the procedure described for **6a-f** in 49% yield as a white solid, mp 123.5 °C (decompose). 1H NMR (400 MHz, $DMSO-d_6$) δ 10.35 (s, 1H), 9.51 (s, 1H), 8.73 (s, 1H), 8.68 (s, 1H), 8.25 (t, $J = 5.9$ Hz, 1H), 7.78 (d, $J = 8.1$ Hz, 2H), 7.15 (d, $J = 8.2$ Hz, 2H), 6.58 (s, 1H), 4.82 – 4.61 (m, 1H), 4.21 (d, $J = 5.8$ Hz, 2H), 3.17 (d, $J = 4.4$ Hz, 1H), 3.05 (s, 6H), 2.49 – 2.41 (m, 2H), 2.11 (t, $J = 7.4$ Hz, 2H), 2.04 – 1.87 (m, 6H), 1.73 – 1.60 (m, 2H), 1.57 – 1.43 (m, 4H), 1.33 – 1.18 (m, 4H). ^{13}C NMR (101 MHz, $DMSO-d_6$) δ 172.40, 169.52, 163.36, 155.95, 152.56, 151.66, 140.13, 132.42, 131.97, 127.85, 118.49, 111.86, 101.13, 65.38, 57.43, 42.09, 35.84, 32.72, 30.01, 28.94, 28.87, 25.77, 25.51, 24.60. ESI-HRMS m/z calcd for $C_{29}H_{40}N_7O_4^+$ 550.3136, found 550.3146 $[M + H]^+$. HPLC purity 97%.

4.1.51. methyl 8-((6-((tert-butoxycarbonyl)amino)pyridin-3-yl)amino)-8-oxooctanoate (29). To a two-necked flask, suberic acid monomethyl ester (**1c**) (531 mg, 2.82 mmol), tert-butyl (5-aminopyridin-2-yl)carbamate (590 mg, 2.82 mmol), EDCI (649 mg, 3.38 mmol), DMAP (35 mg, 0.28 mmol), DIEA (437 mg, 3.38 mmol) and DMF (10 mL) were charged. The mixture was stirred at room temperature for 12 hours, then quenched by water. The mixture was extracted by ethyl acetate, and the combined organic layer was washed with brine solution and dried by anhydrous magnesium sulphate. The solvent was evaporated, and the residue was purified by silica gel column chromatography (petroleum ether–ethyl acetate, gradient 100:00 \rightarrow 50:50) to obtain 570 mg (53 %) of **29** as a white solid, mp 164.4 °C. 1H NMR (400 MHz, $Chloroform-d$) δ 8.39 (s, 1H), 8.01 (s, 1H), 7.96 – 7.86 (m, 2H), 7.55 (s, 1H), 3.66 (s, 3H), 2.46 – 2.09 (m, 4H), 1.77 – 1.67 (m, 2H), 1.66 – 1.57 (m, 2H), 1.51 (s, 9H), 1.41 – 1.30 (m, 4H). ^{13}C NMR (101 MHz, $CDCl_3$) δ 174.32, 171.55, 152.45, 148.25, 139.21, 130.63, 130.13, 112.27, 81.09, 51.55, 37.12, 33.91, 28.70, 28.64, 28.29, 25.23, 24.63. ESI-HRMS m/z calcd for $C_{19}H_{30}N_3O_5^+$ 380.2180, found 380.2181 $[M + H]^+$. HPLC purity 99%.

4.1.52. methyl 8-((6-aminopyridin-3-yl)amino)-8-oxooctanoate (30). To a suspension of compound

(29) (570 mg, 1.5 mmol) in 10 mL THF were added concentrated HCl 10 mL, and the mixture was stirred for 1 hour. This solvent was basified to pH > 8 with aqueous Na₂CO₃ solution and extracted with ethyl acetate. The organic phase was dried over Na₂SO₄, filtered and evaporated. The residue was purified by silica gel column chromatography (dichloromethane – methanol, gradient 100:0 → 95:5) to obtain 275 mg (66%) of **30** as a white solid, mp 129.1 °C. ¹H NMR (400 MHz, DMSO-d₆) δ 9.51 (s, 1H), 8.04 (d, *J* = 2.6 Hz, 1H), 7.53 (dd, *J* = 8.8, 2.7 Hz, 1H), 6.39 (d, *J* = 8.8 Hz, 1H), 5.65 (s, 2H), 3.57 (s, 3H), 2.29 (t, *J* = 7.4 Hz, 2H), 2.22 (t, *J* = 7.4 Hz, 2H), 1.59 – 1.47 (m, 4H), 1.32 – 1.23 (m, 4H). ¹³C NMR (101 MHz, DMSO-d₆) δ 173.80, 171.13, 156.64, 139.98, 130.74, 126.18, 107.84, 51.62, 36.37, 33.70, 28.78, 28.68, 25.47, 24.78. ESI-HRMS *m/z* calcd for C₁₄H₂₂N₃O₃⁺ 280.1656, found 280.1657 [*M* + H]⁺. HPLC purity 99%.

4.1.53.

methyl

8-((6-((7-cyclopentyl-6-(dimethylcarbamoyl)-7H-pyrrolo[2,3-d]pyrimidin-2-yl)amino)pyridin-3-yl)amino)-8-oxooctanoate (31). The title compound was prepared from compound **4** (586 mg, 2 mmol), compound **36** (558 mg, 2 mmol), Pd(OAc)₂ (11 mg, 0.05 mmol), BINAP (62 mg, 0.1 mmol), Cs₂CO₃ (1.37 g, 4.2 mmol) and 1,4-dioxane (20 mL) using the procedure described for **5a-f** in 46% yield as a white solid, mp 205.9 °C. ¹H NMR (400 MHz, DMSO-d₆) δ 9.92 (s, 1H), 9.61 (s, 1H), 8.80 (s, 1H), 8.50 (d, *J* = 2.6 Hz, 1H), 8.25 (d, *J* = 9.0 Hz, 1H), 7.96 (dd, *J* = 9.0, 2.7 Hz, 1H), 6.62 (s, 1H), 4.74 (p, *J* = 8.9 Hz, 1H), 3.58 (s, 3H), 3.05 (s, 6H), 2.49 – 2.38 (m, 2H), 2.30 (td, *J* = 7.4, 1.5 Hz, 4H), 2.04 – 1.89 (m, 4H), 1.73 – 1.46 (m, 6H), 1.30 (p, *J* = 3.7 Hz, 4H). ¹³C NMR (101 MHz, DMSO-d₆) δ 173.80, 171.63, 163.31, 154.91, 152.55, 151.49, 149.23, 139.47, 132.65, 130.60, 128.87, 112.60, 112.21, 100.97, 57.43, 51.62, 36.51, 33.70, 31.64, 30.20, 28.78, 28.69, 25.35, 24.78, 24.71. ESI-HRMS *m/z* calcd for C₂₈H₃₈N₇O₄⁺ 536.2980, found 536.2979 [*M* + H]⁺. HPLC purity 96%.

4.1.54. N1-(6-((7-cyclopentyl-6-(dimethylcarbamoyl)-7H-pyrrolo[2,3-d]pyrimidin-2-yl)amino)

pyridin-3-yl)-N8-hydroxyoctanediamide (32). The title compound was prepared from compound **31** (1.03 g, 1.92 mmol), solution of hydroxylamine (50% in water, 10 mL) and CH₃OH (40 mL) using the procedure described for **6a-f** in 64% yield as a white solid, mp 118.0 °C (decompose). ¹H NMR (400

1 MHz, DMSO- d_6) δ 9.93 (s, 1H), 9.72 (s, 1H), 8.82 (s, 1H), 8.53 (d, J = 2.6 Hz, 1H), 8.26 (d, J = 9.0 Hz,
2 1H), 7.97 (dd, J = 9.1, 2.7 Hz, 1H), 6.62 (s, 1H), 4.74 (p, J = 8.9 Hz, 1H), 3.05 (s, 6H), 2.47 – 2.38 (m,
3 2H), 2.31 (t, J = 7.4 Hz, 2H), 2.20 (t, J = 7.3 Hz, 2H), 2.04 – 1.87 (m, 4H), 1.74 – 1.46 (m, 6H), 1.37 –
4 1.23 (m, 4H). ^{13}C NMR (101 MHz, DMSO- d_6) δ 175.00, 171.65, 163.31, 154.91, 152.57, 151.49,
5 149.23, 139.52, 132.66, 130.60, 128.91, 112.59, 112.19, 100.99, 57.44, 36.55, 34.16, 30.20, 28.88,
6 28.81, 25.41, 24.88, 24.71. ESI-HRMS m/z calcd for $\text{C}_{27}\text{H}_{37}\text{N}_8\text{O}_4^+$ 537.2932, found 537.2930 $[\text{M} + \text{H}]^+$.
7 HPLC purity 98%.

8
9
10
11
12
13
14
15
16 **4.1.55. methyl 8-((5-nitropyridin-2-yl)amino)-8-oxooctanoate (33).** To a suspension of suberic acid
17 monomethyl ester (**1c**) (5.65 g, 30 mmol) in 50 mL THF were added SOCl_2 (8.41 g, 66 mmol) and
18 heated for 3 h at 60°C. The reaction was cooled to room temperature, the solvent was removed under
19 reduced pressure, and the residue was added 50 mL THF, 50 mL pyridine and 5-nitropyridin-2-amine
20 (4.17 g, 30 mmol). The mixture was heated for 3 h at 60°C. The reaction was cooled to room
21 temperature, the solvent was removed under reduced pressure, and the residue was added water 200 mL,
22 and extracted by ethyl acetate. The combine organic was washed by water and brine. The organic phase
23 was dried over MgSO_4 , filtered and evaporated. The residue was purified by silica gel column
24 chromatography (petroleum ether–ethyl acetate, gradient 100:00 \rightarrow 60:40) to obtain 913.2 mg (10%)
25 of **33** as a brown solid, mp 172.3 °C. ^1H NMR (400 MHz, DMSO- d_6) δ 11.19 (s, 1H), 9.16 (d, J = 2.8
26 Hz, 1H), 8.59 (dd, J = 9.3, 2.9 Hz, 1H), 8.30 (d, J = 9.3 Hz, 1H), 3.57 (s, 3H), 2.45 (t, J = 7.4 Hz, 2H),
27 2.29 (t, J = 7.4 Hz, 2H), 1.64 – 1.47 (m, 4H), 1.28 (p, J = 3.6 Hz, 4H). ^{13}C NMR (101 MHz, DMSO- d_6)
28 δ 173.80, 173.57, 156.63, 145.21, 140.12, 134.67, 112.86, 51.64, 36.57, 33.66, 28.63, 24.94, 24.72.
29 ESI-HRMS m/z calcd for $\text{C}_{14}\text{H}_{20}\text{N}_3\text{O}_5^+$ 310.1397, found 310.1393 $[\text{M} + \text{H}]^+$. HPLC purity 98%.

30
31
32
33
34
35
36
37
38
39
40
41
42
43
44
45
46
47
48
49 **4.1.56. methyl 8-((5-aminopyridin-2-yl)amino)-8-oxooctanoate (34).** To a suspension of compound
50 **33** (913 mg, 2.94 mmol) in 10 mL ethanol and 10 mL ethyl acetate were added Palladium 10% on
51 Carbon (91 mg, wetted with ca. 55% Water) and ammonium formate (927 mg, 14.7 mmol) and the
52 flask was purged with N_2 . Then the flask was sealed and the mixture was heated for 12 h at 80°C. The
53
54
55
56
57
58
59
60

reaction was cooled to rt, and added 200 mL ethyl acetate. The organic was washed by water and brine. The organic phase was dried over MgSO_4 , filtered and evaporated. The residue was purified by silica gel column chromatography (dichloromethane – methanol, gradient 100:0 \rightarrow 95:5) to obtain 728.6 mg (88%) of **34** as a brown solid, mp 112.0 °C. ^1H NMR (400 MHz, Chloroform-*d*) δ 8.71 (m, 1H), 7.99 (d, J = 8.8 Hz, 1H), 7.72 (d, J = 2.8 Hz, 1H), 7.08 – 7.02 (m, 1H), 3.73 (s, 2H), 3.63 (s, 3H), 2.36 – 2.21 (m, 4H), 1.71 – 1.52 (m, 4H), 1.37 – 1.23 (m, 4H). ^{13}C NMR (101 MHz, CDCl_3) δ 174.25, 171.29, 143.85, 139.46, 133.91, 124.89, 115.00, 51.51, 37.37, 33.96, 28.82, 28.79, 25.27, 24.72. ESI-HRMS m/z calcd for $\text{C}_{14}\text{H}_{22}\text{N}_3\text{O}_3^+$ 280.1656, found 280.1655 $[\text{M} + \text{H}]^+$. HPLC purity 99%.

4.1.57.**methyle**

8-((5-((7-cyclopentyl-6-(dimethylcarbamoyl)-7H-pyrrolo[2,3-d]pyrimidin-2-yl)amino)pyridin-2-yl)amino)-8-oxooctanoate (35). The title compound was prepared from compound **4** (586 mg, 2 mmol), compound **34** (559 mg, 2 mmol), $\text{Pd}(\text{OAc})_2$ (11 mg, 0.05 mmol), BINAP (62 mg, 0.1 mmol), Cs_2CO_3 (1.37 g, 4.2 mmol) and 1,4-dioxane (20 mL) using the procedure described for **5a-f** in 77% yield as a light-brown solid, mp 153.9 °C. ^1H NMR (400 MHz, Chloroform-*d*) δ 8.64 (s, 1H), 8.49 (d, J = 2.5 Hz, 1H), 8.29 (dd, J = 9.1, 2.9 Hz, 1H), 8.22 (d, J = 9.0 Hz, 1H), 6.43 (s, 1H), 4.75 (t, J = 8.9 Hz, 1H), 3.64 (d, J = 1.4 Hz, 2H), 3.14 (s, 6H), 2.56 – 2.43 (m, 2H), 2.38 (t, J = 7.5 Hz, 2H), 2.28 (t, J = 6.7 Hz, 2H), 2.09 – 1.92 (m, 4H), 1.76 – 1.56 (m, 6H), 1.42 – 1.29 (m, 4H). ^{13}C NMR (101 MHz, CDCl_3) δ 179.05, 174.27, 163.84, 154.75, 152.04, 150.52, 146.03, 136.78, 133.47, 132.68, 129.47, 114.43, 112.35, 101.06, 58.09, 51.50, 37.30, 34.01, 31.47, 30.20, 28.84, 27.75, 25.19, 24.75, 24.48. ESI-HRMS m/z calcd for $\text{C}_{28}\text{H}_{38}\text{N}_7\text{O}_4^+$ 536.2980, found 536.2985 $[\text{M} + \text{H}]^+$. HPLC purity 99%.

4.1.58. 2-chloro-N-cyclopentyl-5-nitropyrimidin-4-amine (38). 2,4-dichloro-5-nitropyrimidine (1.94 g, 10 mmol) and DIEA (1.29 g, 10 mmol) were dissolved in ethyl acetate (20 mL) and cooled to -40 °C. Cyclopentylamine (1.94 g, 10 mmol) was dissolved in ethyl acetate (20 mL) and added dropwise. After the completion of the dropwise addition, the cooling bath was removed and the reaction mixture was stirred at room temperature for about 2 hours. Then the organic added ethyl acetate (200 mL), the organic was washed by saturated citric acid aqueous solution, water and brine. The organic

phase was dried over MgSO_4 , filtered and the solvent evaporated to obtain 2.42 g (99%) of **38** as a yellow solid, mp 126.3 °C. ^1H NMR (400 MHz, Chloroform-*d*) δ 9.01 (s, 1H), 8.37 (s, 1H), 4.58 (h, J = 7.0 Hz, 1H), 2.32 – 2.08 (m, 2H), 1.87 – 1.61 (m, 4H), 1.64 – 1.42 (m, 2H). ^{13}C NMR (101 MHz, CDCl_3) δ 164.14, 157.09, 154.98, 126.46, 53.27, 33.02, 23.73. ESI-HRMS m/z calcd for $\text{C}_9\text{H}_{12}\text{ClN}_4\text{O}_2^+$ 243.0643, found 243.0645 $[\text{M} + \text{H}]^+$. HPLC purity 97%.

4.1.59. 2-chloro-N4-cyclopentylpyrimidine-4,5-diamine (39). To a suspension of compound **38** (2.42 g, 10 mmol) in 50 mL ethanol were added stannous chloride dihydrate (9.03 g, 40 mmol), and the mixture was heated for 2 hours at reflux. The reaction was cooled to room temperature and added ethyl acetate (250 mL). The solvent was washed by saturated sodium carbonate solution, water and brine. The organic phase was dried over MgSO_4 , filtered and evaporated. The residue was purified by silica gel column chromatography (dichloromethane – methanol, gradient 100:0 \rightarrow 90:10) to obtain 1.8 g (85%) of **39** as a black solid, mp 47.8 °C. ^1H NMR (400 MHz, Chloroform-*d*) δ 7.54 (s, 1H), 5.18 (d, J = 7.3 Hz, 1H), 4.46 – 4.27 (m, 1H), 3.10 (s, 3H), 2.26 – 1.89 (m, 2H), 1.80 – 1.51 (m, 4H), 1.52 – 1.32 (m, 2H). ^{13}C NMR (101 MHz, CDCl_3) δ 156.84, 152.63, 141.35, 123.75, 52.55, 33.16, 23.73. ESI-HRMS m/z calcd for $\text{C}_9\text{H}_{14}\text{ClN}_4^+$ 213.0902, found 213.0902 $[\text{M} + \text{H}]^+$. HPLC purity 95%.

4.1.60. 2-chloro-9-cyclopentyl-9H-purine (40). To a suspension of compound **39** (4.02 g, 18.81 mmol) in 100 mL DMF was added triethyl orthoformate (17.32 g, 188.1 mmol) and MgSO_4 (2.26 g, 18.81 mmol), and the mixture was heated for 2 hours at 130 °C. The reaction was cooled to room temperature, the solvent was removed under reduced pressure, and added ethyl acetate (200 mL). The solvent was washed by water and brine. The organic phase was dried over MgSO_4 , filtered and evaporated. The residue was purified by silica gel column chromatography (petroleum ether–ethyl acetate, gradient 100:00 \rightarrow 50:50) to obtain 1.97 g (47%) of **40** as a brown solid, mp 117.1 °C. ^1H NMR (400 MHz, Chloroform-*d*) δ 8.94 (s, 1H), 8.13 (s, 1H), 5.08 – 4.73 (m, 1H), 2.38 – 2.22 (m, 2H), 2.05 – 1.89 (m, 4H), 1.86 – 1.73 (m, 2H). ^{13}C NMR (101 MHz, CDCl_3) δ 154.07, 153.20, 150.03, 144.33, 133.45, 56.14, 32.73, 23.85. ESI-HRMS m/z calcd for $\text{C}_{10}\text{H}_{12}\text{ClN}_4^+$ 223.0745, found 223.0743

[M + H]⁺. HPLC purity 98%.

4.1.61. methyl 8-((4-((9-cyclopentyl-9H-purin-2-yl)amino)phenyl)amino)-8-oxooctanoate (41).

The title compound was prepared from compound **40** (445 mg, 2 mmol), compound **3e** (558 mg, 2mmol), Pd(OAc)₂ (11 mg, 0.05 mmol), BINAP (62 mg, 0.1 mmol), Cs₂CO₃ (1.37 g, 4.2 mmol) and 1,4-dioxane (20 mL) using the procedure described for **5a-f** in 77% yield as a white solid, mp 156.7 °C. ¹H NMR (400 MHz, Chloroform-*d*) δ 8.74 (s, 1H), 7.84 (s, 1H), 7.82 – 7.67 (m, 2H), 7.67 – 7.60 (m, 2H), 7.53 – 7.47 (m, 2H), 4.81 (p, *J* = 7.5 Hz, 1H), 3.64 (s, 3H), 2.29 (ddt, *J* = 19.5, 12.2, 6.6 Hz, 6H), 2.12 – 1.99 (m, 2H), 1.94 (tt, *J* = 6.9, 3.7 Hz, 2H), 1.85 – 1.65 (m, 4H), 1.60 (p, *J* = 7.3 Hz, 2H), 1.35 (qd, *J* = 8.1, 5.1, 4.6 Hz, 4H). ¹³C NMR (101 MHz, CDCl₃) δ 174.29, 171.31, 156.10, 152.58, 149.25, 141.42, 136.29, 132.60, 128.91, 120.64, 119.25, 55.98, 51.53, 37.44, 33.95, 32.28, 28.82, 28.77, 25.45, 24.71, 24.11. ESI-HRMS *m/z* calcd for C₂₅H₃₃N₆O₃⁺ 465.2609, found 465.2613 [M + H]⁺. HPLC purity 99%.

4.1.62. N1-(4-((9-cyclopentyl-9H-purin-2-yl)amino)phenyl)-N8-hydroxyoctanediamide (42). The

title compound was prepared from compound **41** (350 mg, 0.75 mmol), solution of hydroxylamine (50% in water, 5 mL) and CH₃OH (5 mL) using the procedure described for **6a-f** in 45% yield as a yellow solid, mp 177.2 °C (decompose). ¹H NMR (400 MHz, DMSO-*d*₆) δ 10.35 (s, 1H), 9.75 (s, 1H), 9.53 (s, 1H), 8.73 (d, *J* = 35.5 Hz, 2H), 8.26 (s, 1H), 7.73 (d, *J* = 8.4 Hz, 2H), 7.50 (d, *J* = 8.6 Hz, 2H), 4.99 – 4.73 (m, 1H), 2.37 – 2.00 (m, 6H), 2.00 – 1.81 (m, 4H), 1.71 (s, 2H), 1.53 (d, *J* = 31.4 Hz, 4H), 1.28 (s, 4H). ¹³C NMR (101 MHz, DMSO-*d*₆) δ 171.15, 169.56, 156.47, 152.46, 149.46, 142.99, 136.75, 133.46, 128.80, 119.91, 119.03, 55.87, 36.74, 32.72, 31.90, 28.92, 28.89, 25.59, 25.52, 24.22. ESI-HRMS *m/z* calcd for C₂₄H₃₂N₇O₃⁺ 466.2561, found 466.2563 [M + H]⁺. HPLC purity 96%.

4.1.63. 5-chloro-3-cyclopentyl-3H-[1,2,3]triazolo[4,5-*d*]pyrimidine (43). To a suspension of

2-chloro-N4-cyclopentyl pyrimidine-4,5-diamine (**39**) (2.13 g, 10 mmol) in con. HCl (20 mL) was stirred for 15 mins at 0°C. Then NaNO₂ (828 mg, 12 mmol) was dissolved in water (5 mL) and added dropwise. After the completion of the dropwise addition, the cooling bath was removed and the reaction mixture was stirred at room temperature for about 3 hours. Then the reaction poured into 200 mL

sodium bicarbonate solution, and extracted by ethyl acetate. The combine organic was washed by water and brine. The organic phase was dried over MgSO_4 , filtered and evaporated. The residue was purified by silica gel column chromatography (petroleum ether–ethyl acetate, gradient 100:00 \rightarrow 60:40) to obtain 1.45 g (65%) of **43** as a white solid, mp 64.9 °C. ^1H NMR (400 MHz, Chloroform- d) δ 9.34 (s, 1H), 5.32 (p, J = 7.1 Hz, 1H), 2.40 – 2.18 (m, J = 6.5 Hz, 4H), 2.10 – 1.96 (m, 2H), 1.90 – 1.66 (m, 2H). ^{13}C NMR (101 MHz, CDCl_3) δ 158.34, 153.04, 150.47, 135.13, 59.53, 32.70, 24.42. ESI-HRMS m/z calcd for $\text{C}_9\text{H}_{11}\text{ClN}_5^+$ 224.0697, found 224.0697 $[\text{M} + \text{H}]^+$. HPLC purity 99%.

4.1.64.

methyl

8-((4-((3-cyclopentyl-3H-[1,2,3]triazolo[4,5-d]pyrimidin-5-yl)amino)phenyl)amino)

-8-oxooctanoate (44). The title compound was prepared from compound **43** (336 mg, 1.5 mmol), compound **3e** (461 mg, 1.65mmol), $\text{Pd}(\text{OAc})_2$ (8 mg, 0.04 mmol), BINAP (47 mg, 0.08 mmol), Cs_2CO_3 (538 mg, 1.65 mmol) and 1,4-dioxane (15 mL) using the procedure described for **5a-f** in 77% yield as a yellow solid, mp 131.6 °C. ^1H NMR (400 MHz, Chloroform- d) δ 9.09 (s, 1H), 7.93 (s, 1H), 7.66 (d, J = 8.8 Hz, 3H), 7.59 – 7.51 (m, 2H), 5.21 (p, J = 7.3 Hz, 1H), 3.65 (s, 3H), 2.35 (t, J = 7.5 Hz, 2H), 2.29 (q, J = 6.4, 5.5 Hz, 6H), 2.09 – 1.95 (m, 3H), 1.86 – 1.66 (m, 4H), 1.61 (p, J = 7.3 Hz, 2H), 1.36 (dt, J = 8.5, 5.1 Hz, 4H). ^{13}C NMR (101 MHz, CDCl_3) δ 174.32, 171.40, 158.02, 152.57, 150.11, 135.07, 133.60, 132.23, 120.59, 120.04, 58.87, 51.56, 37.47, 33.95, 32.25, 28.81, 28.76, 25.42, 24.70, 24.66. ESI-HRMS m/z calcd for $\text{C}_{24}\text{H}_{32}\text{N}_7\text{O}_3^+$ 466.2561, found 466.2567 $[\text{M} + \text{H}]^+$. HPLC purity 99%.

4.1.65.

N1-(4-((3-cyclopentyl-3H-[1,2,3]triazolo[4,5-d]pyrimidin-5-yl)amino)phenyl)-N8-

hydroxyoctanediamide (45). The title compound was prepared from compound **44** (150 mg, 0.32 mmol), solution of hydroxylamine (50% in water, 3 mL) and ethanol (5 mL) using the procedure described for **6a-f** in 32% yield as a yellow solid, mp 199.4 °C (decompose). ^1H NMR (400 MHz, DMSO- d_6) δ 11.96 (s, 1H), 10.16 (s, 1H), 9.82 (s, 1H), 9.31 (s, 1H), 7.76 (d, J = 8.6 Hz, 2H), 7.56 (d, J = 8.7 Hz, 2H), 5.24 (p, J = 7.3 Hz, 1H), 2.34 – 2.15 (m, 8H), 2.01 – 1.85 (m, 2H), 1.76 (p, J = 7.8, 5.6 Hz, 2H), 1.54 (dt, J = 32.4, 7.0 Hz, 4H), 1.40 – 1.24 (m, 4H). ^{13}C NMR (101 MHz, DMSO- d_6) δ 175.02, 171.31, 158.48, 153.36, 149.97, 135.36, 134.68, 131.90, 120.11, 119.80, 58.71, 36.76, 34.15, 32.11,

28.90, 28.82, 25.52, 24.89, 24.76. ESI-HRMS m/z calcd for $C_{23}H_{31}N_8O_3^+$ 467.2514, found 467.2543 [$M + H$] $^+$. HPLC purity 98%.

4.1.66. 7-cyclopentyl-2-((4-(8-hydroxyoctanamido) phenyl) amino)-N, N-dimethyl-7H-pyrrolo[2,3-d] pyrimidine-6-carboxamide (46). To a suspension of compound (**5e**) (268 mg, 0.5 mmol) in 5 mL THF were added $LiAlH_4$ (29 mg, 0.75 mmol) at 0°C. After the completion of the addition, the cooling bath was removed and the reaction mixture was stirred at room temperature for about 4 hours. The reaction added NaOH aqueous solution (0.03 mL, 2N) and water 0.1 mL, filtered and washed by dichloromethane. The organic phase was washed by water and brine. The organic phase was dried over Na_2SO_4 , filtered and evaporated. The residue was purified by silica gel column chromatography (dichloromethane – methanol, gradient 100:0 → 90:10) to obtain 144 mg (57%) of **46** as a yellow solid, mp 159.7 °C. 1H NMR (400 MHz, $DMSO-d_6$) δ 9.82 – 9.64 (m, 1H), 9.54 – 9.36 (m, 1H), 8.71 (q, $J = 5.5, 4.6$ Hz, 1H), 7.84 – 7.66 (m, 2H), 7.50 (d, $J = 7.2$ Hz, 2H), 6.56 (q, $J = 6.1, 5.0$ Hz, 1H), 4.70 (q, $J = 9.4, 8.7$ Hz, 1H), 4.34 (d, $J = 6.8$ Hz, 1H), 3.03 (s, 6H), 2.48 (s, 2H), 2.25 (d, $J = 8.1$ Hz, 2H), 1.96 (dd, $J = 13.7, 7.3$ Hz, 4H), 1.60 (d, $J = 30.4$ Hz, 4H), 1.39 (s, 2H), 1.27 (d, $J = 8.2$ Hz, 6H). ^{13}C NMR (101 MHz, $DMSO-d_6$) δ 171.18, 163.37, 156.02, 152.57, 151.71, 136.75, 133.40, 131.80, 119.78, 118.92, 111.72, 101.19, 61.15, 57.39, 36.78, 35.14, 32.99, 30.02, 29.25, 29.22, 25.89, 25.65, 24.64. ESI-HRMS m/z calcd for $C_{28}H_{39}N_6O_3^+$ 507.3078, found 507.3080 [$M + H$] $^+$. HPLC purity 99%.

4.1.67. 8-((4-((7-cyclopentyl-6-(dimethylcarbamoyl)-7H-pyrrolo [2,3-d]pyrimidin-2-yl)amino)phenyl) amino)-8-oxooctanoic acid (47). To a suspension of compound (**5e**) (536 mg, 1 mmol) in THF/ CH_3OH/H_2O (5 mL/5 mL /5 mL) were added NaOH (60 mg, 4.5 mmol) and the mixture was stirred for 12 hours at room temperature. The reaction added saturated ammonium chloride aqueous solution (20 mL) and extracted by ethyl acetate. The organic phase was washed by water and brine. The organic phase was dried over $MgSO_4$, evaporated and the residue was purified by recrystallization (ethanol/ toluene) to obtain 484 mg (93%) of **47** as an orange solid, mp 218.7 °C. 1H NMR (400 MHz, $DMSO-d_6$) δ 12.01 (s, 1H), 9.75 (s, 1H), 9.46 (s, 1H), 8.71 (s, 1H), 7.75 (d, $J = 8.4$ Hz,

2H), 7.52 (d, $J = 8.5$ Hz, 2H), 6.55 (s, 1H), 4.72 (p, $J = 8.9$ Hz, 1H), 3.04 (d, $J = 7.5$ Hz, 6H), 2.50 – 2.39 (m, 2H), 2.27 (t, $J = 7.4$ Hz, 2H), 2.20 (t, $J = 7.3$ Hz, 2H), 2.02 – 1.90 (m, 4H), 1.70 – 1.54 (m, 4H), 1.55 – 1.46 (m, 2H), 1.35 – 1.25 (m, 4H). ^{13}C NMR (101 MHz, DMSO- d_6) δ 174.47, 170.66, 162.89, 155.54, 152.04, 151.24, 136.28, 132.92, 131.31, 119.33, 118.44, 111.24, 100.69, 56.91, 36.25, 34.55, 33.61, 29.55, 28.43, 28.34, 25.06, 24.38, 24.16. ESI-HRMS m/z calcd for $\text{C}_{28}\text{H}_{37}\text{N}_6\text{O}_4^+$ 521.2871, found 521.2872 $[\text{M} + \text{H}]^+$. HPLC purity 99%.

4.1.68. N1-(4-((7-cyclopentyl-6-(dimethylcarbamoyl)-7H-pyrrolo [2,3-d]pyrimidin-2-yl)amino)phenyl) -N8,N8-dimethyloctanediamide (48). To a two-necked flask, compound (**47**) (0.21 mmol, 110 mg), dimethylamine (0.42 mmol, 0.21 mL, 2.0mol/l in THF), EDCI (0.32 mmol, 61 mg), HOBt (0.25 mmol, 34 mg), DIEA (0.42 mmol, 54 mg) and THF (5 mL) were charged. The mixture was stirred at room temperature for 12 hours, then quenched by water. The mixture was extracted by ethyl acetate, and the combined organic layer was washed with brine solution and dried by anhydrous magnesium sulphate. The solvent was evaporated, and the residue was purified by silica gel column chromatography (dichloromethane – methanol, gradient 100:0 \rightarrow 94:6) to obtain 70.2 mg (61%) of **48** as a yellow solid, mp 169.5 $^{\circ}\text{C}$. ^1H NMR (400 MHz, DMSO- d_6) δ 9.76 (s, 1H), 9.46 (s, 1H), 8.71 (s, 1H), 7.74 (d, $J = 8.5$ Hz, 2H), 7.52 (d, $J = 8.5$ Hz, 2H), 6.56 (s, 1H), 4.72 (p, $J = 8.8$ Hz, 1H), 3.04 (s, 6H), 2.92 (s, 3H), 2.78 (s, 3H), 2.49 – 2.41 (m, 2H), 2.26 (q, $J = 8.0$ Hz, 4H), 2.04 – 1.88 (m, 4H), 1.72 – 1.52 (m, 4H), 1.48 (t, $J = 7.3$ Hz, 2H), 1.35 – 1.21 (m, 4H). ^{13}C NMR (101 MHz, DMSO- d_6) δ 172.32, 171.17, 163.38, 156.04, 152.54, 151.73, 136.76, 133.42, 131.81, 119.79, 118.91, 111.73, 101.18, 57.40, 37.12, 36.76, 35.19, 35.06, 32.74, 30.03, 29.07, 25.59, 25.02, 24.65. ESI-HRMS m/z calcd for $\text{C}_{30}\text{H}_{42}\text{N}_7\text{O}_3^+$ 548.3344, found 548.3346 $[\text{M} + \text{H}]^+$. HPLC purity 99%.

4.2 Biology:

4.2.1. Materials and Methods. Human lung cancer cell line A549 and H460 cells, human breast cancer cell line MDA-MB-231 and T47D cells, human hepatic cancer cell lines HEPG2 and HEP3B, 4T1 triple negative breast cancer cells were purchased from ATCC. All the cell lines were recently

1 authenticated by cellular morphology and the short tandem repeat analysis at Microread Inc. (Beijing,
2 China; May 2014) according to the guideline from ATCC.
3

4
5 **4.2.2. Cytotoxicity Assays.** Cells were seeded at a cell density of 3×10^3 cells/0.1 mL/well in a
6 96-well plate. The compounds were added 24h postplating at the indicated concentrations. Cell counts
7 were determined from duplicate wells 72h post-treatment. The total number of viable cells was
8 determined using the CCK-8 assay (Promega, WI) in conjunction with the Microplate reader (Promega,
9 WI).
10
11

12
13
14
15
16 **4.2.3. Kinase Inhibition Assays.** Kinase inhibition profiles were determined using KinaseProfiler
17 services provided by Eurofins, and ATP concentrations used are the K_m of corresponding kinases. The
18 binding affinities of **6e** projected on the human kinome tree were generated using the online Kinome
19 Render program.⁵⁹
20
21

22
23
24
25 **4.2.4. Cell Cycle Assay.** The different cell lines were plated onto 100 mm² dishes at a cell density of
26 1.0×10^6 cells/dish. All cells were treated with increasing concentrations of the indicated compounds
27 24h post plating. Cells were harvested 24h post-treatment, washed in phosphate buffered saline (PBS),
28 and fixed in ice cold 70% ethanol for at least 24 h. The fixed cells were then washed with room
29 temperature PBS and stained with propidium iodide (50 mg/mL) in the presence of RNase A (0.5 mg)
30 for 30 min at 37 °C. The stained cells were then analyzed using a Flow Cytometer. and the resulting
31 data analyzed with cell cycle analysis software (Modfit, BD).
32
33
34
35
36
37
38
39
40

41
42 **4.2.5. Apoptosis Assay.** Cells (3×10^5 cells/mL) were seeded in six-well plates and treated with
43 compounds at different concentration for 48 h. The cells were then harvested by trypsinization and
44 washed twice with cold PBS. After centrifugation and removal of the supernatants, cells were
45 resuspended in 500 μ L of $1 \times$ binding buffer which was then added to 5 μ L of annexin V-FITC and
46 incubated at room temperature for 15 min. After adding 10 μ L of PI the cells were incubated at room
47 temperature for another 15 min in dark. The stained cells were analyzed by a Flow Cytometer. All
48 experiments were performed three times.
49
50
51
52
53
54
55
56
57
58
59
60

4.2.6. Western blotting. Cell lysates from different cell lines were prepared with RIPA buffer in the presence of protease inhibitor cocktails and Phosphatase Inhibitor Cocktail 2 and 3 (P8340, P5726 and P0044, Sigma-Aldrich, St Louis, MO, USA). Protein (20-50 μ g) was separated by 8–15% Tris-acrylamide gels and transferred onto PVDF membrane the membrane was blocked in 5% skim milk, subsequently incubated with primary antibodies at 4°C over night followed by incubation with peroxidase-conjugated goat anti-mouse IgG or goat anti-rabbit IgG and developed with Pierce ECL reagent (cat. #17153, Millipore, Billerica, MA, USA). Antibody information: anti-phosphospecific Rb^{Ser807/811} (Cell Signaling Technology; catalogue no. 8516), Rb (Cell Signaling; catalogue no. 9309), Acetyl-Histone H3 (Cell Signaling Technology, catalogue no. 9649), phosphospecific p53^{Ser15} (Cell Signaling Technology; catalogue no. 9286), and Caspase 3 (Santa Cruz; catalogue no. 271028).

4.2.7. Immunofluorescence staining. Briefly, cells obtained and seeded on glass coverslips in complete 1640 in order to induce cell adhesion and then incubation with the inhibitors at different concentration. After 24h, the cells were fixed in 4% paraformaldehyde, permeabilized in 0.15% Triton X-100, saturated using 4% BSA in PBS at room temperature for 1h, and incubated overnight with anti-CDK4 or anti- acetyl histone H3 at 1:200 dilutions in PBS-4% BSA and then with a FITC-conjugated secondary antibody. Slides were mounted in glycerol-DABCO and observed using a Nikon Eclipse E600 microscope equipped with a digital camera. Images were elaborated only for brightness and contrast using Adobe Photoshop 7.

4.2.8. In vivo Assay. The experimental procedures of the animal study were proved by the Animal Care and Use Committee at Nankai University. 4T1 triple negative breast cancer cells (5×10^4) were injected bilaterally in the mammary fat pads of 6–8 week old female BALB/c mice (Taconic, NY). Once the tumors grew to a volume of approximately 100mm³, they were placed into five treatment groups (n = 4, with a total tumor number of 20). The mice were treated daily for 18 days by via intraperitoneal administration or 24 days via oral gavage. Body weights and tumor size were determined every other day. Tumor measurements were used using a digital vernier caliper, and the volumes were determined using the following calculation: (short²) \times long \times 0.5. Experiments were performed under an

approved IACUC protocol according to federal and institutional guidelines and regulations. Tumor measurements were used using a digital vernier caliper, and the volumes were determined using the following calculation: $(\text{short}^2) \times \text{long} \times 0.5$. Inhibition rate of tumor growth was calculated using the following formula: $100 \times \{1 - [(\text{tumor volume}_{\text{final}} - \text{tumor volume}_{\text{initial}}) \text{ for 9m-treated group}] / [(\text{tumor volume}_{\text{final}} - \text{tumor volume}_{\text{initial}}) \text{ for the vehicle-treated group}]\}$.

4.2.9. Immunohistochemistry staining. Immunohistochemistry staining was performed on the tumour BALB/c mice by using antibody against Bcl2, (BDbioscience, USA), p-Rb (Cell Signaling Technology, USA) separately, followed by the standard labelled streptavidin–biotin method by using the 3,3'-Diaminobenzidine (DAB) substrate. The images were recorded on an Olympus BX51 Epi-fluorescent microscope (Olympus Co. Tokyo, Japan) based on the images observed under a 20 × objective.

4.2.10. Procedure for LogP and LogD_{7.4} determination. LogP and LogD_{7.4} was determined by using well-known 'shake-flask' method and the concentrations of the test compound in the two phases were determined by HPLC (Shimadzu Prominence-i LC-2030C 3D system. column, InertSustain C18, 4.6 mm × 250 mm, 5 μm; mobile phase, gradient elution of methanol/H₂O; low rate, 1.0 mL/min; UV wavelength, 190–800 nm; temperature, 40 °C; injection volume, 10 μL).

The LogP was calculated by employing the following equation:

$\text{LogP} = \log (C_{\text{OCT}}/C_{\text{H}_2\text{O}})$; C_{OCT} , $C_{\text{H}_2\text{O}}$ were the compound's concentration in two phases

$\text{LogD}_{7.4} = \log (C_{\text{OCT}}/C_{\text{PBS}})$; C_{OCT} , C_{PBS} were the compound's concentration in two phases

4.2.11. Aqueous solubility determination. 1 mg of **6e** was weighed into 1-mL PBS at 7.4 and 1 mg of methanesulfonic acid formulation was weighed into 1-mL water. The samples were sonicated, vortexed and equilibrated by stirring at 100 rpm for 24 h and subsequently left standing, unstirred, for an additional 24 h at room temperature. At the end of equilibration, the entire sample volume was filtered manually through a 2.5 μm glass fiber syringe filter. The filtrate was subsequently analyzed by HPLC for solubility and the solubility of the samples determined in triplicate.

4.2.12. Assessments of Pharmacokinetic Properties. The pharmacokinetics analysis of **6e** was conducted in male Sprague–Dawley rats (Chinese Academy of Medical Science, Beijing, China). Briefly, catheters were surgically placed into the jugular veins of the rats to collect serial blood samples. **6e** was dissolved in saline with 5% (v/v) DMSO. The animals were administered a single dose of 20 mg/kg **6e** by iv and ip after fasting overnight. Blood was collected and centrifuged immediately to isolate plasma. The plasma concentrations were determined using high performance liquid chromatography with HPLC analysis on a Shimadzu Prominence-i LC-2030C 3D system.

4.2.13. Statistical analysis. Values were expressed as means±s.e.m. Significance was determined by χ^2 test, others were determined by Student's t-test. A value of $P < 0.05$ was used as the criterion for statistical significance. *Indicates significant difference with $P < 0.05$, **indicates significant difference with $P < 0.01$, ***indicates significant difference with $P < 0.001$.

ASSOCIATED CONTENT

The Supporting Information is available free of charge on the ACS Publications website.

Supporting Information

The pharmacophore features we defined based on the complex structure between CDK4 and HDAC1 with their ligands; Preliminary screen of dual-action compounds; In vitro growth inhibitory activities of dual-action compounds; The GI_{50} value of compound **6e**; Kinase Profiling Results of compound **6e**; molecular docking of the best candidate for enzymes inhibition; 1H and ^{13}C spectra of compounds; ESI-HRMS Spectra and HPLC Purity Analysis for Compound **6e** (PDF)

Molecular formula strings (CSV)

AUTHOR INFORMATION

Corresponding Author

* Y. F.: phone, +86 22 23509482; e-mail: yanfan@nankai.edu.cn.

*R.X.: phone, +86 22 23509482; e-mail: rxiang@nankai.edu.cn.

Author Contributions

[†]Y. L. and X. L. contributed equally to this work.

Notes

The authors declare no competing financial interest.

ACKNOWLEDGMENTS

This work was supported by the Project of Science and Technology Assistance in Developing Countries (KY201501006) and the National Natural Science Foundation of China (81470354) and the Natural Science Foundation of Tianjin (17JCQNJC13500)

ABBREVIATIONS USED

CDKs: cyclin-dependent kinases; HDACs: Histone deacetylases; SAR: structure-activity relationship; IC₅₀: half-maximal inhibitory concentrations; EDCI: 1-ethyl-3-(3-dimethylaminopropyl) carbodiimide; HOBt: 1-hydroxybenzotriazole; DIEA: *N,N*-diisopropylethylamine; DCM, dichloromethane; DMF, *N,N*-dimethylformamide.

References:

1. Asghar, U.; Witkiewicz, A. K.; Turner, N. C.; Knudsen, E. S. The history and future of targeting cyclin-dependent kinases in cancer therapy. *Nat. Rev. Drug Discovery* **2015**, *14*, 130-146.
2. Grana, X.; Reddy, E. P. Cell cycle control in mammalian cells: Role of cyclins, cyclin dependent kinases (cdks), growth suppressor genes and cyclin-dependent kinase inhibitors (ckis). *Oncogene* **1995**, *11*, 211-219.
3. Malumbres, M.; Barbacid, M. To cycle or not to cycle: A critical decision in cancer. *Nat. Rev. Cancer* **2001**, *1*, 222-231.
4. Malumbres, M.; Barbacid, M. Cell cycle, cdks and cancer: A changing paradigm. *Nat. Rev. Cancer* **2009**, *9*, 153.
5. Baker, S. J.; Reddy, E. P. Cdk4: A key player in the cell cycle, development, and cancer. *Genes Cancer* **2012**, *3*, 658-669.
6. Dickson, M. A. Molecular pathways: Cdk4 inhibitors for cancer therapy. *Clinical cancer research : an official journal of the American Association for Cancer Research* **2014**, *20*, 3379-3383.
7. Lim, J. S. J.; Turner, N. C.; Yap, T. A. Cdk4/6 inhibitors: Promising opportunities beyond breast

cancer. *Cancer Discovery* **2016**, *6*, 697-699.

8. O'Leary, B.; Finn, R. S.; Turner, N. C. Treating cancer with selective cdk4/6 inhibitors. *Nat. Rev. Clin. Oncol.* **2016**, *13*, 417.

9. Sherr, C. J.; Beach, D.; Shapiro, G. I. Targeting cdk4 and cdk6: From discovery to therapy. *Cancer Discovery* **2016**, *6*, 353-367.

10. Di Giovanni, C.; Novellino, E.; Chilin, A.; Lavecchia, A.; Marzaro, G. Investigational drugs targeting cyclin-dependent kinases for the treatment of cancer: An update on recent findings (2013-2016). *Expert Opin. Invest. Drugs* **2016**, *25*, 1215-1230.

11. Hamilton, E.; Infante, J. R. Targeting cdk4/6 in patients with cancer. *Cancer Treat. Rev.* **2016**, *45*, 129.

12. Lu, H.; Chang, D. J.; Baratte, B.; Meijer, L.; Schulze-Gahmen, U. Crystal structure of a human cyclin-dependent kinase 6 complex with a flavonol inhibitor, fisetin. *J. Med. Chem.* **2005**, *48*, 737-743.

13. Sanchez-Martinez, C.; Gelbert, L. M.; Lallena, M. J.; de Dios, A. Cyclin dependent kinase (cdk) inhibitors as anticancer drugs. *Bioorg. Med. Chem. Lett.* **2015**, *25*, 3420-3435.

14. Rader, J.; Russell, M. R.; Hart, L. S.; Nakazawa, M. S.; Belcastro, L. T.; Martinez, D.; Li, Y.; Carpenter, E. L.; Attiyeh, E. F.; Diskin, S. J.; Kim, S.; Parasuraman, S.; Caponigro, G.; Schnepf, R. W.; Wood, A. C.; Pawel, B.; Cole, K. A.; Maris, J. M. Dual cdk4/cdk6 inhibition induces cell-cycle arrest and senescence in neuroblastoma. *Clin. Cancer Res.* **2013**, *19*, 6173-6182.

15. Logan, J. E.; Mostofizadeh, N.; Desai, A. J.; Von Euw, E.; Conklin, D.; Konkankit, V.; Hamidi, H.; Eckardt, M.; Anderson, L.; Chen, H. W.; Ginther, C.; Taschereau, E.; Bui, P. H.; Christensen, J. G.; Belldgrun, A. S.; Slamon, D. J.; Kabbinavar, F. F. Pd-0332991, a potent and selective inhibitor of cyclin-dependent kinase 4/6, demonstrates inhibition of proliferation in renal cell carcinoma at nanomolar concentrations and molecular markers predict for sensitivity. *Anticancer Res.* **2013**, *33*, 2997-3004.

16. Finn, R. S.; Dering, J.; Conklin, D.; Kalous, O.; Cohen, D. J.; Desai, A. J.; Ginther, C.; Atefi, M.; Chen, I.; Fowst, C. Pd 0332991, a selective cyclin d kinase 4/6 inhibitor, preferentially inhibits

- proliferation of luminal estrogen receptor-positive human breast cancer cell lines in vitro. *Breast Cancer Res.* **2009**, *11*, 1-13.
17. Toogood, P. L.; Harvey, P. J.; Repine, J. T.; Sheehan, D. J.; VanderWel, S. N.; Zhou, H. R.; Keller, P. R.; McNamara, D. J.; Sherry, D.; Zhu, T.; Brodfuehrer, J.; Choi, C.; Barvian, M. R.; Fry, D. W. Discovery of a potent and selective inhibitor of cyclin-dependent kinase 4/6. *J. Med. Chem.* **2005**, *48*, 2388-2406.
18. Baughn, L. B.; Di Liberto, M.; Wu, K.; Toogood, P. L.; Louie, T.; Gottschalk, R.; Niesvizky, R.; Cho, H.; Ely, S.; Moore, M. A. S.; Chen-Kiang, S. A novel orally active small molecule potently induces G₁ arrest in primary myeloma cells and prevents tumor growth by specific inhibition of cyclin-dependent kinase 4/6. *Cancer Res.* **2006**, *66*, 7661-7667.
19. Reddy, M. V. R.; Akula, B.; Cosenza, S. C.; Athuluridivakar, S.; Mallireddigari, M. R.; Pallela, V. R.; Billa, V. K.; Subbaiah, D. R. C. V.; Bharathi, E. V.; Vasquez-Del Carpio, R.; Padgaonkar, A.; Baker, S. J.; Reddy, E. P. Discovery of 8-cyclopentyl-2-[4-(4-methyl-piperazin-1-yl)-phenylamino]-7-oxo-7,8-dihydro-pyrido[2,3-d]pyrimidine-6-carbonitrile (7x) as a potent inhibitor of cyclin-dependent kinase 4 (cdk4) and ampk-related kinase 5 (arks). *J. Med. Chem.* **2014**, *57*, 578-599.
20. Heilmann, A. M.; Perera, R. M.; Ecker, V.; Nicolay, B. N.; Bardeesy, N.; Benes, C. H.; Dyson, N. J. Cdk4/6 and igf1 receptor inhibitors synergize to suppress the growth of p16ink4a-deficient pancreatic cancers. *Cancer Res.* **2014**, *74*, 3947-3958.
21. Van Dort, M. E.; Hong, H.; Wang, H.; Nino, C. A.; Lombardi, R. L.; Blanks, A. E.; Galbán, S.; Ross, B. D. Discovery of bifunctional oncogenic target inhibitors against allosteric mitogen-activated protein kinase (mek1) and phosphatidylinositol 3-kinase (pi3k). *J. Med. Chem.* **2016**, *59*, 2512-2522.
22. Daniele, S.; Sestito, S.; Pietrobono, D.; Giacomelli, C.; Chiellini, G.; Di Maio, D.; Marinelli, L.; Novellino, E.; Martini, C.; Rapposelli, S. Dual inhibition of pdk1 and aurora kinase a: An effective strategy to induce differentiation and apoptosis of human glioblastoma multiforme stem cells. *ACS Chem. Neurosci.* **2017**, *8*, 100-114.

23. Xu, B. W.; Konze, K. D.; Jin, J.; Wang, G. G. Targeting ezh2 and prc2 dependence as novel anticancer therapy. *Exp. Hematol.* **2015**, *43*, 698-712.
24. Peserico, A.; Simone, C. Physical and functional hat/hdac interplay regulates protein acetylation balance. *J. Biomed. Biotechnol.* **2011**, *2011*, 1-10.
25. Witt, O.; Deubzer, H. E.; Milde, T.; Oehme, I. Hdac family: What are the cancer relevant targets? *Cancer Lett.* **2009**, *277*, 8-21.
26. West, A. C.; Johnstone, R. W. New and emerging hdac inhibitors for cancer treatment. *J. Clin. Invest.* **2014**, *124*, 30-39.
27. Khan, O.; La Thangue, N. B. Hdac inhibitors in cancer biology: Emerging mechanisms and clinical applications. *Immunol. Cell Biol.* **2012**, *90*, 85-94.
28. Chen, J. B.; Chern, T. R.; Wei, T. T.; Chen, C. C.; Lin, J. H.; Fang, J. M. Design and synthesis of dual-action inhibitors targeting histone deacetylases and 3-hydroxy-3-methylglutaryl coenzyme a reductase for cancer treatment. *J. Med. Chem.* **2013**, *56*, 3645-3655.
29. Yang, E. G.; Mustafa, N.; Tan, E. C.; Poulsen, A.; Ramanujulu, P. M.; Chng, W. J.; Yen, J. J. Y.; Dymock, B. W. Design and synthesis of janus kinase 2 (jak2) and histone deacetylase (hdac) bispecific inhibitors based on pacritinib and evidence of dual pathway inhibition in hematological cell lines. *J. Med. Chem.* **2016**, *59*, 8233-8262.
30. Ko, K. S.; Steffey, M. E.; Brandvold, K. R.; Soellner, M. B. Development of a chimeric c-src kinase and hdac inhibitor. *ACS Med. Chem. Lett.* **2013**, *4*, 779-783.
31. Sun, K. M.; Atoyan, R.; Borek, M. A.; Dellarocca, S.; Samson, M. E. S.; Ma, A. W.; Xu, G. X.; Patterson, T.; Tuck, D. P.; Viner, J. L.; Fattaey, A.; Wang, J. Dual hdac and pi3k inhibitor cudc-907 downregulates myc and suppresses growth of myc-dependent cancers. *Mol. Cancer Ther.* **2017**, *16*, 285-299.
32. Huang, J. M.; Sheard, M. A.; Ji, L. Y.; Sposto, R.; Keshelava, N. Combination of vorinostat and flavopiridol is selectively cytotoxic to multidrug-resistant neuroblastoma cell lines with mutant tp53. *Mol. Cancer Ther.* **2010**, *9*, 3289-3301.

33. Cho, Y. S.; Angove, H.; Brain, C.; Chen, C. H. T.; Cheng, H.; Cheng, R.; Chopra, R.; Chung, K.; Congreve, M.; Dagostin, C.; Davis, D. J.; Felten, R.; Giraldes, J.; Hiscock, S. D.; Kim, S.; Kovats, S.; Lagu, B.; Lewry, K.; Loo, A.; Lu, Y. P.; Luzzio, M.; Maniara, W.; McMenamin, R.; Mortenson, P. N.; Benning, R.; O'Reilly, M.; Rees, D. C.; Shen, J. Q.; Smith, T.; Wang, Y. P.; Williams, G.; Woolford, A. J. A.; Wrona, W.; Xu, M.; Yang, F.; Howard, S. Fragment-based discovery of 7-azabenzimidazoles as potent, highly selective, and orally active cdk4/6 inhibitors. *ACS Med. Chem. Lett.* **2012**, *3*, 445-449.
34. Tarcsay, A.; Keseru, G. M. Contributions of molecular properties to drug promiscuity miniperspective. *J. Med. Chem.* **2013**, *56*, 1789-1795.
35. Salmi-Smail, C.; Fabre, A.; Dequiedt, F.; Restouin, A.; Castellano, R.; Garbit, S.; Roche, P.; Morelli, X.; Brunel, J. M.; Collette, Y. Modified cap group suberoylanilide hydroxamic acid histone deacetylase inhibitor derivatives reveal improved selective antileukemic activity. *J. Med. Chem.* **2010**, *53*, 3038-3047.
36. Wang, T.; Sepulveda, M.; Gonzales, P.; Gately, S. Identification of novel hdac inhibitors through cell based screening and their evaluation as potential anticancer agents. *Bioorg. Med. Chem. Lett.* **2013**, *23*, 4790-4793.
37. He, R.; Chen, Y. F.; Chen, Y. H.; Ougolkov, A. V.; Zhang, J. S.; Savoy, D. N.; Billadeau, D. D.; Kozikowski, A. P. Synthesis and biological evaluation of triazol-4-ylphenyl-bearing histone deacetylase inhibitors as anticancer agents. *J. Med. Chem.* **2010**, *53*, 1347-1356.
38. Lu, C. C.; Zhang, K.; Zhang, Y.; Tan, M. J.; Li, Y. J.; He, X. W.; Zhang, Y. K. Preparation and characterization of vorinostat-coated beads for profiling of novel target proteins. *J. Chromatogr. A* **2014**, *1372*, 34-41.
39. Le Brazidec, J. Y.; Pasis, A.; Tam, B.; Boykin, C.; Wang, D. P.; Marcotte, D. J.; Claassen, G.; Chong, J. H.; Chao, J. H.; Fan, J. H.; Nguyen, K.; Silvian, L.; Ling, L.; Zhang, L.; Choi, M.; Teng, M.; Pathan, N.; Zhao, S.; Li, T.; Taveras, A. Structure-based design of 2,6,7-trisubstituted-7h-pyrrolo[2,3-d]pyrimidines as aurora kinases inhibitors. *Bioorg. Med. Chem. Lett.* **2012**, *22*, 4033-4037.

40. Mazitschek, R.; Patel, V.; Wirth, D. F.; Clardy, J. Development of a fluorescence polarization based assay for histone deacetylase ligand discovery. *Bioorg. Med. Chem. Lett.* **2008**, *18*, 2809-2812.
41. Kiriy, N.; Bocharova, V.; Kiriy, A.; Stamm, M.; Krebs, F. C.; Adler, H. J. Designing thiophene-based azomethine ligomers with tailored properties: Self-assembly and charge carrier mobility. *Chem. Mater.* **2004**, *16*, 4765-4771.
42. Garofalo, A.; Farce, A.; Ravez, S.; Lemoine, A.; Six, P.; Chavatte, P.; Goossens, L.; Depreux, P. Synthesis and structure-activity relationships of (aryloxy)quinazoline ureas as novel, potent, and selective vascular endothelial growth factor receptor-2 inhibitors. *J. Med. Chem.* **2012**, *55*, 1189-1204.
43. Brain, C.; Thomas; Cho, Y. S.; Giraldes, J., William; Lagu, B.; Levell, J.; Luzzio, M.; Perez, L., Blas; Wang, Y.; Yang, F. Pyrrolopyrimidine compounds as inhibitors of cdk4/6. WO 2011101409 A1, 08/25/2011, 2011.
44. Qin, M. Z.; Wang, T. T.; Xu, B. X.; Ma, Z. H.; Jiang, N.; Xie, H. B.; Gong, P.; Zhao, Y. F. Novel hydrazone moiety-bearing aminopyrimidines as selective inhibitors of epidermal growth factor receptor t790m mutant. *Eur. J. Med. Chem.* **2015**, *104*, 115-126.
45. Denny, W. A. D., Ellen Myra; Kramer, James Bernard; Mc Namara, Dennis Joseph; Rewcastle, Gordon William; Showalter, Howard Daniel Hollis; Toogood, Peter Laurence. Preparation of pteridinones as kinase inhibitors. WO 2001019825 A1, 03/22/2001, 2001.
46. Andrews, D., Michael; Jones, C., David; Simpson, I.; Ward, R., Andrew. 2-anilnopyurin-8-ones as inhibitors of tk/mps1 for the treatment of proliferative disorders. WO 2009024824 A1, 02/26/2009, 2009.
47. Yamashita, Y.; Mutoh, Y.; Yamasaki, R.; Kasama, T.; Saito, S. Synthesis of [3]rotaxanes that utilize the catalytic activity of a macrocyclic phenanthroline-Cu complex: remarkable effect of the length of the axle precursor. *Chem. Eur. J.* **2015**, *21*, 2139-2145.
48. Wang, T.; Lamb, M. L.; Scott, D. A.; Wang, H.; Block, M. H.; Lyne, P. D.; Lee, J. W.; Davies, A. M.; Zhang, H. J.; Zhu, Y. Y.; Gu, F.; Han, Y. X.; Wang, B.; Mohr, P. J.; Kaus, R. J.; Josey, J. A.; Hoffmann, E.; Thress, K.; MacIntyre, T.; Wang, H. Y.; Omer, C. A.; Yu, D. W. Identification of

- 4-aminopyrazolylpyrimidines as potent inhibitors of trk kinases. *J. Med. Chem.* **2008**, *51*, 4672-4684.
49. VanderWel, S. N.; Harvey, P. J.; McNamara, D. J.; Repine, J. T.; Keller, P. R.; Quin, J.; Booth, R. J.; Elliott, W. L.; Dobrusin, E. M.; Fry, D. W.; Toogood, P. L. Pyrido[2,3-d]pyrimidin-7-ones as specific inhibitors of cyclin-dependent kinase 4. *J. Med. Chem.* **2005**, *48*, 2371-2387.
50. Chen, Y.; Lopez-Sanchez, M.; Savoy, D. N.; Billadeau, D. D.; Dow, G. S.; Kozikowski, A. P. A series of potent and selective, triazolylphenyl-based histone deacetylases inhibitors with activity against pancreatic cancer cells and plasmodium falciparum. *J. Med. Chem.* **2008**, *51*, 3437-3448.
51. Cholody, W. M.; Kosakowska-Cholody, T.; Hollingshead, M. G.; Hariprakash, H. K.; Michejda, C. J. A new synthetic agent with potent but selective cytotoxic activity against cancer. *J. Med. Chem.* **2005**, *48*, 4474-4481.
52. Chen, P.; Lee, N. V.; Hu, W. Y.; Xu, M. R.; Ferre, R. A.; Lam, H.; Bergqvist, S.; Solowiej, J.; Diehl, W.; He, Y. A.; Yu, X.; Nagata, A.; VanArsdale, T.; Murray, B. W. Spectrum and degree of cdk drug interactions predicts clinical performance. *Mol. Cancer Ther.* **2016**, *15*, 2273-2281.
53. Eswar, N.; Eramian, D.; Webb, B.; Shen, M. Y.; Sali, A. Protein structure modeling with modeller. *Methods Mol Biol* **2008**, *426*, 145-159.
54. Delano, W. L. The pymol molecular graphics system, version 1.7; schrödinger, llc: New york, 2014.
55. Munster, P. N.; Troso-Sandoval, T.; Rosen, N.; Rifkind, R.; Marks, P. A.; Richon, V. M. The histone deacetylase inhibitor suberoylanilide hydroxamic acid induces differentiation of human breast cancer cells. *Cancer Res.* **2001**, *61*, 8492-8497.
56. Wang, H.; Nicolay, B. N.; Chick, J. M.; Gao, X.; Geng, Y.; Ren, H.; Gao, H.; Yang, G.; Williams, J. A.; Suski, J. M.; Keibler, M. A.; Sicinska, E.; Gerdemann, U.; Haining, W. N.; Roberts, T. M.; Polyak, K.; Gygi, S. P.; Dyson, N. J.; Sicinski, P. The metabolic function of cyclin d3-cdk6 kinase in cancer cell survival. *Nature* **2017**, *546*, 426-430.
57. Pabla, N.; Gibson, A. A.; Buege, M.; Ong, S. S.; Li, L.; Hu, S.; Du, G.; Sprowl, J. A.; Vasilyeva, A.; Janke, L. J.; Schlatter, E.; Chen, T.; Ciarimboli, G.; Sparreboom, A. Mitigation of acute kidney injury by cell-cycle inhibitors that suppress both cdk4/6 and oct2 functions. *Proceedings of the National Academy*

1 *of Sciences of the United States of America* **2015**, *112*, 5231-5236.

2 58. Eschbach, R. S.; Kazmierczak, P. M.; Heimer, M. M.; Todica, A.; Hirner-Eppeneder, H.; Schneider,
3 M. J.; Keinrath, G.; Solyanik, O.; Olivier, J.; Kunz, W. G.; Reiser, M. F.; Bartenstein, P.; Ricke, J.; Cyran,
4 C. C. (18)f-fdg-pet/ct and diffusion-weighted mri for monitoring a braf and cdk 4/6 inhibitor
5 combination therapy in a murine model of human melanoma. *Cancer imaging : the official publication*
6 *of the International Cancer Imaging Society* **2018**, *18*, 2.

7 59. Chartier, M.; Chenard, T.; Barker, J.; Najmanovich, R. Kinome render: A stand-alone and
8 web-accessible tool to annotate the human protein kinome tree. *PeerJ* **2013**, *1*, e126.
9
10
11
12
13
14
15
16
17
18
19
20
21
22
23
24
25
26
27
28
29
30
31
32
33
34
35
36
37
38
39
40
41
42
43
44
45
46
47
48
49
50
51
52
53
54
55
56
57
58
59
60

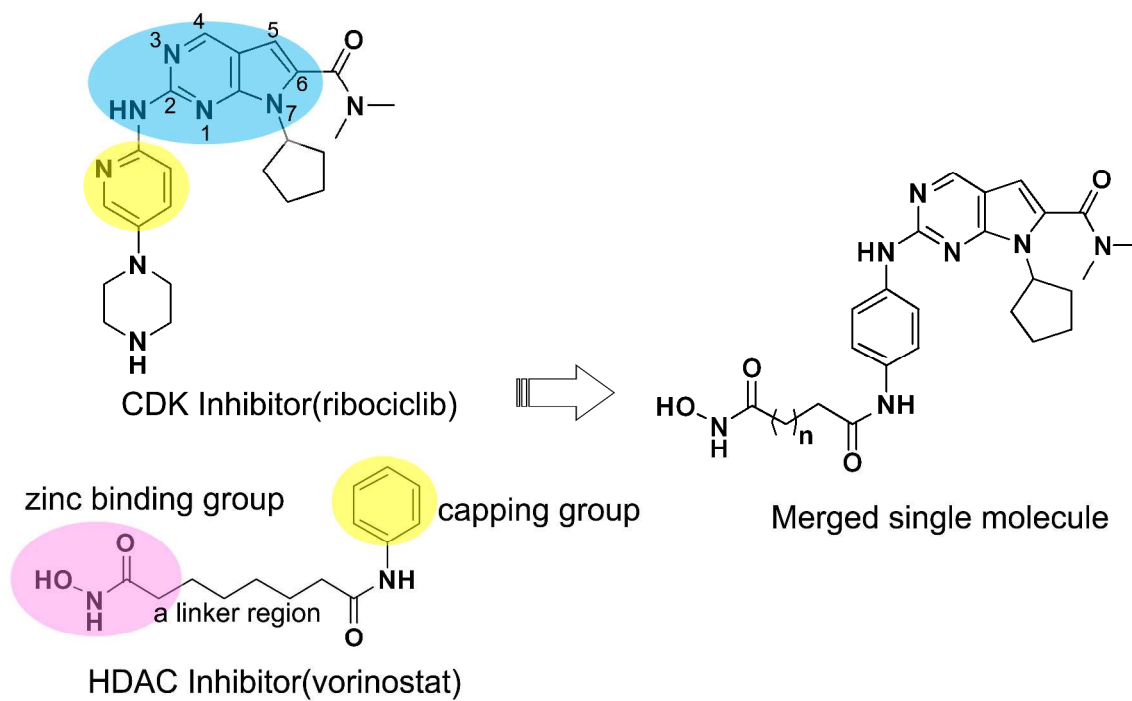


Figure 1. Schematic showing design for merged CDK-HDAC pharmacophore.

1a: $n = 4$
1b: $n = 5$
1c: $n = 6$
1d: $n = 7$

2a: $R^1 = 2\text{-NH}_2$
2b: $R^1 = 3\text{-NH}_2$
2c: $R^1 = 4\text{-NH}_2$

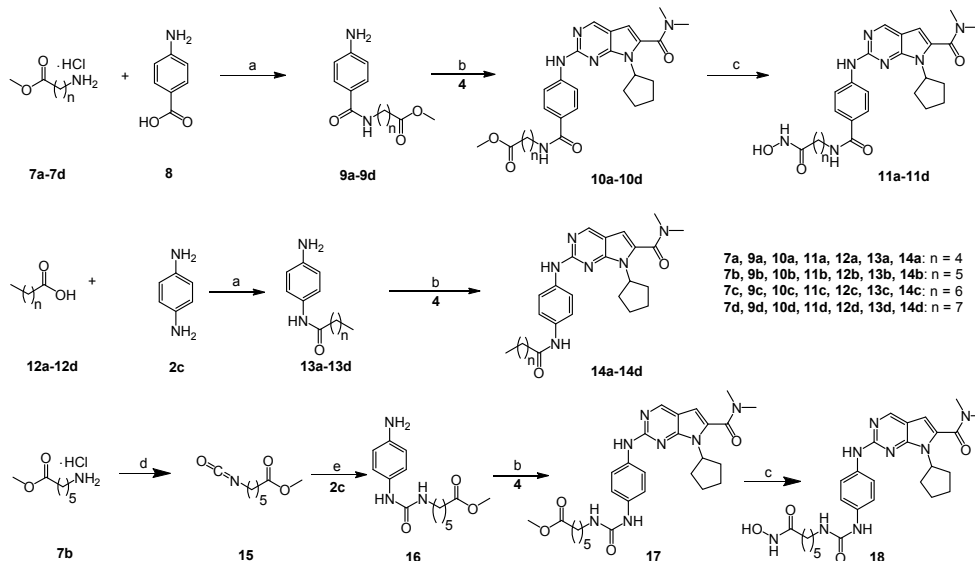
3a: $n = 6, R^1 = 2\text{-NH}_2$
3b: $n = 6, R^1 = 3\text{-NH}_2$
3c: $n = 4, R^1 = 4\text{-NH}_2$
3d: $n = 5, R^1 = 4\text{-NH}_2$
3e: $n = 6, R^1 = 4\text{-NH}_2$
3f: $n = 7, R^1 = 4\text{-NH}_2$

4

5a, 6a: $n = 6$
5b, 6b: $n = 6$

6a-6f

5c, 6c: $n = 4$
5d, 6d: $n = 5$
5e, 6e: $n = 6$
5f, 6f: $n = 7$

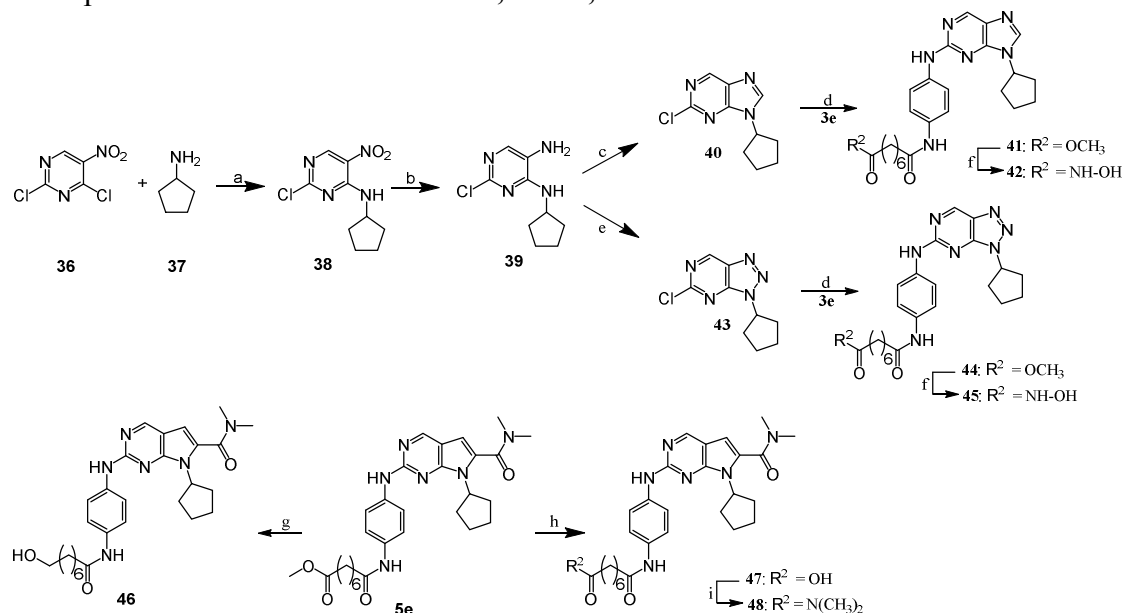


59
ACS Paragon Plus Environment

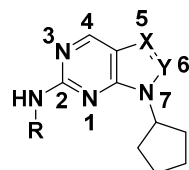
[illegible]

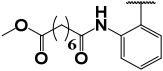
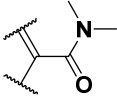
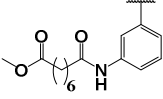
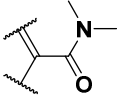
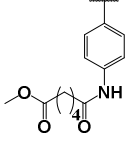
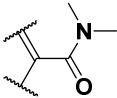
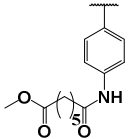
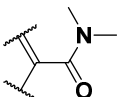
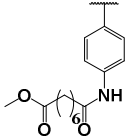
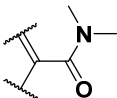
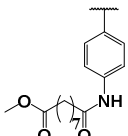
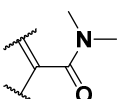
^a Reagents and conditions: (a) Pd(OAc)₂, BINAP, Cs₂CO₃, 100 °C, 12 h, 79% yield for **27**, 46% yield for **31**, 77% yield for **35**; (b) con HCl, THF, 84% yield for **20** over two steps, 66% yield for **30**; (c) N₂H₄·H₂O (80%), EtOH, 80°C, 6 h, 79% yield; (d) EDCI, HOBT, DIEA, rt, 12 h, 72% yield for **22**, 32% yield for **23**, 49% yield for **24**, 67% yield for **26**; (e) NH₂OH, CH₃OH, reflux, 18 h, 67% yield for **25**, 49% yield for **28**, 64% yield for **32**; (f) 5-nitropyridin-2-amine, SOCl₂, pyridine, THF, 80°C, 6 h, 10% yield; (g) Pd/C, HCOONH₄, EtOH, 80°C, 12 h, 88% yield.

Scheme 3. Preparation of Derivatives of **41-42, **44-45**, **46-48**^a**

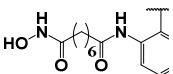
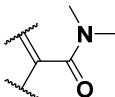
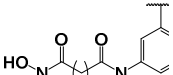
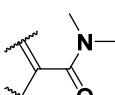
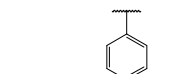
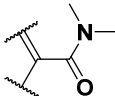
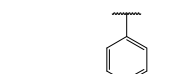
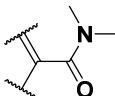
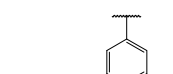
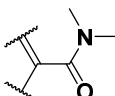
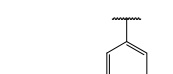
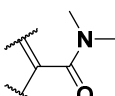
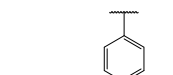
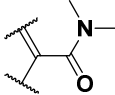
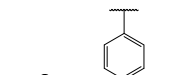
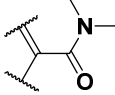
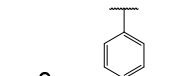
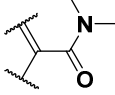
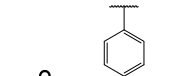
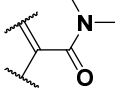
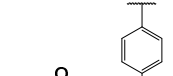
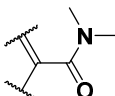


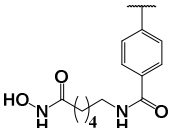
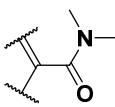
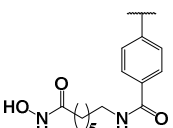
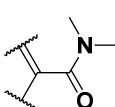
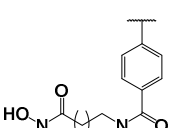
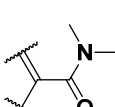
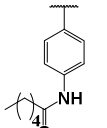
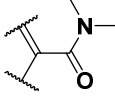
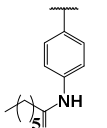
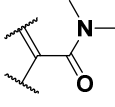
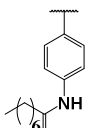
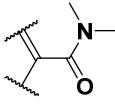
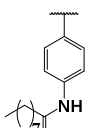
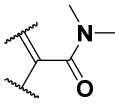
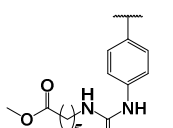
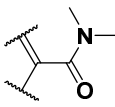
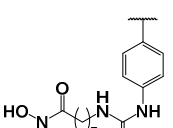
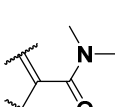
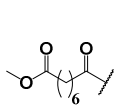
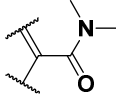
^aReagents and conditions: (a) DIEA, EA, -40°C to rt, 2 h, 99% yield; (b) $\text{SnCl}_2 \cdot 2\text{H}_2\text{O}$, EtOH, reflux, 2 h, 85% yield; (c) triethylorthoformate, MgSO_4 , DMF, 130°C, 2h, 47% yield; (d) $\text{Pd}(\text{OAc})_2$, BINAP, Cs_2CO_3 , 100 °C, 12 h, 77% yield for **41**, 45% yield for **44**; (e) NaNO_2 , con HCl, 0°C to rt, 3.25h, 65% yield; (f) NH_2OH , CH_3OH , reflux, 18 h, 45% yield for **42**, 32% yield for **45**; (g) LiAlH_4 , THF, 0°C to rt, 4 h, 57% yield; (h) NaOH, THF/ CH_3OH / H_2O , rt, 12 h, 93% yield; (i) $\text{HN}(\text{CH}_3)_2$, EDCI, HOBT, DIEA, rt, 12 h, 61% yield.

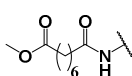
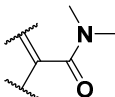
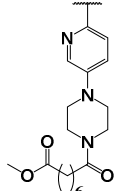
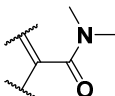
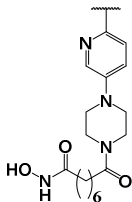
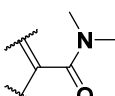
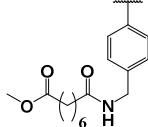
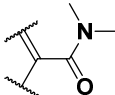
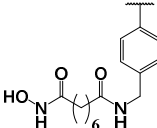
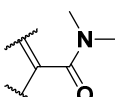
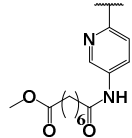
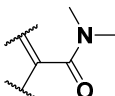
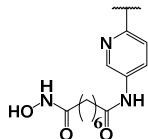
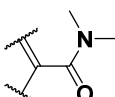
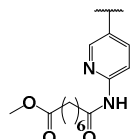
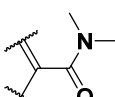
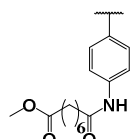
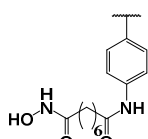
Table 1. IC₅₀ Values for Enzymatic Inhibition of CDK4 and HDAC1

Compound	R	X	Y	IC ₅₀ (nM) ^a	
				CDK4	HDAC1
CDK Inhibitor					
(ribociclib)	--	--	--	13	--
HDAC Inhibitor					
(vorinostat)	--	--	--	--	27
5a		CH		>5000	--
5b		CH		26	--
5c		CH		4.8	--
5d		CH		10	--
5e		CH		12	>5000
5f		CH		24	--

1
2
3
4
5
6
7
8
9
10
11
12
13
14
15
16
17
18
19
20
21
22
23
24
25
26
27
28
29
30
31
32
33
34
35
36
37
38
39
40
41
42
43
44
45
46
47
48
49
50
51
52
53
54
55
56
57
58
59
60

6a		CH		>5000	37
6b		CH		30	3.1
6c		CH		11	27
6d		CH		10	0.84
6e		CH		8.8	2.2
6f		CH		8.1	3.0
10a		CH		6.3	--
10b		CH		7.3	--
10c		CH		11	--
10d		CH		8.2	--
11a		CH		11	--

11b		CH		9.6	0.53
11c		CH		12	1.4
11d		CH		26	1.6
14a		CH		10	>5000
14b		CH		27	--
14c		CH		29	--
14d		CH		123	--
17		CH		23	--
18		CH		8.4	1.6
22		CH		>5000	--

23		CH		>5000	--
24		CH		13	>5000
25		CH		13	39
27		CH		25	--
28		CH		10	53
31		CH		47	>5000
32		CH		93	423
35		CH		16	--
41		N	CH	>5000	>5000
42		N	CH	>5000	2.6

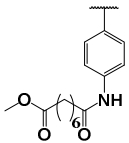
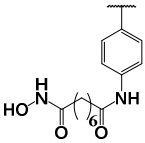
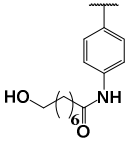
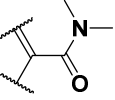
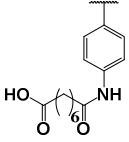
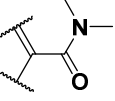
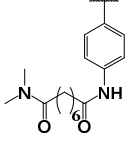
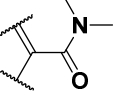
44		N	N	857	>5000
45		N	N	1140	433
46		CH		10	>5000
47		CH		18	>5000
48		CH		16	>5000

Table 2. Cytotoxic Activity of compound **6e** against cancer cell lines

Cell lines	IC ₅₀ value (μM)		
	CDK Inhibitor	Compound 6e	HDAC Inhibitor
	ribociclib		vorinostat
4T1	>10	1.11 ± 0.45	4.76 ± 0.69
MDA-MB-231	>10	1.86 ± 0.45	2.59 ± 0.95
MDA-MB-468	>10	1.82 ± 0.35	2.69 ± 0.86
T47D	6.23 ± 4.04	2.59 ± 0.59	3.01 ± 1.13
A549	>10	1.33 ± 0.57	3.70 ± 0.18
H1299	5.46 ± 2.65	1.87 ± 0.27	3.46 ± 0.47
H460	>10	3.78 ± 0.86	6.29 ± 1.37
Hep G2	>10	3.37 ± 0.33	2.57 ± 0.43
Hep 3B	>10	1.24 ± 0.27	2.30 ± 0.46

The IC₅₀ values are shown in the forms. The cytotoxic effect of compounds were assayed using CCK-8 assay with 72 hours incubation. Data are mean ± SD values from three independent experiments.

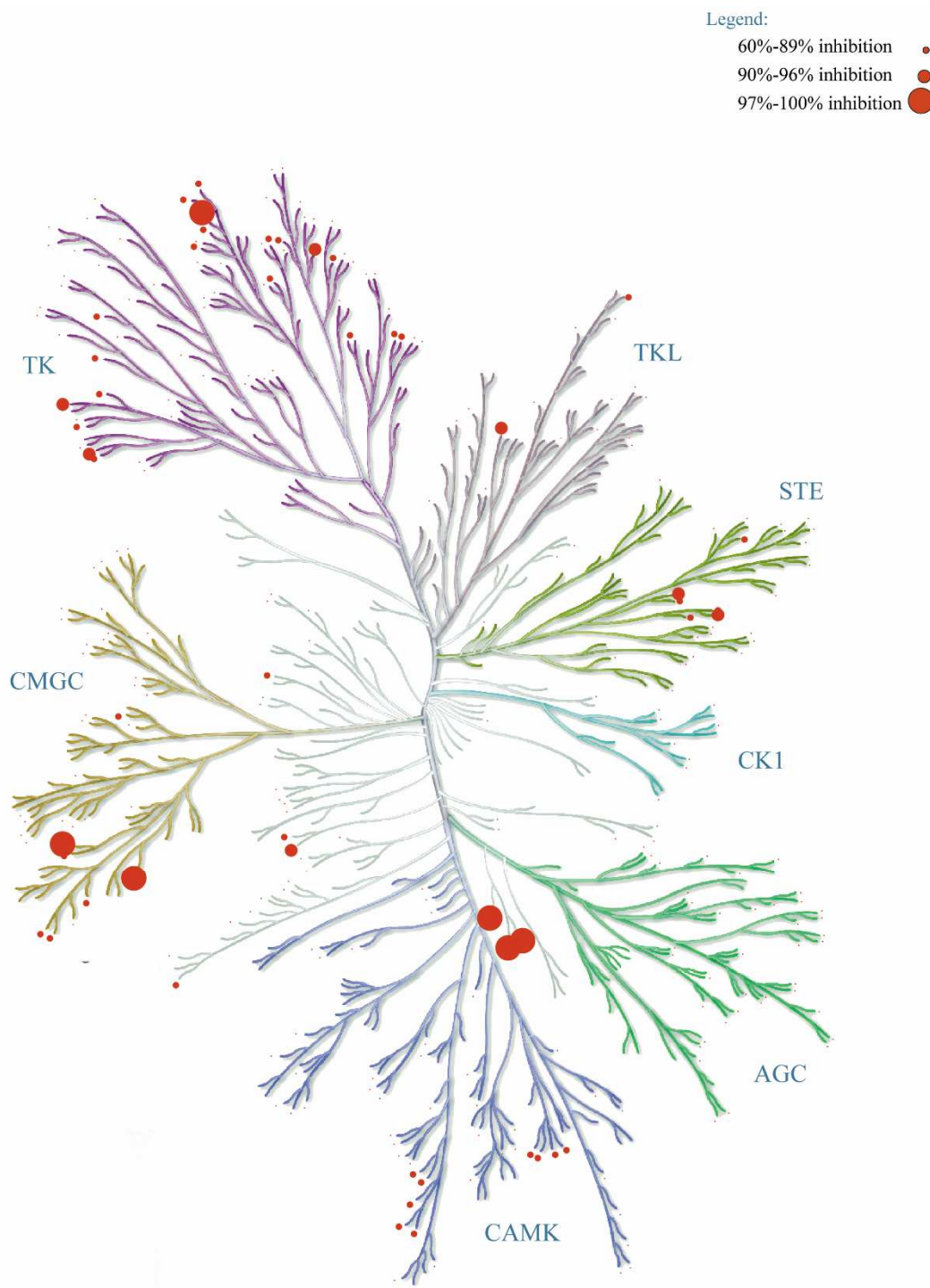


Figure 2. Kinase binding selectivity for compound **6e** shown on the human kinome dendrogram. The inhibition rates were determined using the KinaseProfiler of Eurofins. The figure was generated by using an online Kinome Render program (<http://bcb.med.usherbrooke.ca/kinomerenderLig.php>).

Table 3. Kinase inhibition profile of compound **6e** against selected protein kinases ^a

Kinase	IC ₅₀ (μM)	Kinase	Inhibition(%) at 1 μM
CDK4/cyclinD3(h)	0.0088	CDK1/cyclinB(h)	55
CDK9/cyclin T1(h)	0.009	CDK2/cyclinA(h)	71
Aurora-A(h)	0.012	CDK2/cyclinE(h)	66
Aurora-B(h)	0.019	CDK3/cyclinE(h)	68
Aurora-C(h)	0.022	CDK4/cyclinD3(h)	101
CaMKK2(h)	0.053	CDK5/p25(h)	78
Flt4(h)	0.043	CDK5/p35(h)	72
LIMK1(h)	0.044	CDK6/cyclinD3(h)	70
TAO2(h)	0.084	CDK7/cyclinH/MAT1(h)	-11
TrkA(h)	0.031	CDK9/cyclin T1(h)	97

^aIC₅₀ values and inhibition values were determined using KinaseProfiler by Eurofins. The data represent the mean values of two independent experiments.

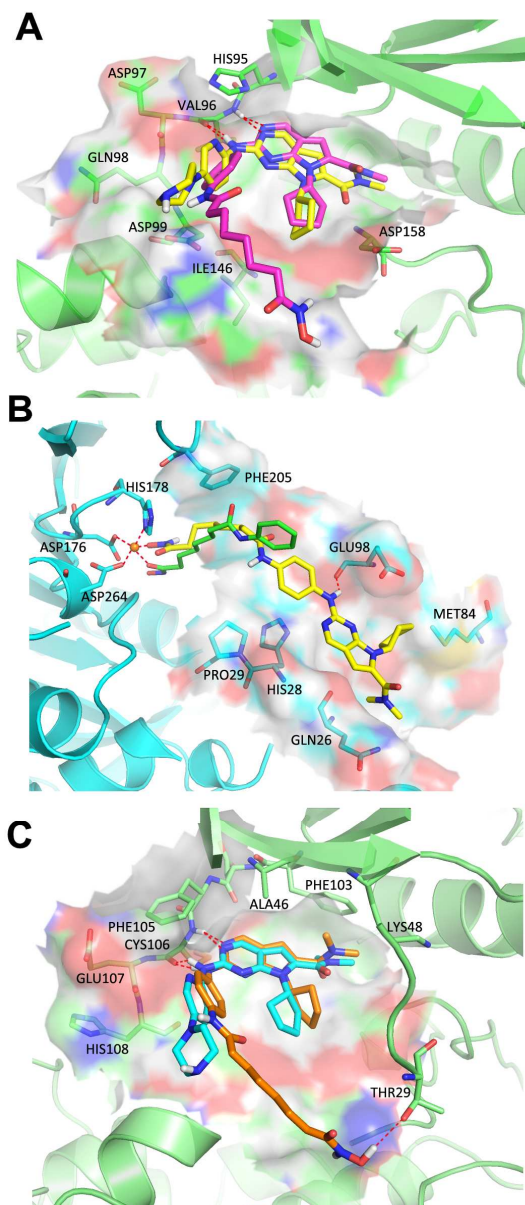


Figure 3. (A) Representation of the predicted binding modes of compound 6e (purple) and ribociclib (yellow) in the ATP pocket of CDK4 which employed CDK6 (PDB entry: 4EZ5) as the template for homology modeling. Dash lines indicate the H-bond interaction between compounds and CDK4. (B) Predicted binding mode of compound 6e (yellow) and vorinostat (green) with HDAC1. The crystal structure of HDAC1 was taken from the RCSB Protein Data Bank (PDB entry: 4BKX). (C) Proposed binding mode of compound 6e (orange) and ribociclib (cyan) within the active site of CDK9 (PDB code 4BCF). The dash lines represent the H-bond interaction between compounds and CDK9.

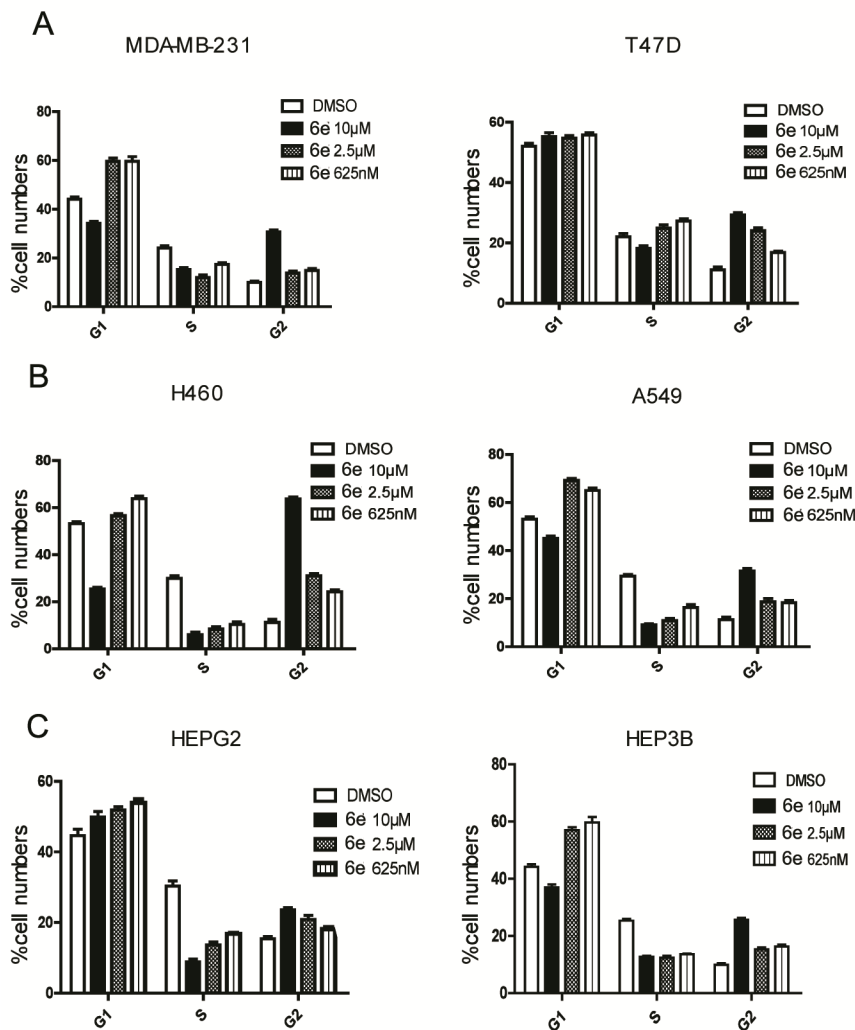


Figure 4. Effect of compound 6e on cell cycle progression of human tumor cell lines. Compound 6e induces G2 arrest in high concentration and induces G1 arrest in low concentration. (A) MDA-MB-231 and T47D cell lines; (B) H460 and A549 cell lines; (C) HepG2 and Hep3B cell lines;

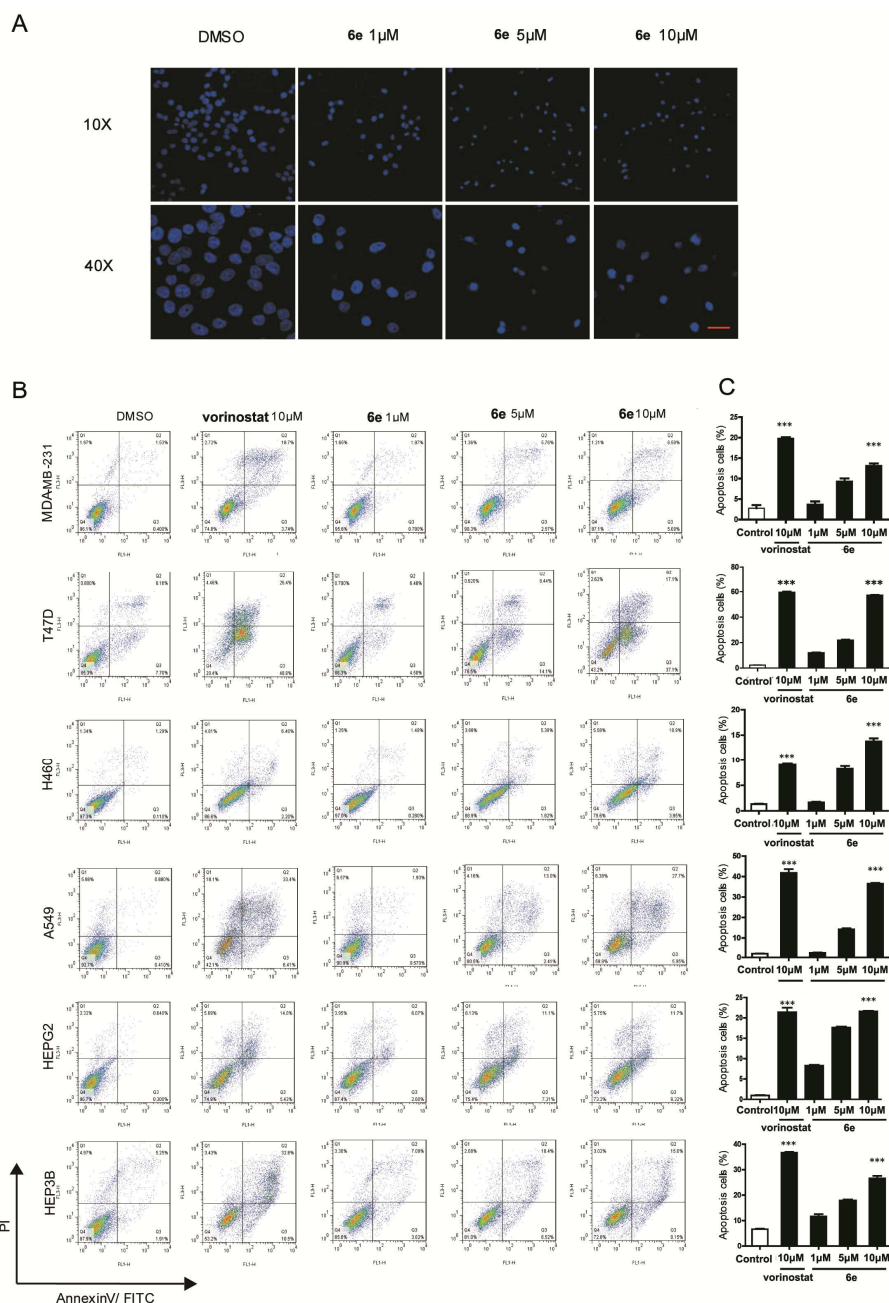
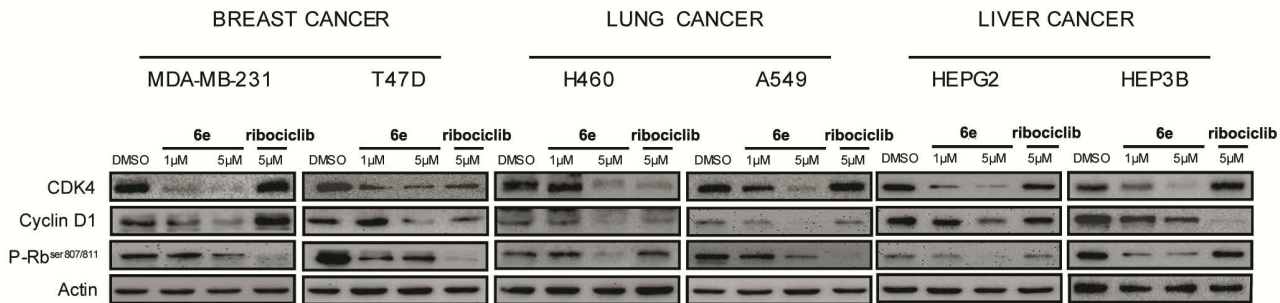


Figure 5. Compound **6e** induces cell apoptosis in vitro. (A) Hoechst 33342 nuclear staining of T47D cell line, showing the basal level of cells with apoptotic bodies in untreated control (left) and a dose-dependent increase in the number of apoptotic cells after treatment with compound **6e**. Representative pictures, scale bar 20 μ m. (B) Flow cytometry and (C) quantitative analysis of apoptotic cells. Cells were incubated with the indicated concentrations of compound **6e** or vorinostat for 48 h and were stained with FITC-Annexin V/PI, followed by flow cytometry analysis. Data are expressed as means \pm SD of the percentages of apoptotic cells from three independent experiments, ***P < 0.001.

1
2
3
4
5
6
7
8
9
10
11
12
13
14
15
16
17
18
19
20
21
22
23
24
25
26
27
28
29
30
31
32
33
34
35
36
37
38
39
40
41
42
43
44
45
46
47
48
49
50
51
52
53
54
55
56
57
58
59
60

A



B

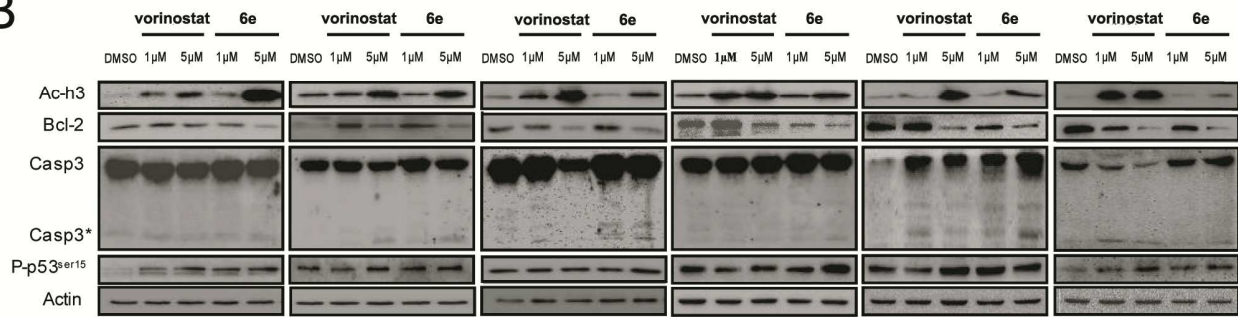


Figure 6. Western blotting analysis for inhibition of (A) CDK4 and (B) histone acetylation pathway. Breast cell lines (MDA-MB-231 and T47D), lung cancer cell lines(H460 and A549) and liver cancer cell lines (HepG2 and Hep3B) were treated with 1 and 5 μM of compound **6e** and vorinostat for 48 h.

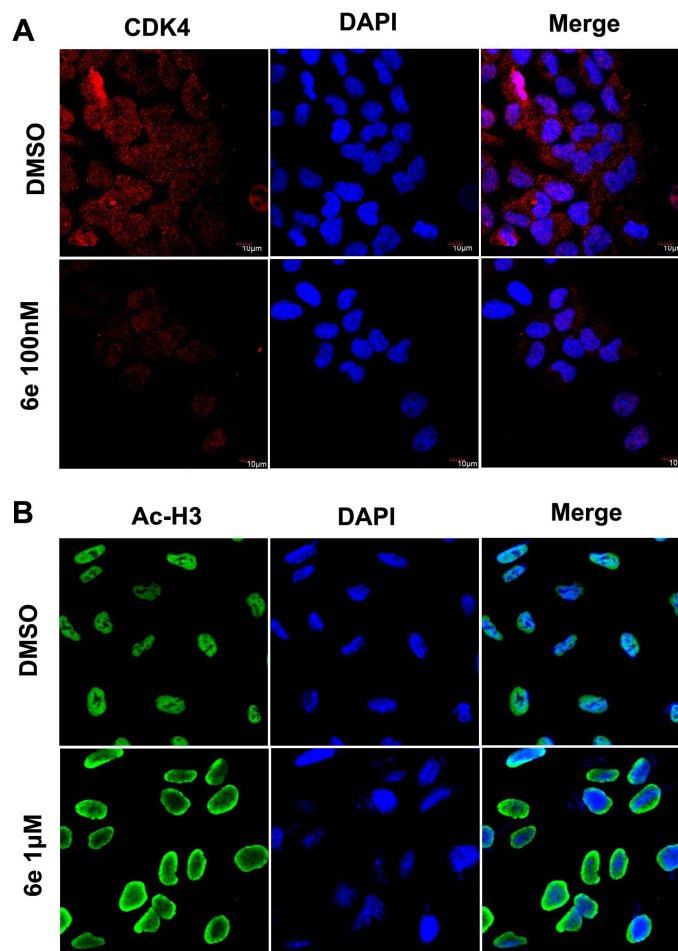


Figure 7. Immunofluorescence staining of (A) CDK4 in untreated cells (control, upper panel) or treated with compound **6e** (lower panel) at 100 nM and (B) acetyl-histone H3 in untreated cells (control, upper panel) or treated with compound **6e** (lower panel) at 1 μM. Nuclei were counterstained with DAPI. The merged images are shown in the right column. Representative images, scale bar 10 μm.

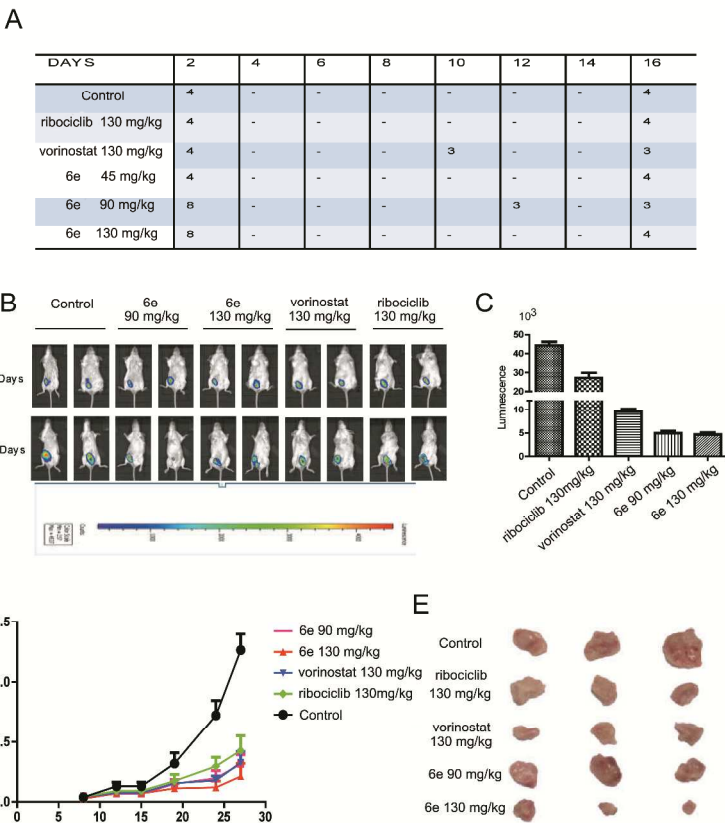


Figure 8. In vivo antitumor efficacy of compound **6e** against 4T1 tumor xenograft models with IP administration. (A) Effects of compound **6e**, ribociclib and vorinostat on toxicity and animal survival. (B) Representative animals injected with 5×10^4 Fluc-4T1 shows significant bioluminescence activity at day 8 and day 25. (C) Quantitative analysis of tumor inhibitory responses by bioluminescence imaging signals at day 25 demonstrated that compound **6e** showed significantly better inhibitory. (D) and (E) Tumor volumes were recorded. Animals were treated with solvent control, compound **6e** at doses of 90 and 130 mg/kg/day, ribociclib and vorinostat at a dose of 130 mg/kg/day through IP injection.

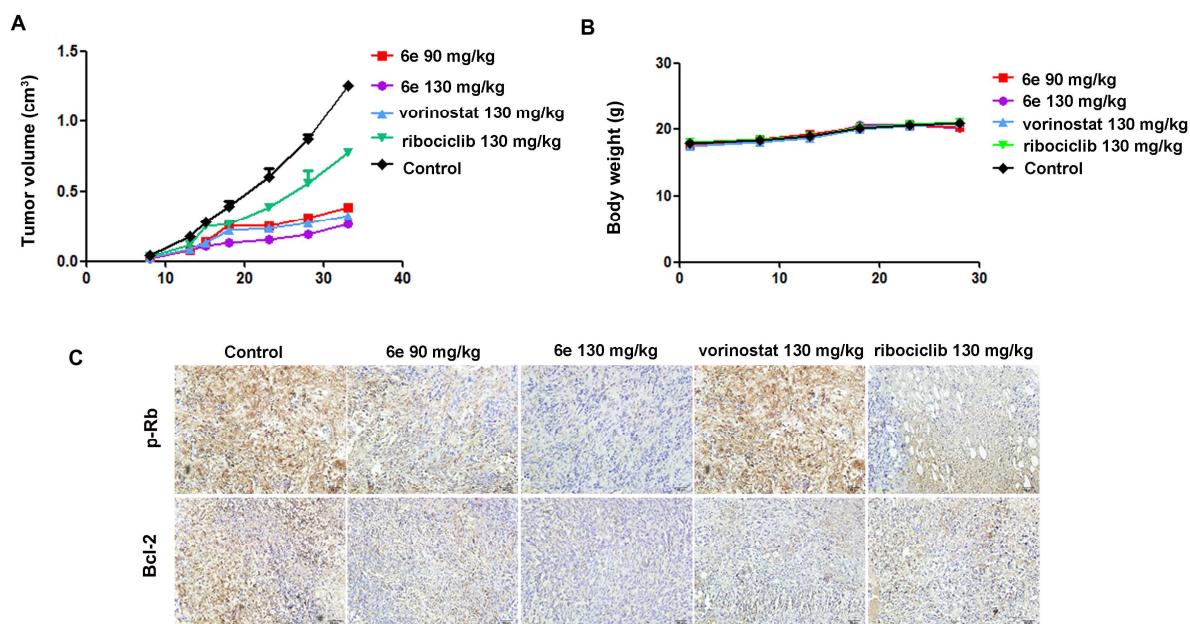
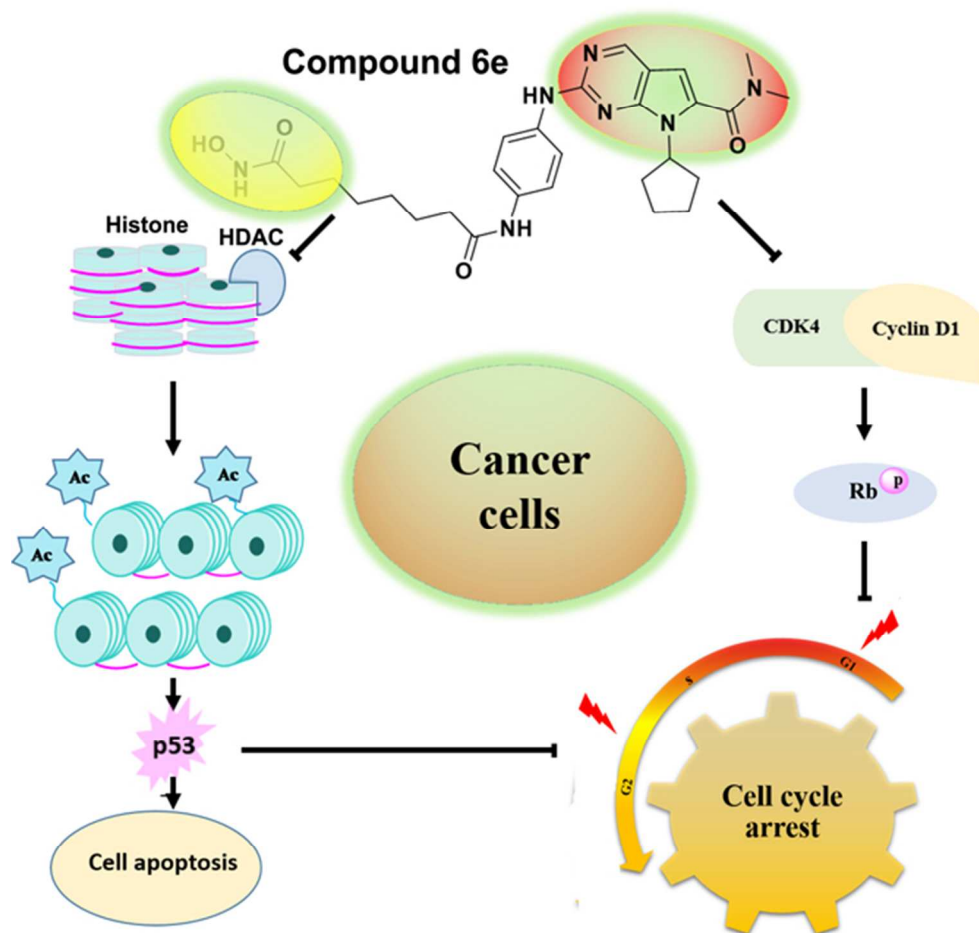


Figure 9. In vivo antitumor efficacy of compound **6e** against 4T1 tumor xenograft models with oral administration. (A) Antitumor efficacy of **6e**, ribociclib and vorinostat treated 4T1 xenograft tumor. (B) Average body weights for **6e**, ribociclib and vorinostat treated mice groups. (C) p-Rb and Bcl-2 staining of tumor tissues showing the down-regulation in **6e** groups compared to other groups. Scale bar, 50 μ m.

1
2
3
4
5
6
7
8
9
10
11
12
13
14
15
16
17
18
19
20
21
22
23
24
25
26
27
28
29
30
31
32
33
34
35
36
37
38
39
40
41
42
43
44
45
46
47
48
49
50
51
52
53
54
55
56
57
58
59
60

Table 4. Pharmacokinetic Characteristics of Compound **6e**

parameter	iv (20mg/kg)	ip (20mg/kg)	po (20mg/kg)
AUC _{0-∞} (μg/L*h)	6158	2133.7	1130.6
C _{max} (μg/L)	3853	359.8	136.8
T _{max}	--	0.262	1.8
F(%)	--	34.7	18.4
MRT _{0-∞} (h)	14.07	13.75	20.3
V _{ss} (L/kg)	48.99	119.94	431.52
CL(L/h/kg)	4.14	12.61	20.62
t _{1/2} (h)	10.76	9.65	14.91



A novel, highly potent, selective inhibitor 6e targeting both CDK4/9 and HDAC1 have been designed and synthesized. 6e with excellent CDK4/9 inhibitory activity of $IC_{50} = 8.8$ nM and $IC_{50} = 12$ nM, respectively and HDAC1 inhibitory activity of $IC_{50} = 2.2$ nM, can effectively induce apoptosis of human breast, lung and liver cancer cell lines. The kinase profiling of compound 6e against a panel of 375 kinases showed excellent selectivity and specificity. Mice bearing breast cancer treated with 6e showed significant antitumor efficacy.

57x55mm (300 x 300 DPI)